Durham E-Theses

New and renewable energy and environmental engineering

Shatat, Mahmoud I. M.

How to cite:

NEW AND RENEWABLE ENERGY AND ENVIRONMENTAL ENGINEERING

MSc Thesis

In

SOLAR WATER DESALINATION

by

Mahmoud I. M. Shatat

0 7 OCT 2008

School of Engineering
Durham University
UK
2008
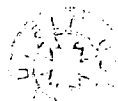
Durham University

School of Engineering

MSc Thesis

In

Solar Water Desalination

by

Mahmoud I. M. Shatat

Supervisors

Dr. Khamid Mahkamov   **Dr. Karen Johnson**

It is worth mentioning that three papers have been produced from this thesis

DEDICATION

To The My Loving Memory of My Parents, My Wife and My Unseen Son Omar, Whom I Shall Remember

ACKNOWLEDGEMENT

I'm so grateful to my supervisors, Dr. Khamid Mahkamov and Dr. Karen Johnson, who gave me their invaluable suggestions and comments and assisted me in conducting this study in the most useful way.

I'm deeply indebted to the Durham Palestine Educational Trust (DPET) and to all its donors and supporters for giving me the scholarship which has enabled me to study for the MSc in New and Renewable Energy and Environmental Engineering at Durham University.

I would also thank Mr. Vin McIntyre for his help and fatherly assistance and the staff of the Durham thermo fluids laboratory, especially Colin Wintrip and Gary Parker

DECLARATION

The material contained within this thesis has not previously been submitted for a degree at Durham University or any other university. The research reported within this thesis has been conducted by the author unless indicated otherwise.

This work has been documented in part in the following publications:

[1] Shatat M., Mahkamov K., and Johnson K. Experimental and Theoretical Investigations of Performance of Multi-Stage Solar Still Water Desalination Unit Coupled with an Evacuated Tube Solar Collector. *Proceedings of the ASME 2nd International Conference on Energy Sustainability*. August 10-14, 2008 Jacksoville, Florida, USA.

[2] Shatat M., and Mahkamov K. (2008). Determination of Rational Design Parameters of a Multi-Stage Solar Water Desalination Still Using Transient Mathematical Modeling. *Renewable Energy*.

[3] Shatat M., and Mahkamov K. (2008). Survey of Water Desalination using Conventional and Renewable Energy Sources Submitted to *Journal of Renewable and Sustainable Energy Reviews*.

TABLE OF CONTENTS

LIST OF FIGURES

LIST OF TABLES

NOMENCLATURE

$\dot{Q}_H$ Heat energy input (W)

$\dot{m}_e$ Vapour mass flow rate at i^{th} stage (kg/s)

$\Delta\dot{Q}_{lossesi}$ Heat loss rate in the ith stage of the still (W)

M_s Mass of water bed at i^{th} stage (kg)

$\dot{m}_c$ Mass flow rate of water in the solar collector, (kg/s)

$\dot{m}_{qp}$ Mass transfer rate from phase q to phase p

$\dot{m}_{pq}$ Mass transfer from phase p to phase q

C_p Specific heat of water, (J/(kg K))

h_{fg} Latent heat of vaporization of water (J/kg)

h_{fg}^{*} The refined value of latent heat of vaporization of water (J/kg) at the condensation surface

T_{si} Water bed temperature at the ith stage (°C)

T_{ci} Upper surface temperature at the ith stage (°C)

T_{SCinl} Solar collector inlet temperature (°C)

T_{SCoutl} Solar collector outlet temperature (°C)

T_{xi} Heat exchanger inlet temperature (°C)

P_s Vapour pressure at surface of water (Pa)

P_c Vapour pressure at condensing surface (Pa)

h_{sc} Convective heat transfer coefficient (W/(m²K))

h_{ew} Evaporative heat transfer coefficient (W/(m²K))

A_s Surface area of the water body (m²)

G Insolation (W/m²)

$\overline{G}$ Daily average insolation (W/m²)

$A_{collect}$ Solar collector area (m²)

m_{out} Distillate output (kg)

D_h Heat exchanger diameter

l_h Heat exchanger length

$\eta_{distill}$ Water distillation efficiency

$\eta_{overall}$ Overall efficiency of the system

$\vec{F}$ Body force (N)

k_{eff} Effective thermal conductivity

S_h Source term which contains the contribution from radiation (J)

E Energy for each phase (J)

A_{lamp} Total area panel lamps (m^2)

A_{col} Total area of columns between lamps (m^2)

A_{raw} Total area of rows between lamps (m^2)

V_{lamp} Voltage at lamps (Volts)

V_{col} Voltage at columns (Volts)

V_{raw} Voltage at rows (Volts)

$\bar{x}$ Arithmetic mean of sample

x_i Values of sample

n Sample size or number of values

s Standard deviation

t Statistical parameter for significance test in water quality

m_d Daily distillate output (kg/day)

m_y Average annual distillate output (kg)

M Annual cost of desalination system (US$)

P Capital cost (US$)

CRF Capital recovery factor

r The interest rate (%)

n Life of the system (year) in economical study

N The annual salvage value (US$)

S salvage value (US$)

SFF The sinking fund factor

PC Product cost (US$)

C Cost price (US$)

t Thickness (m) in economical study

η_{inv} Inverter losses

η_b Battery losses

S_F Safety factor for PV thermal losses

P_{pv} Peak power of PV

N_{pv} Number of PV modules

C_{Ah} Battery ampere hour capacity

C_{wh} Battery watt hour capacity

GREEK LETTERS

ρ Material density (kg/m^3)

μ Molecular viscosity (kg/m. s)

Ω 1/Siemens

υ mass phase velocity (m/sec)

α_q q_{th} fluid's volume of fraction

SUBSCRIPTS

c Solar collector

h Heat exchanger

SM Still metal

SI Still insulation

SL Labour

SA Additional cost

M Metal

df Degrees of freedom

q Primary phase

p Secondary phase

ABBREVIATIONS

MSF Multi-stage flash distillation

MED Multiple effect evaporation

VC Vapor compression evaporation

RO Reverse osmosis

PV Photovoltaic cells

$PSSH$ Peak sunshine hours

ED Electro dialysis

MD Membrane distillation

HFF Hollow fine fiber

DC An electrical direct current

ppm Part per million

EC Electrical conductivity *(μS/cm)*

NTU Nepholometric turbidity units

TDS Total dissolved solids *(mg/L)*

WHO World health organization

EU European Union

UN United Nations

ABSTRACT

There is an acute scarcity of potable water in many parts of the world, and especially in most of the Middle East region. Important advances have been made in desalination technology but its wide application is restricted by relatively high capital and input energy costs, even when solar energy is used. Until recently, flat-plate solar collectors have usually been employed to distill water in compact desalination systems. Currently, it is possible to replace these collectors by the more advanced evacuated tube collectors, which are now available on the market at a similar price.

The research which is concerned with the development of a novel small scale solar water desalination technology, consists of experimental and theoretical investigations of the operation of a multi stage solar still desalination system coupled with a heat pipe evacuated tube solar collector with an aperture area of about 1.7 m^2.

The multi stage still was tested to recover latent heat from the evaporation and condensation processes in each of its four stages. A number of experimental tests were carried out using a laboratory rig to investigate its water production capacity. Solar radiation (insolation) during a mid-summer day in the Middle East region was simulated by an array of 110 halogen flood lights.

Computational Fluid Dynamics (CFD) modeling of the evaporation and condensation processes in one of the still's stages was conducted using FLUENT 6.2 software. The simulation results demonstrate the importance of the various parameters affecting the total production rate of the solar still and provide detailed information on the temperature distribution and condensate formation inside the solar still. However, it was found that the CFD technique at this stage does not provide accurate quantitative predictions and results obtained can be used only for qualitative analysis. Hence, the use of a lumped parameter mathematical model was preferred for analysis and design purpose.

A lumped parameter model has been developed to describe the system's operation. It consists of a system of ordinary differential equations of energy and mass conservation written for each stage of the still. A MATLAB computer program was written to solve the system of governing equations to simulate the evaporation and condensation processes and the experimental results were used to validate numerical predictions. The experimental and theoretical values for the total daily

distillate output were found to be closely correlated. The test results demonstrate that the system produces about 9 kg of clean water per day and has a distillation efficiency of 90%. The overall efficiency is 33% due to the presence of heat losses in the system. However, this level of efficiency is greater of that for conventional solar stills. Following the experimental calibration of the lumped parameter model, this was used for determination of rational design parameters of the still and it was demonstrated that the performance of the system could be considerably improved to produce 11 kg/m^2 of water per day if the number of stages and evaporation area were 4 and 1 m^2, respectively.

A water quality analysis was performed for the distilled water and the levels of total dissolved solids, electrical conductivity and pH were well within the range defined by the World Health Organization guidelines for drinking water.

An economic study was also conducted for the system and it was shown that the distilled water costs of 0.016 US$/litre with a payback period of 6 months in the Middle East region conditions.

This research demonstrates, empirically and theoretically, the potential role in the field of solar desalination of the multistage solar still coupled to the evacuated tube solar collector. Not only is this system a promising new technology but it could prove to be particularly appropriate in remote and rural areas. Simultaneously this system also uses a completely clean energy source and contributes to tackling environmental pollution, global carbon emissions and climate change problems.

1 Introduction and Overview of Desalination Process

1.1 Introduction

Many countries around the world, especially developing countries and countries in the Middle East region, suffer from a shortage of fresh water. The United Nations (UN) Environment Programme stated that one third of the world's population lives in countries with insufficient freshwater to support the population [1]. Consequently, drinking water of acceptable quality has become a scarce commodity. The total global water reserves are about 1.4 billion cubic kilometers, of which around 97.5% is in the oceans and the remaining 2.5% is fresh water present in the atmosphere, ice mountains and ground water. Of the total, only about 0.014% is directly available for human beings and other organisms [2]. Thus tremendous efforts are now required to make available new water resources in order to reduce the water deficit in countries which have shortages [3].

According to World Health Organization (WHO) guidelines, the permissible limit of salinity in drinking water is 500 ppm and for special cases up to 1000 ppm [4]. Most of the water available on earth has the salinity up to 10,000 ppm and seawater normally has salinity in the range of 35,000–45,000 ppm in the form of total dissolved salts [5].

Desalination is a process in which saline water is separated into two parts, one that has a low concentration of dissolved salts and which is called fresh water, and the other which has a much higher concentration of dissolved salts than the original feed water, and which is usually referred to as brine concentrate [14].

The desalination of seawater has become one of the most important commercial processes to provide fresh water for many communities and industrial sectors. It plays a crucial role in socio-economic development in a number of developing countries, especially in Africa and some countries in the Middle East region, which suffer from a shortage of fresh water. There is extensive R & D activity, especially in the field of renewable energy technologies, to find new and feasible methods to produce drinking water [6&7].

Currently there are more than 7,500 desalination plants in operation worldwide producing several billion gallons of water per day. 57% are in the Middle East [8] where large scale conventional heat and power plants are among the region's most important

commercial processes, as they play a crucial role in providing fresh water for many communal and industrial sectors, especially in areas with a high density of population. However, since they are operated with fossil fuel, they are becoming very expensive to run and the environmental pollution they produce is increasingly recognised as very harmful to the globe.

Moreover, such plants are not economically viable in remote areas, even near a coast where seawater is abundant. Many such areas often also experience a shortage of fossil fuels and an inadequate electricity supply. The development of compact, small-scale systems for water desalination is imperative for the population in such areas [6&7]. Thermal solar energy water desalination is known to be a viable method of producing fresh water from saline water [9] in remote locations; conventional basin solar stills with a relatively large footprint are an example of such simple technology. Furthermore using a clean natural energy resource in water desalination processes will reduce significantly the pollution that causes global warming.

This research presents the development of a novel small scale solar powered water desalination technology. It consists of experimental and theoretical investigations of the operation of a multi stage solar still desalination system coupled with a heat pipe evacuated tube solar collector to investigate the performance of that rig. A mathematical model with a Matlab program code was developed to simulate the evaporation and condensation processes inside the still in addition to CFD simulation using FLUENT 6.2 software.

Water quality analysis of the distillate water product has been performed and reported and a study of the economic feasibility has been also conducted.

This chapter aims to present a review of the published literature on the various desalination technologies and their advantages and disadvantages in addition to their economics. It also presents an introduction to the geographical location and water situation in the Gaza Strip

1.2   Overview of desalination processes

Various desalination processes have been developed, some of which are currently under research and development. The most widely applied and commercially proven technologies can be divided into two types: phase change thermal processes and

membrane processes and, as shown in Figure 1.1., both encompass a number of different processes. In addition, there are the alternative technologies of freezing and ion exchange which are not widely used. All are operated by either a conventional energy or renewable energy to produce fresh water.

1.3   Thermal desalination processes.

Thermal desalination, often called distillation, is one of the most ancient ways of treating seawater and brackish water to make it potable. It is based on the principles of boiling or evaporation and condensation. Water is heated until it reaches the evaporation state. The salt is left behind while the vapour is condensed to produce fresh water [10]. In modern times, the required thermal energy is produced in steam generators, waste heat boilers or by the extraction of back-pressure steam from turbines in power stations [11]. The most common thermal desalination processes are:

- Multi-stage flash distillation (MSF)
- Multiple-effect distillation (MED)
- Vapour-compression evaporation (VC)
- Cogeneration
- Solar water desalination
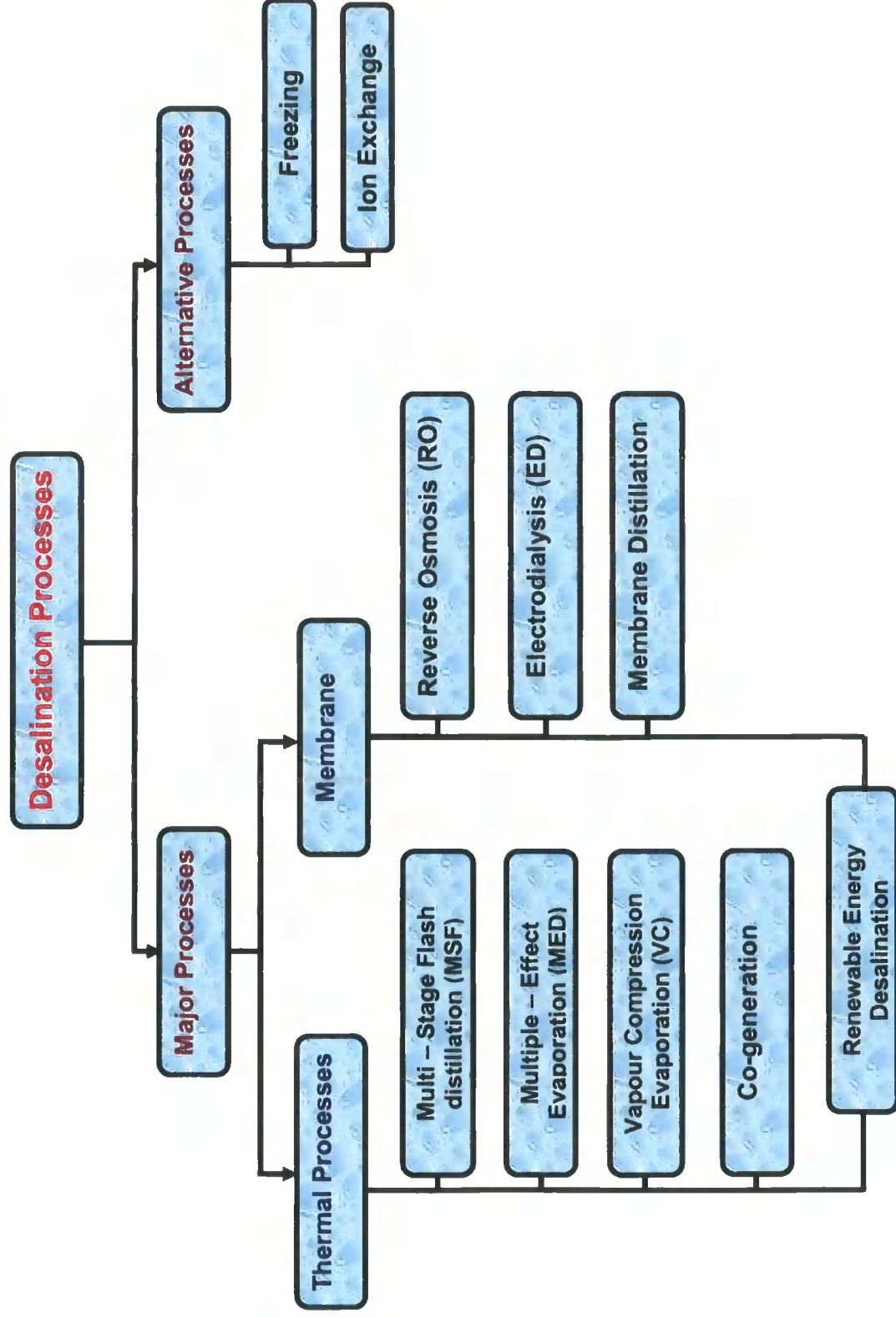
Figure 1-1: Classification of water desalination technologies.

1.3.1 Multi-stage flash distillation (MSF)

Water distillation in a vessel operating at a reduced pressure, and thus providing a lower boiling point for water, has been used for well over a century. In the 1950s, Weirs of Cathcart in Scotland, used this concept to invent the MSF process and it had significant development and wide application throughout the 1960s due to both to its economical scale and its ability to operate on low-grade steam [12].

In the MSF process, illustrated in Figure 1.2, feed water (saline water) is heated in a vessel called the brine heater until it reaches a temperature below the saturation boiling temperature. The heated seawater flows through a series of vessels, in sequence, where the lower ambient pressure causes the water to boil rapidly and vaporize. This sudden introduction of heated water into the reduced-pressure chamber is referred to as the "flashing effect" [13] because the water almost flashes into steam.

A small percentage of this water is converted into water vapour; the percentage mainly dependent on the pressure inside the stage, since boiling continues until the water cools and vaporization stops. The vapour steam generated by flashing is converted to fresh water by being condensed on the tubes of heat exchangers (condenser) that run through each stage. The incoming feed water going to the brine heater cools the tubes. This, in turn, heats up the feed water and increases the thermal efficiency by reducing the amount of thermal energy required in the brine heater to raise the temperature of the seawater.

An MSF unit that used a series of stages set at increasingly lower atmospheric pressures was developed so that the feed water which was passed from one stage to another was boiled repeatedly without adding more heat. Typically, an MSF plant contains between 15 and 25 stages [14].

Distillation processes produce about 50% of the worldwide desalination capacity. and 84% of this is produced by MSF technology. Most MSF plants have been built in the Middle East, where energy resources have been plentiful and inexpensive [15].

1.3.1.1 Advantages and disadvantages of MSF

- MSF plants are relatively simple to construct and operate [13]

- They have no moving parts, other than conventional pumps, and incorporate only a small amount of connection tubing. [13]

- The quality of water effluent contains 2-10 ppm dissolved solids, a high level of purification. Therefore it is re-mineralized in the post treatment process [16].

- The quality of the feed water is not as important as it is in the reverse osmosis system technology [14].

- Operating plants at higher temperatures (over 115°C) improves their efficiency but causes scaling problems where the salts such as calcium sulphate precipitate on the tubes surfaces and create thermal and mechanical problems like tube clogging [14].

- Adding more stages improves the efficiency and increases water production but it increases the capital cost and operational complexity [14].
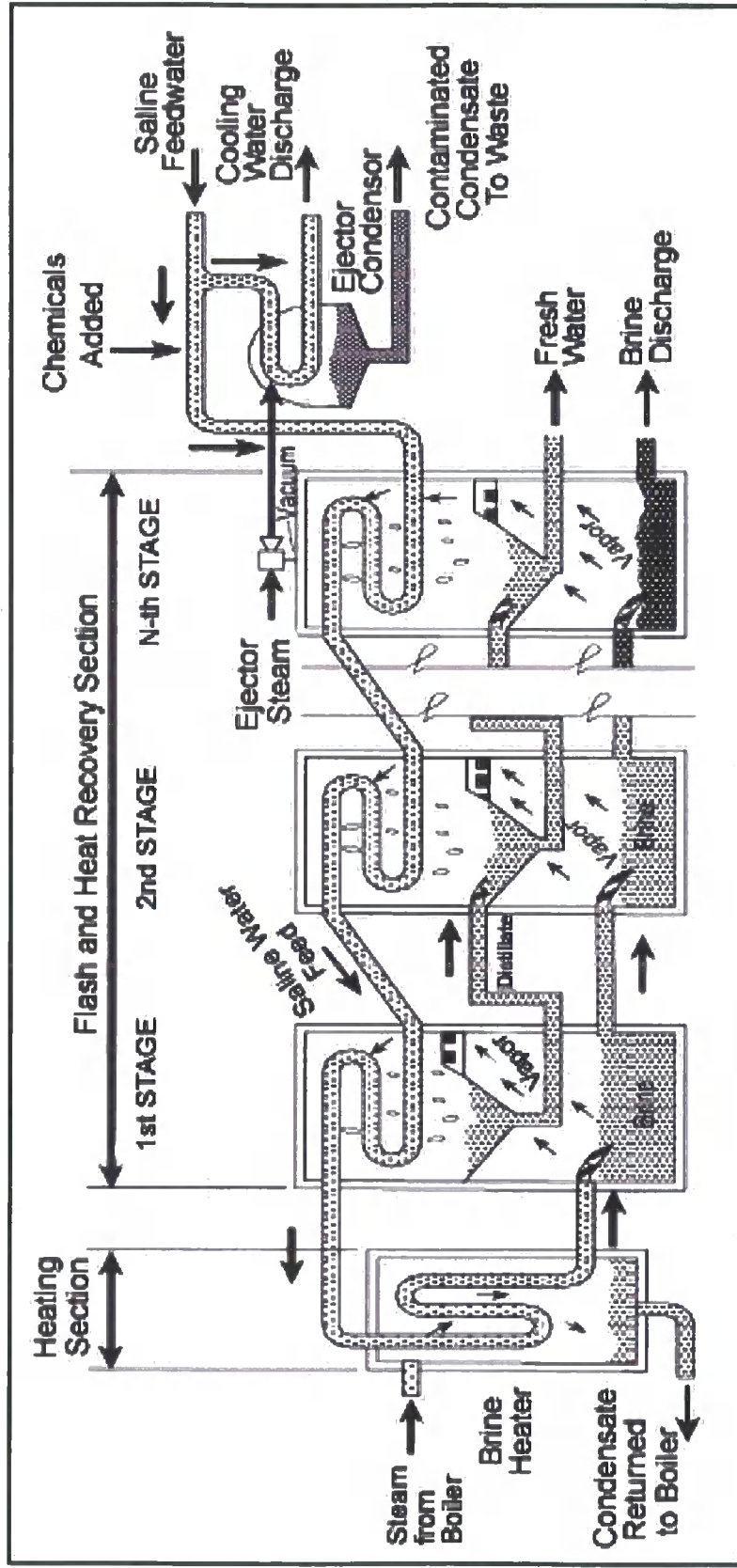
Figure 1-2: Multi stage flashing process - MSF [7]

1.3.2 Multi-effect distillation (MED)

The multiple-effect distillation (MED) process is the oldest large-scale distillation method used for seawater desalination. At present, about 3.5% of the world's desalted water is produced by MED plants [17].High distilled water quality, high unit capacity and high heat efficiency are its most obvious characteristics [17 &18].

In addition, MED has traditionally been used in the industrial distillation sector for the evaporation of juice from sugar cane in the production of sugar and in the production of salt using the evaporative process.

The MED process, like MSF, takes place in a series of vessels or evaporators called effects, and it also uses the principle of evaporation and condensation by reducing the ambient pressure in the various effects. This process permits the seawater feed to undergo multiple boiling without supplying additional heat after the first effect.

The seawater enters the first effect and is raised to boiling point after being preheated in tubes. The seawater is sprayed onto the surface of the evaporator tubes to promote rapid evaporation. The evaporator tubes are heated by externally supplied steam, normally from a dual-purpose power plant. The steam is condensed on the opposite side of the tubes, and the steam condensate is recycled to the power plant for its boiler feed water as shown in Figure 1.3.
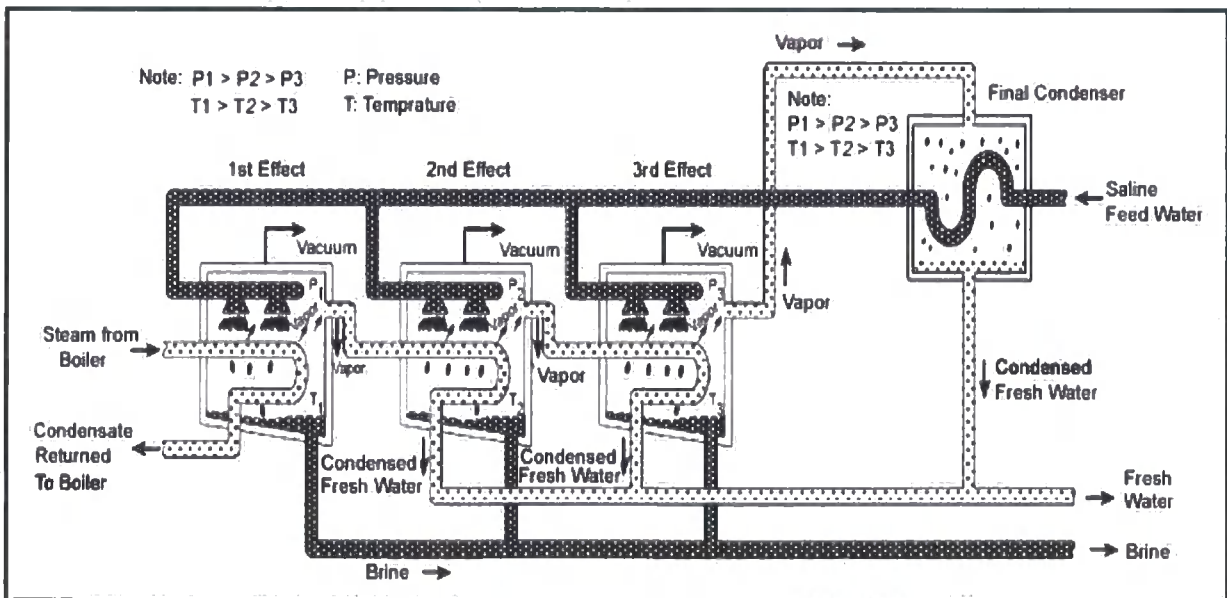
Figure 1-3: Multi effect distillation plant [19]

The MED plant's steam economy is proportional to the number of effects. The total number of effects is limited by the total temperature range available and the minimum allowable temperature difference between one effect and the next effect. Only a portion of the seawater applied to the tubes in the first effect is evaporated. The remaining feed water is fed to the second effect, where it is again applied to a tube bundle. These tubes are in turn heated by the vapours created in the first effect. This vapour is condensed to form the fresh water product, while giving up heat to evaporate a portion of the remaining seawater feed in the next effect.

The process of evaporation and condensation is repeated from effect to effect, each at a successively lower pressure and temperature. This continues for, typically, 4 to 21 effects and a performance ratio between 10 and 18 is found in large plants [20].

1.3.2.1 Advantages and disadvantages of MED

- The MED process is designed to operate at lower temperatures of about 70°C (158°F). This minimizes tube corrosion and the potential of scale formation around the tube surfaces [14].

- The quality of the feed water is not as important as in the reverse osmosis system technology. Hence the pre-treatment and operational costs of MED are low.

- The power consumption of MED is lower than that of MSF plant. [13].

- The performance efficiency in MED plants is higher than in MSF plants; therefore the MED process is more efficient than the MSF process in terms of heat transfer and fresh water production cost [21].

1.3.3 Vapour-compression evaporation (VC)

The vapour compression distillation process is used in combination with other processes like MED and single-effect vapour compression. In this process, the heat for evaporating the seawater comes from the compression of vapour. VC plants take advantage of the principle of reducing the boiling point temperature by reducing the pressure. Two devices, a mechanical compressor (mechanical vapour compression) and a steam jet (thermal vapour compression), are used to condense the water vapour to produce sufficient heat to evaporate incoming seawater, as illustrated in Figure 1.4.

The mechanical compressor is usually electrically or diesel driven. VC units have been built in a variety of configurations to promote the exchange of heat to evaporate the seawater. The compressor creates a vacuum in the evaporator and then compresses the vapour taken from the evaporator and condenses it inside a tube bundle. Seawater is sprayed on the outside of the heated tube bundle where it boils and partially evaporates, producing more vapour. With the steam-jet type of VC distillation unit, called a thermo compressor, a venturi orifice at the steam jet creates and extracts water vapour from the evaporator, creating a lower ambient pressure. The extracted water vapour is compressed by the steam jet. This mixture is condensed on the tube walls to provide the thermal energy (heat of condensation) to evaporate the seawater being applied on the other side of the tube walls in the evaporator.
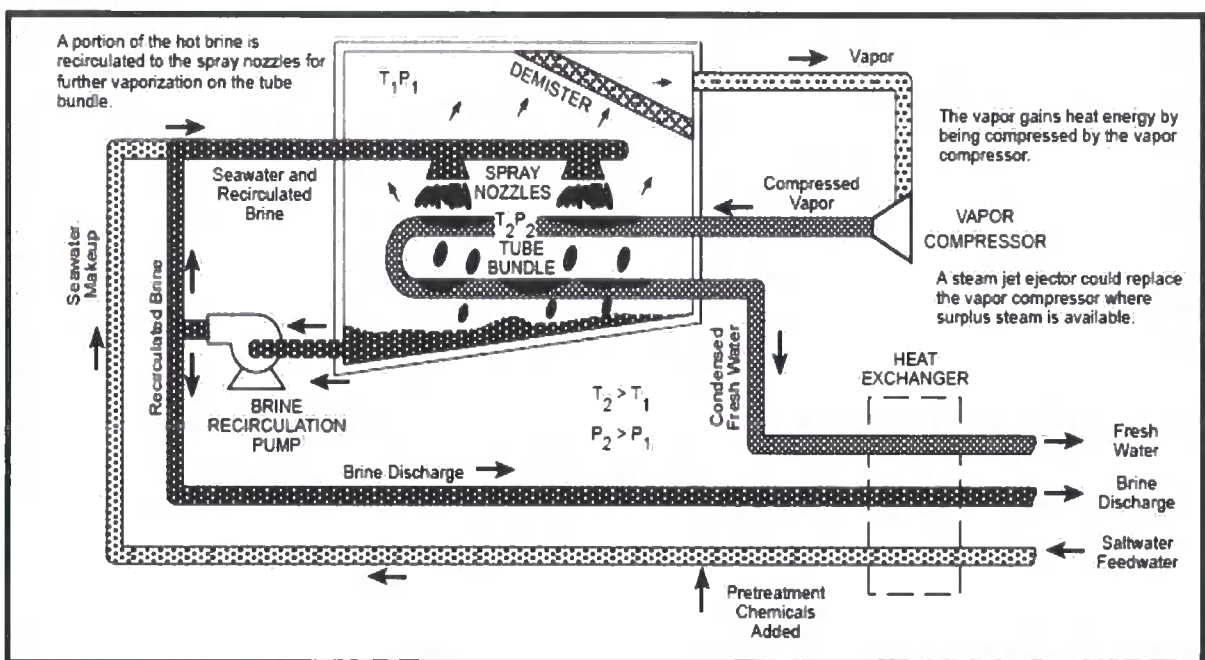
Figure 1-4: Vapor-compression evaporation [14].

1.3.3.1 Advantages and disadvantages of VC

- The simplicity and reliability of plant operation make it an attractive unit for small-scale desalination units. They are usually built up to a capacity of 3000 m^3/day and are often used for resorts, industries and drilling sites where fresh water is not readily available [14].

- The low operating temperature of VC distillation makes it a simple and efficient process in terms of power requirement.

- The low operating temperatures (below 70°C) reduces the potential for scale formation and tube corrosion.

1.3.4 Cogeneration system for power and water desalination.

It is possible to use energy in a dual use or cogeneration systems in which the energy sources can perform several different functions such as electric power generation and water desalination.

Most of the desalinated potable water and electricity in the Arabian Gulf countries, and North Africa are produced by cogeneration plants associated with multi-stage flash (MSF) desalination units operating on seawater [14]. Although other distillation process such as thermal vapor compression and MED are starting to find their way into the market, the MSF process is still considered as the workhorse of the desalination industry. This process has proven its reliability and flexibility over almost 50 years of plant design and operation. For large desalination capacity, the MSF process can be considered as the only candidate commercially. However, on the cogeneration plant side, the situation is different in that several alternatives are commercially available to provide the required electrical power and steam for desalination [22].

In cogeneration plants, the electricity is produced with high pressure steam to operate the turbines; the steam produced by boilers at temperatures up to 540 °C. As this steam expands in turbines its temperature and energy level are reduced. As previously stated, distillation plants need steam with temperatures lower than 120 °C and this can be obtained easily at the end of the turbine after much of its energy has been utilized in electric power generation. This steam is used in the desalination process and the condensate from the steam is then returned to the boiler to be reheated again for use in the turbine.

The main advantage of this system is that it uses much less fuel than each plant operating separately and energy costs are a crucial factor in any desalination process. In contrast, one of the disadvantages is the permanent coupling between the desalination plant and the power plant which can create a problem in water production

when the demand of electricity is reduced or when the turbine or generator is down for repair.

The size of the desalination plant that can be efficiently integrated with a power cogeneration plant so that the ratio of desalted water to power production is consistent with water and power requirements of the community it serves.

Cogeneration plants have also reduced power costs. Meanwhile other types of cogeneration plants have achieved lower costs by benefiting from heat recovery systems on gas turbines, heat pumps and other industrial processes such as burning solid wastes in an incinerator [6].

1.3.5 Economics of thermal desalination processes

Thermal process desalination plants, which use conventional sources of energy and which usually have large production capacities are more expensive than membrane plants because of the large quantities of fuel required to vaporize salt water. The membrane method is a separation process using a permeable membrane to move either water or salt to induce two zones of differing concentrations to produce fresh water without the need for heating or phase change, [25] as described in the following sections. It is also more economical for brackish water desalination. [45] In the case of multi-effect distillation (MED), the cost for large systems with a daily production from 91,000 m^3 to 320,000 m^3 ranges between 0.52\$/m^3 and 1.01\$/m^3. These costs refer to examples of plants built between 1999 and 2006 with the most recent having lower costs and the older installations being the most expensive [45].

For medium size systems, with a daily production from 12,000 m^3 to 55,000 m^3, the cost ranges between 0.95\$/m^3 and 1.5\$/m^3. For small systems with a daily capacity around 100 m^3, the cost varies between 2.50 and 10 \$/m^3.

For the MSF method, the cost can vary between 0.52\$/m^3 and 1.75\$/m^3 for systems with a daily production of 23,000 m^3 to 528,000 m^3. The cost is reduced when MSF is coupled with electric power generation in a cogeneration plant.

VC is used mainly for small systems with production of around 1000 m^3/day, and a cost that ranges between and 2.01 and 2.66 US\$/m^3 [23,24]. Table 1.1 shows the water unit cost for various thermal desalination processes.

Desalination process	Capacity of desalination plant (m³/day)	Desalination cost per m³ (US$)
Multi effect distillation MED	Less than 100	2.5 – 10
	12,000 – 55,000	0.95 – 1.95
	Greater than 91,000	0.52 – 1.01
Multi stage flash MSF	23,000 – 528,000	0.52 – 1.75
Vapour compression	1000 – 1200	2.01 – 2.66

Table 1-1: Cost of desalinated water in thermal processes.

1.4 Membrane processes

Synthetic membranes were first introduced in separation processes in the 1960s but they began to play an increasingly crucial role in water desalination in the 1980s. Originally, membrane applications were limited to municipal water treatment such as microfiltration and desalination but, with the development of new membrane types, uses have expanded to cover not only the water industry but also high return processes such as chemical separations, enzyme concentration and beverage purification.

This technology uses a relatively permeable membrane to move either water or salt to induce two zones of differing concentrations to produce fresh water. These processes are also useful in municipal water treatment; RO (reverse osmosis) and ED (electrodialysis) are replacing phase-change desalting technologies for supplying water to coastal and island communities all over the world. Reverse osmosis, in particular, is becoming an economical alternative to the traditional water softening processes [25].

Membrane technology includes several processes but the principal difference between them lies in the size of the entities, ions, molecules and suspended particles that are retained or allowed to pass through the membranes. Typical separation processes are nano filtration, ultra filtration, micro filtration and filtration used in the pre-treatment stages of desalination to remove large particles, bacteria, ions, and for water softening [13]. Table 1.2 summarizes the membrane separation processes and Figure 1.5 shows the effective range of membrane processes and applications.

This section looks at the following process

- Reverse osmosis (RO)
- Electrodialysis (ED)

- Membrane distillation (MD)

Separation process	Pore size or maximum molecular weight range [a]	Operating pressure (kPa)	Substances removed	Alternative traditional water treatment method
Microfiltration	0.1 to 10 microns	140 to 5,000	Bacteria, viruses, larger colloidal particles, precipitates and coagulates	Ozonation, chlorination, sand-bed filtration, bioreactors, coagulation and sedimentation
Ultrafiltration	10 to 1,000 Å 1,000 to 500,000 daltons	200 to 1,000	High molecular weight proteins, large organic molecules and pyrogens	Sand-bed filtration, bioreactors and active carbon treatment
Nano filtration	2 to 70 Å 180 to 10,000 daltons	550 to 1,400	Large divalent and some monovalent ions, colourants and odorants	Lime/soda softening and ion exchange
Reverse osmosis	1 to 70 Å	1,400 to 7,000	All of the above in addition to monovalent ions	Evaporation, freezing and electrodialysis

Note: Å = angstroms; kPa = kilopascals
a/ The maximum molecular weight range, expressed in Daltons, refers to the molecular weight cut-off (MWCO) allowed by membrane pores.

Table 1-2: Characterization of membrane separation processes

Source: Adapted from J.E. Stratton, "Food online", Department of Food Science and Technology, University of Nebraska [25]
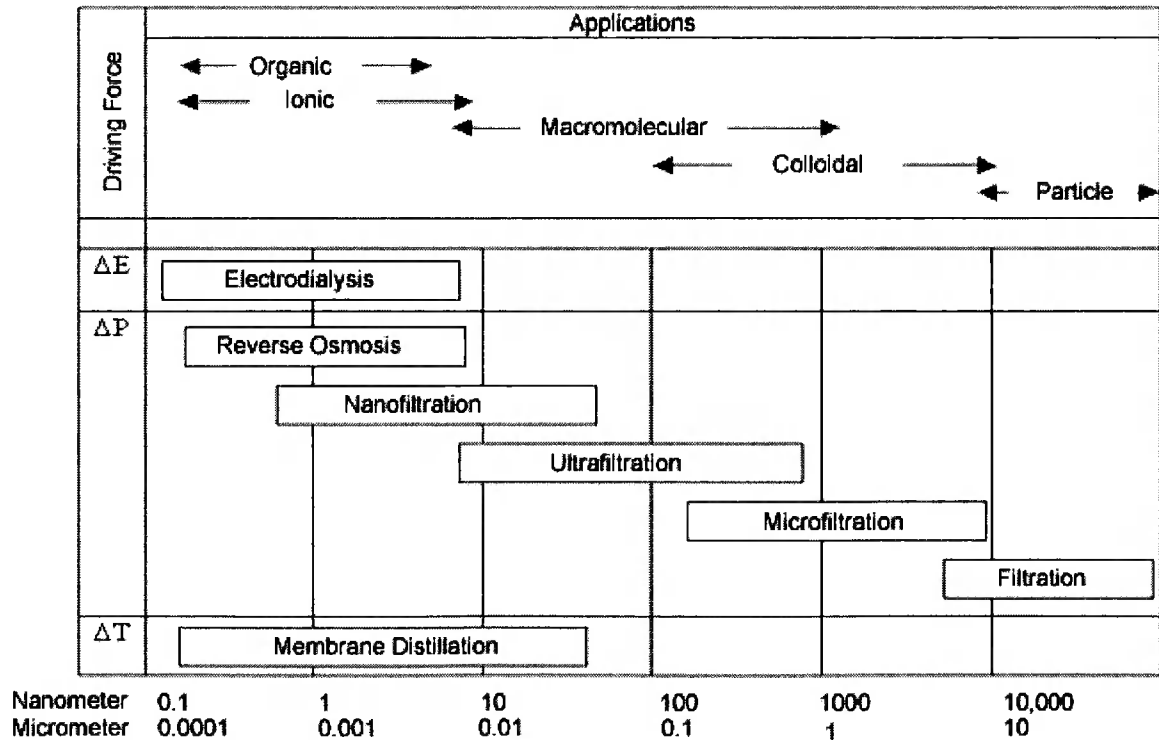
Figure 1-5: Effective range of membrane processes and applications [25]

1.4.1 Reverse osmosis (RO)

The reverse osmosis process is relatively new in comparison to other technologies and was introduced as a successful commercialized technology in water desalination in the early 1970s. RO is a membrane separation process in which the water from a pressurized saline solution is separated from the solutes (the dissolved material) by flowing through a membrane without the need for heating or phase change. The major energy required is for pressurizing the feed water [14]. It can also be described as a process of forcing a solvent from a region of high solute concentration through a membrane to a region of low solute concentration by applying a pressure in excess of the osmotic pressure, as shown in Figure 1.6. Thus, water flows in the reverse direction to the natural flow across the membrane, leaving the dissolved salts behind with an increase in salt concentration [26].
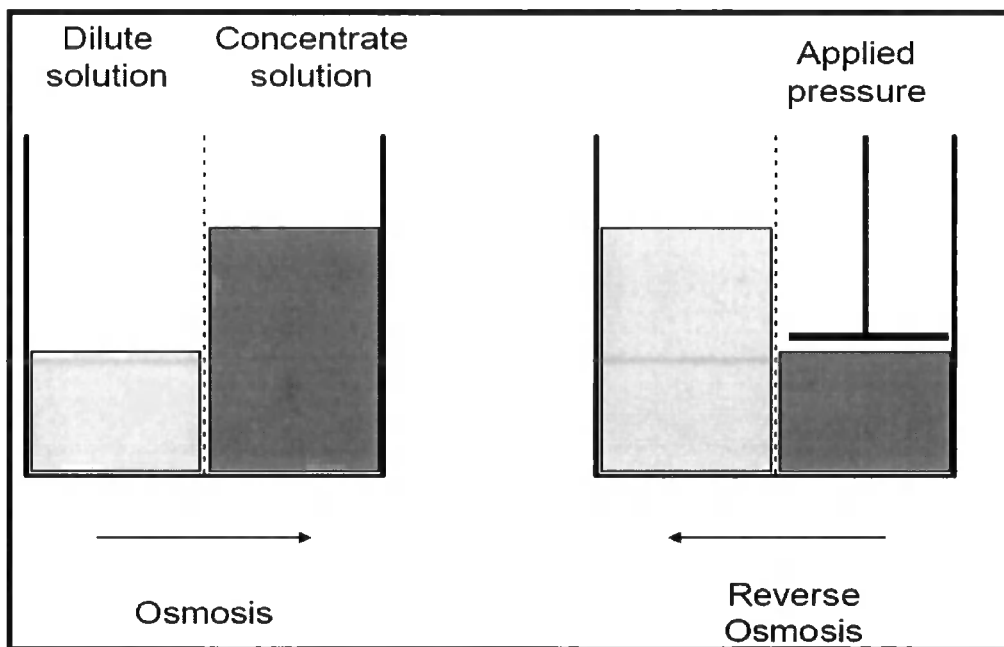
Figure 1-6: Osmosis and reverse osmosis processes

A typical large saline water RO plant consists of five major components, a saline water supply system, a feed water pre-treatment system, high pressure pumping, RO modules (membrane separation) and post-treatment system as shown in Figure 1.7 [27]

In the recent years the largest RO desalination plants have been built in the Middle East and particularly in Saudi Arabia. A plant in Jeddah produces 15 million gallon per

day (MGD) while the Al Jubail and Yanbu RO plants have capacities of 24 MGD and 33.8 MGD respectively.[27, 28]
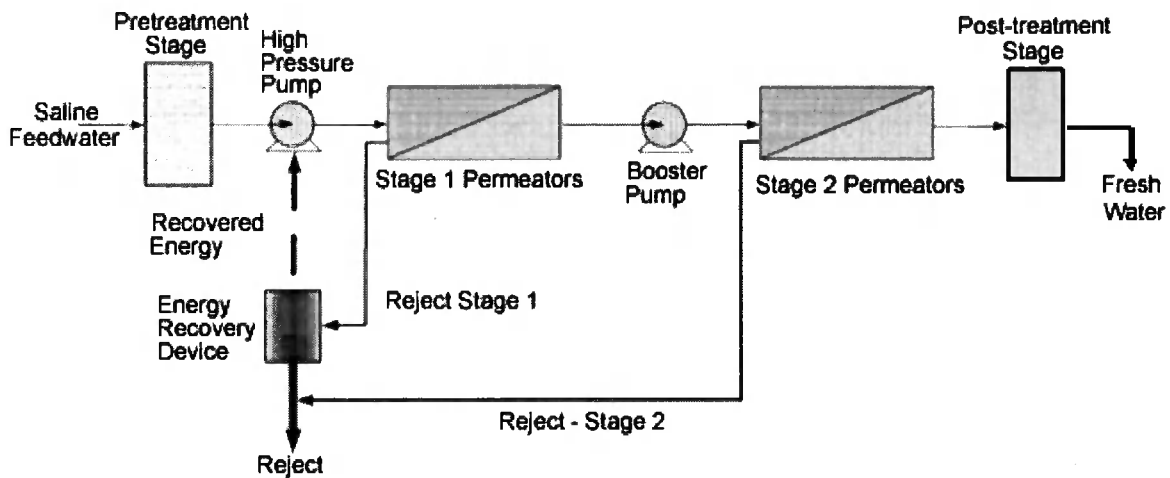
Figure 1-7: Basic components of reverse osmosis plant - adapted from [29].

1.4.1.1 Seawater supply system

An open intake channel supplies the plant with raw seawater which is pumped through trash racks and travelling screens to remove debris [30].

1.4.1.2 Pre Treatment

Pre-treatment is very important in the RO process because it protects membrane surfaces from fouling and also provides protection to the high-pressure pumps and the RO section of the plant. The nature of the pre-treatment depends largely on the feed water characteristics, the membrane type and configuration, the recovery ratio and the required product water quality.

In this stage the seawater is treated against debris, particles and suspended solids by a multimedia gravity filter that removes particles larger than 10 microns. The water is biologically disinfected by injecting chemicals like sodium hypochlorite to remove algae and bacteria and to prevent microorganism growth. Also added are ferric chloride as a flocculant and sulphuric acid to adjust pH and control scale formation [27].

1.4.1.3 High pressure pumping

The high-pressure pump supplies the appropriate pressure needed to enable the water to pass through the membrane where the semi-permeable membrane restricts the passage of dissolved salts while permitting water to pass through. Then the concentrated brine water is discharged into the sea. This pressure ranges from 15 to 25 bar for brackish water and from 54 to 80 bar for sea water [14&20].

1.4.1.4 RO modules (Membrane Separation)

The membrane must be strong enough to withstand the drop of the entire pressure across it. A relatively small amount of salts passes through the membrane and appear in the permeate [14]. In principle, RO membranes should be semi-permeable, possessing a high degree of water permeability but presenting an impenetrable barrier to salts. A membrane should have a large surface area to allow maximum flow.

There are membranes available which are suitable for pump operation up to 84 kg/cm^2 discharge pressure. This pressure ranges from 54 to 80 bars for seawater, depending on its salt content. Most RO applications require two or more modules arranged to operate in series [31] as shown in Figure 1.8.
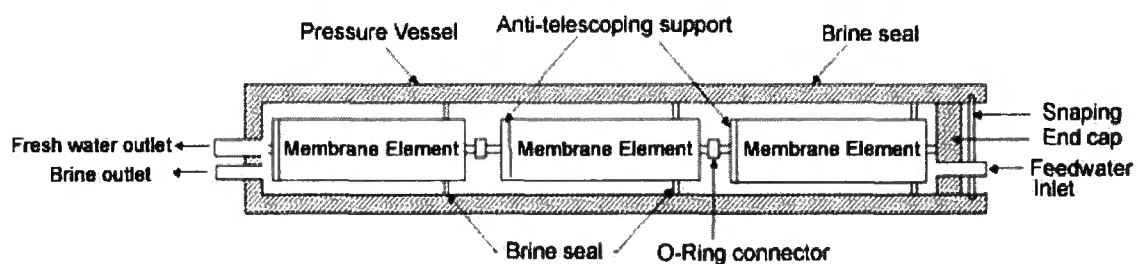
Figure 1-8: Cross-section of a pressure vessel with three membrane elements [14]

RO membranes are made in a variety of configurations. Two of the most commercially successful membranes are spiral wound and hollow fine fibre (HFF) and both of these are used to desalt brackish water and seawater [32].

- **Spiral wound membrane**

This type of membrane element is most commonly manufactured as a flat sheet of either a cellulose diacetate and triacetate blend or a thin film composite usually made

from polyamide, polysulphone, or polyurea polymers. The configuration is illustrated in Figure 1.9 [19].
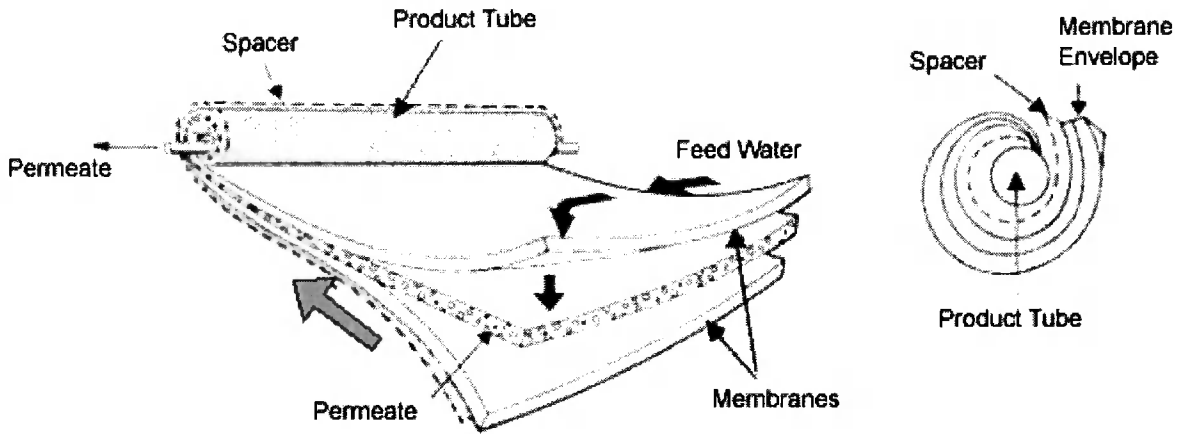
Figure 1-9: Cutaway view of a spiral wound membrane element [19]

- **Hollow fine fibre (HFF) membrane**

HFF is a U-shaped fibre bundle housed in a pressure vessel. The membrane materials are based on cellulose triacetate and polyamide and its arrangement allows the highest specific surface area of all the module configurations, resulting in compact plants. Figure 1.10 illustrates the HFF formation [19].
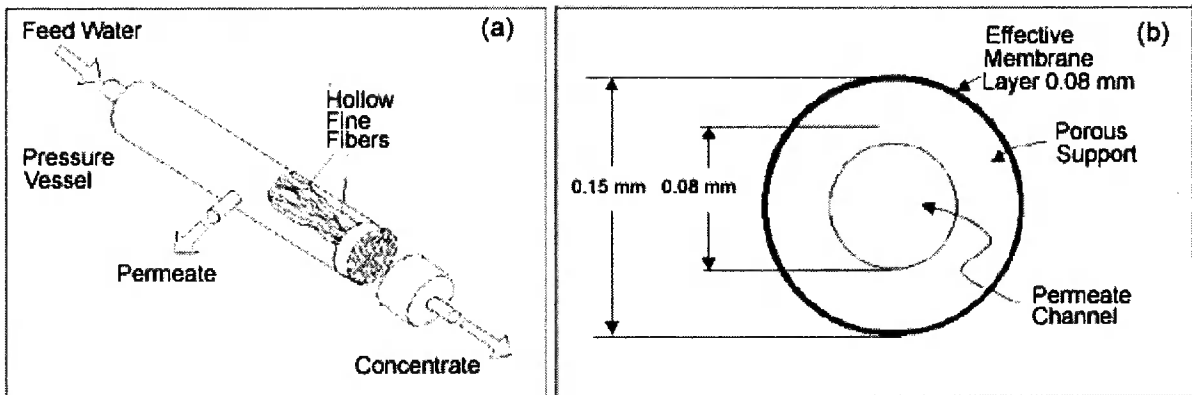
Figure 1-10: Hollow fine fiber membrane module [19]

1.4.1.5 Post treatment

The post-treatment generally stabilizes the water and might include pH adjustment by adding lime to meet the potable water specifications, and the removal of dissolved gases such as hydrogen sulphide and carbon dioxide [20].

1.4.1.6 Advantages and disadvantages of RO process

- Material corrosion problems are significantly less compared with MSF and MED processes due to the ambient temperature conditions.

- Polymeric materials are utilized as much as possible rather than the use of metal alloys [20].

- Two developments have also helped to reduce the operating cost of RO plants during the past decade:

  - The development of operational membranes with high durability and lower prices.

  - The use of energy recovery devices that are connected to the concentrated stream as it leaves the pressure vessel. The concentrated brine loses only about 1–4 bar relative to the applied pressure from the high-pressure pump. The devices are mechanical and generally consist of turbines or pumps that can convert a pressure difference into rotating energy that can be used to reduce energy costs.

- Reverse osmosis units sold for residential water filtration require very large quantities of water since they recover only 5-15% of the feed water that enters the filter. In seawater systems, for every 5 gallons of usable water, 40-90 gallons of water are sent to the wastewater system [14].

- Membrane scaling caused by the precipitation of salts is a common problem in the RO process but it is less than in MSF.

- Membranes are liable to be fouled (plugged) by large particles but this can be avoided by pre-filtering the feed water through a 5-10 micron cartage micro filter. Biological fouling can be caused by the formation of micro-organism colonies and by entrapping dead and live organisms. Colloidal fouling is caused by the settlement on membrane surfaces of colloids from an accumulation of aluminum silicate and clays and from soap detergents and organic materials. [13]

1.4.2 Electrodialysis (ED)

ED was commercially introduced in the early 1960s, about 10 years before RO. It provided a cost-effective way to desalt brackish water and spurred considerable interest

in the whole field of using desalting technologies to produce potable water for municipal use [14]. It also has many other applications in the environmental and biochemical industries as well as in the production of table salt. [13,33]

Electrodialysis is an electrochemical separation process that employs electrically charged ion exchange membranes with an electrical potential difference as a driving force. It depends on the fact that most salts dissolved in water are ionic, being either positively (cationic) or negatively (anionic) charged and they migrate toward electrodes with an opposite electric charge. Membranes can be constructed to permit the selective passage of either cations or anions.

1.4.2.1 Electrodialysis system configuration

The ED system consists of the following elements, as shown in Figure 1.11

- Electrical direct current (DC) power supply to maintain electrical potential between the electrodes, causing ions in the feed stream to migrate through the selective membranes.
- Supply of pressurized water across the membrane.
- Pre-treatment water unit such as filters.
- Single-stage or multiple-stage membrane stacks to achieve demineralization.
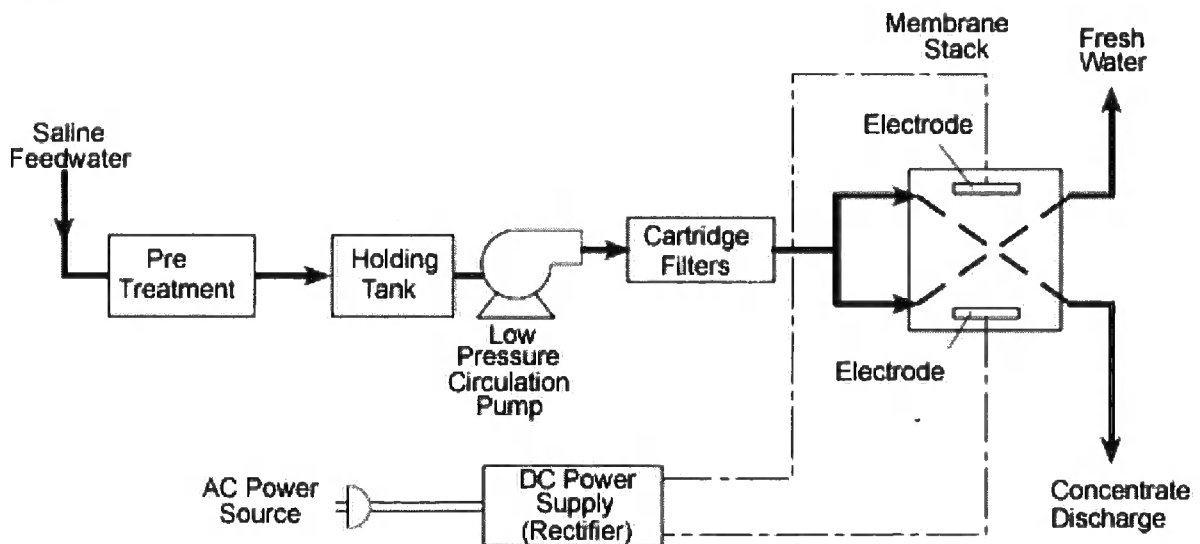
Figure 1-11: Electrodialysis system configuration [14]

To desalinate water, individual membranes that will allow either cations or anions (but not both) to pass are placed between a pair of electrodes. These membranes are

arranged alternately, with an anion selective membrane followed by a cation selective membrane.

A spacer sheet that permits water to flow along the face of the membrane is placed between each pair of membranes. One spacer provides a channel that carries feed (and product) water, while the next carries brine. As the electrodes are charged and saline feed water flows along the product water spacer at right angles to the electrodes, the anions (such as sodium and calcium) in the water are attracted and diverted through the membrane towards the positive electrode. This dilutes the salt content of the water in the product water channel.

The anions pass through the anion-selective membrane, but cannot pass any further than the cation-selective membrane, which blocks their path and traps the anions in the brine stream. Similarly, cations (such as chloride or carbonates) under the influence of the negative electrode move in the opposite direction through the cation-selective membrane to the concentrate channel on the other side. Here, the cations are trapped because the next membrane is anion selective and prevents further movement towards the electrode as shown in Figure 1.12. The design of the system should take into consideration scaling formation; therefore chemicals may be added to the streams to reduce the potential for scaling. [13, 14]

1.4.2.2 Advantages and disadvantages of ED

- It has the capability of high recovery in terms of more fresh water product and less brine [14].
- ED is feasible for brackish water with a salinity of less than 6 g/L of dissolved solids, but not suitable for water with dissolved solids of less than 0.4 g/L.
- The desalination of water with concentrations of dissolved solids higher than 30 g/L, like seawater, is possible but it is not economically viable [34].
- The major energy requirement is the direct current to separate the ionic substances in the membrane.
- Energy usage is proportional to the salts removed.
- It can treat feed water with a higher level of suspended solids than RO.
- Chemical usage for pre-treatment is low [14].
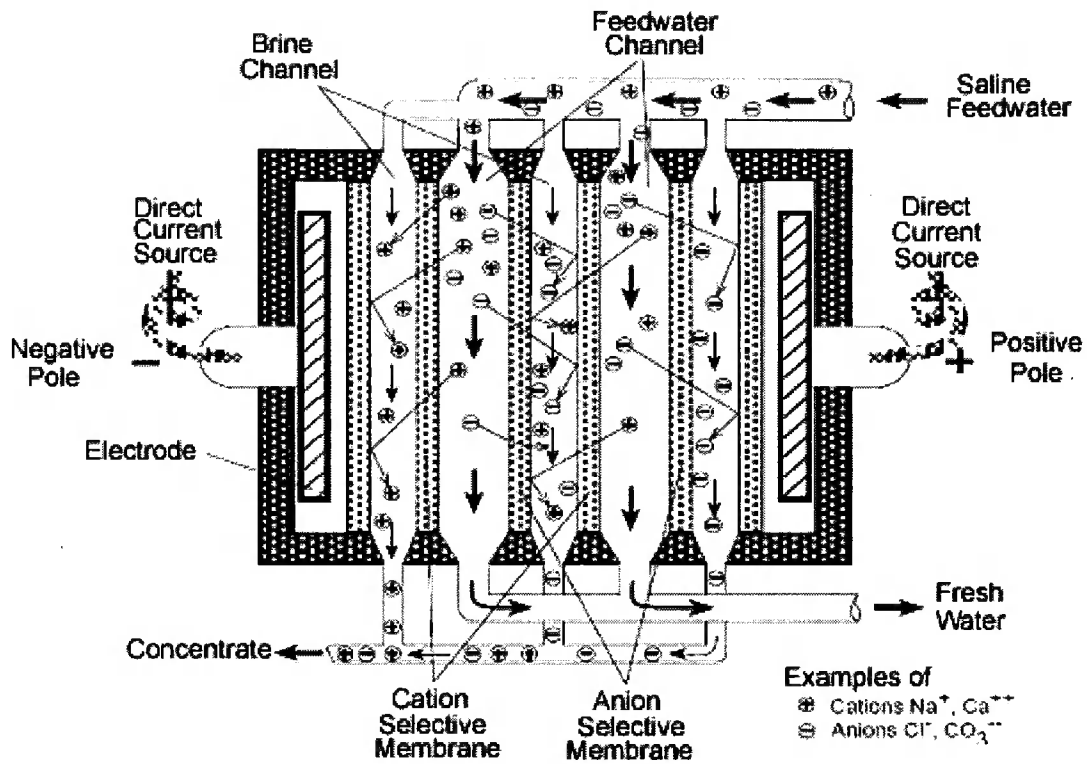
Figure 1-12: Movement of ions in the electrodialysis process –adapted from [14]

1.4.3 Membrane distillation (MD)

Membrane distillation was developed commercially on a small scale in the 1980s [13] but it has not achieved great commercial success. The process combines the use of distillation and membranes and is, essentially, an evaporation process. Saline water is warmed to enhance vapour production and this vapour is exposed to a membrane that can pass water vapour but not liquid water. After the vapour passes through the membrane, it is condensed on a cooler surface to produce fresh water. In the liquid form, the fresh water cannot pass back through the membrane, so it is collected as the fresh water product [14].

1.4.3.1 Advantages and disadvantages of MD

- The main advantages are its simplicity and the low temperature rise it requires to operate. These facilitate the use of membrane distillation in experimental solar desalting units. [1314].
- Membrane distillation requires more space than other membrane processes [14].

- Energy consumption is approximately the same as that of MSF and MED plants. [13, 14].

- The MD process requires that the feed water should be free of organic pollutants; this explains the limited use of this method. [13]

1.4.4 Economics of water desalination using membrane processes.

The cost of membrane desalination technology has steadily decreased from its commercial introduction in 1970s until today, despite rising energy prices. Recent developments in membrane materials, pumping and energy recovery systems have dramatically reduced the energy consumption in RO desalination processes as shown in Figure 1.13 [35, 36].
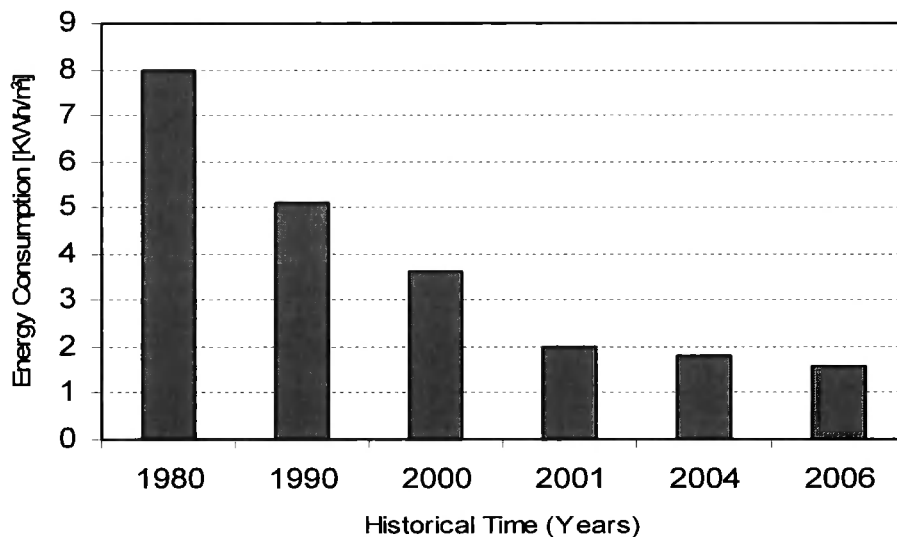
Figure 1-13: Development of achievable energy consumption in RO desalination processes.

The cost of water desalination in membrane processes varies according to the type and composition of the feed water. Large scale RO plants can use brackish water containing total dissolved solids (TDS) of from 2000 ppm to 10,000 ppm [37] but, as TDS concentrations increase, the unit cost of the desalinated water also increases. The cost of brackish water desalination in Jordan with a TDS concentration of 2300 ppm is 0.26$/m^3 while in Florida for brackish water with a TDS of 5000 ppm it is 0.27$/m^3 [38]. In small scale RO units, the costs are greater. For example, the cost of a desalination unit of 1000 m^3/day ranges from 0.78$/m^3 to 1.23$/m^3 [39&40] or even 1.33$/m^3 [41].

For the desalination of seawater, the RO method has been used more and more in recent years, as the cost of membranes has fallen but it is still costly [42]. For instance, the estimated water production cost for the world's largest RO seawater desalination plant at Ashkelon in Israel with a capacity of 320,000 m^3/day was 0.52US$/$m^3$ in 2007 [43] and costs at an RO plant with a capacity of 94,600 m^3/day in Tampa Bay in USA was reported to be at $0.56/$m^3$ [44]. Table 1.3 shows typical costs for RO desalination of brackish water and seawater. [45]

Type of feed water	Capacity of desalination plant (m^3/day)	Desalination cost per m^3 (US$)
Brackish water	Less than 20	5.63 – 12.9
	20 – 1200	0.78 – 1.33
	40,000 – 46,000	0.26 – 0.54
Seawater	Less than 100	1.5 – 18.75
	250 – 1000	1.25 – 3.93
	15,000 – 60,00	0.48 – 1.62
	100,000 – 320,000	0.45 – 0.66

Table 1-3: Cost of desalinated water in membrane (RO) plants

1.5 Renewable energy desalination

The coupling of renewable energy sources and desalination such as solar, wind and geothermal energy with desalination systems holds great promise for tackling water scarcity. An effective integration of these technologies will allow countries to address water shortage problems with a domestic energy source that does not produce air pollution or contribute to the global problem of climate change due to lower conventional energy consumption and lower gas emissions. Meanwhile the cost of desalination and renewable energy systems are steadily decreasing, while fossil fuel prices are rising and its supplies are being depleted. The desalination units powered by renewable energy systems are uniquely suited to provide water and electricity in remote areas where water and electricity infrastructures are currently lacking [46].

The majority of desalination systems that use a renewable energy source can be divided into three categories: wind, solar (photovoltaics or solar collectors) and those that use geothermal energy. These renewable energy sources can be coupled with thermal distillation or membrane desalination systems as shown in Figure 1.14 to

produce water. In some cases [47] these systems are connected with a conventional source of energy (e.g. local electricity grid) in order to minimize the variations in the level of energy production and consequently water production. [45]. When renewable energy sources are used to operate the RO plants, the cost was found to dramatically increase to (10.32$/m^3), due to the fact that the output efficiency of renewable energy devices is low and the capital cost is very high [48].Hence, new developments in renewable energy should provide more reliable devices at lower cost in the future.

```
                    ┌ ─ ─ ─ ─ ─ ─ ─ ─ ─ ─ ─ ┐
                    I Renewable Energy Resources I
                    └ ─ ─ ─ ─ ─ ─ ┬ ─ ─ ─ ─ ─ ─ ┘

      Geothermal              Solar                    Wind

   ┌─────┴─────┐        ┌──────┴──────┐              Electricity
  Heat    Electricity  PV      Solar Thermal              │
   │          │         │   ┌────┬──────┐                 │
  MSF        RO      Electricity Direct  Solar            RO
  MED        ED          │    Process  Collectors         ED
  VC         MD         RO       │    ┌────┐               MD
  MD                    ED      SD    MSF
                        MD      HD    MED
                                      VC
                                      MD
```
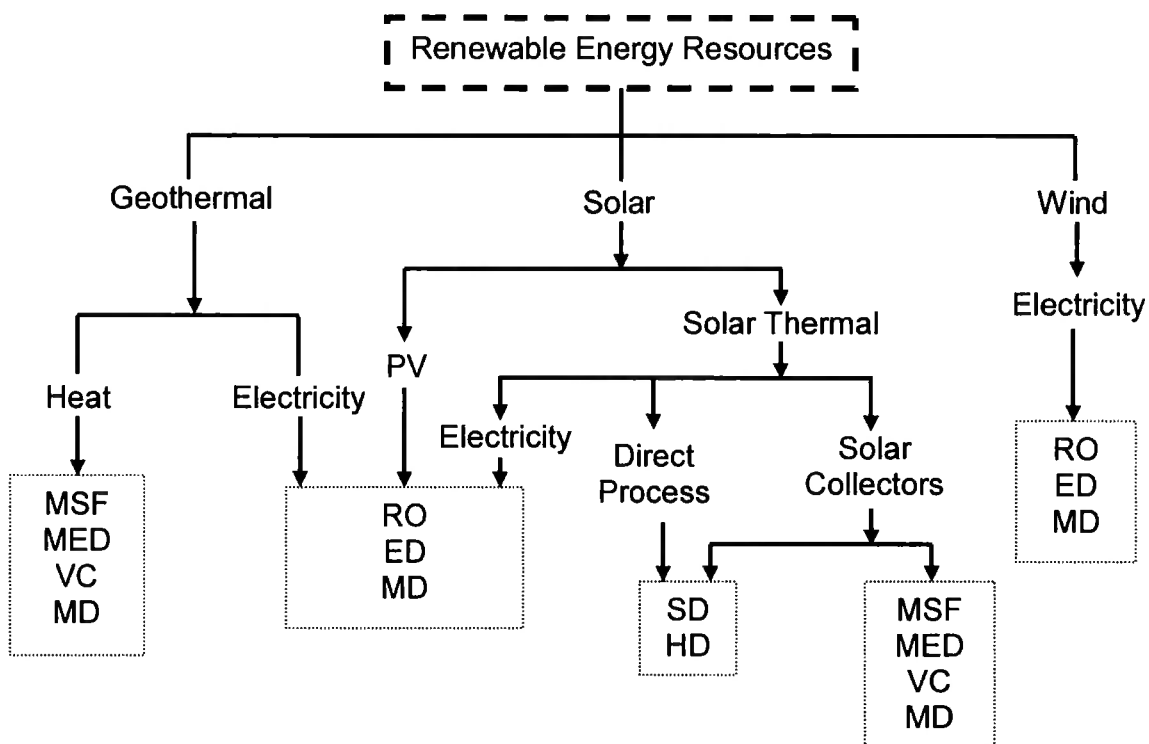
Figure 1-14: Combinations of renewable energy resources with water desalination technologies adapted from [47].

1.5.1   Solar powered water desalination

1.5.1.1 Introduction to solar energy

The sun was adored by many ancient civilizations as a powerful God and solar energy is the oldest energy source used by human beings. The first known practical application was in drying for food preservation.

Scientists have long looked at solar radiation as a source of energy, trying to convert it into a useful form for direct utilization. Archimedes, the Greek mathematician and philosopher (287–212 BC), used the sun's reflected heat to burn the Roman fleet in the Bay of Syracuse [49]. During the 18th century, the French naturalist Boufon experimented with various solar energy devices which he called 'hot mirrors burning at long distance [50].

Most forms of energy are solar in origin. Oil, coal, natural gas and wood were originally produced by photosynthetic processes [51]. Even wind and tide energy have a solar origin since they are caused by differences in temperature in various regions of the earth. The great advantages of solar energy, compared with other forms of energy, are that it is clean, sustainable and can be used without any environmental pollution.

Solar energy is used to heat and cool buildings, to heat water for domestic and industrial uses, to heat swimming pools, to power refrigerators, to operate engines and pumps, to desalinate water for drinking purposes, to generate electricity, in chemistry applications, and for many more functions.

The decision about which source of energy to use should be made on the basis of economic, environmental and safety considerations. Because of its desirable environmental and safety advantages, it is widely believed that, where possible, solar energy should be utilized instead of energy derived from fossil fuels, even when the costs involved are slightly higher [52]. This section focuses on the desalination of saline water by using solar energy.

1.5.1.2 Introduction to water desalination by solar power

Solar water desalination has a long history. The first documented use of solar stills was in the sixteenth century and, in 1872, the Swedish engineer, Carlos Wilson, built a large-scale solar still to supply a mining community in Chile with drinking water [53].

Solar desalination using humidification and dehumidification is a promising technique for producing fresh water, especially in remote and sunny regions. It has the potential to make a significant contribution to providing humans with fresh water using a renewable, free and environmentally-friendly energy source [54].

Solar energy can be used to convert saline water into fresh water with simple, low cost and economical technology and thus it is suitable for small communities, rural areas, and areas where the income level is very low [55]. Recent developments have demonstrated that solar powered desalination processes are better than the alternatives, including electrodialysis, reverse osmosis and freezing, for fresh water provision in remote rural areas [56].

Solar powered desalination processes are generally divided into two categories, direct and indirect systems.

1.5.1.3 Direct systems

The direct systems are those where the heat gaining and desalination processes take place naturally in the same device. The basin solar still represents its simplest application, the still working as a trap for solar radiation that passes through a transparent cover.

Solar Still

Solar still distillation represents a natural hydrologic cycle on a small scale. The basic design of a solar still, which is similar to a greenhouse, is shown in Figure 1.15. Solar energy enters the device through a sloping transparent glass or plastic panel and heats a basin of salt water. The basin is generally black to absorb energy more efficiently. The heated water evaporates and then condenses on the cooler glass panels. The condensed droplets run down the panels and are collected for use as fresh water.

Experience proves that about $1m^2$ of ground will produce 3 - 4 litres per day of freshwater Because of this low production, it is important to minimize capital costs by using very inexpensive construction materials. Efforts have been made by various researchers to increase the efficiency of solar stills by changing the design, by using additional effects such as multi stage evacuated stills and by adding wicking material, etc. and these modifications have increased production per unit area [14].

In the simple solar still shown in Figure 1.15, the latent heat of condensation is dissipated to the environment. However, the latent heat of condensation can be used to preheat the feed water, and this obviously leads to an improvement in the still efficiency.
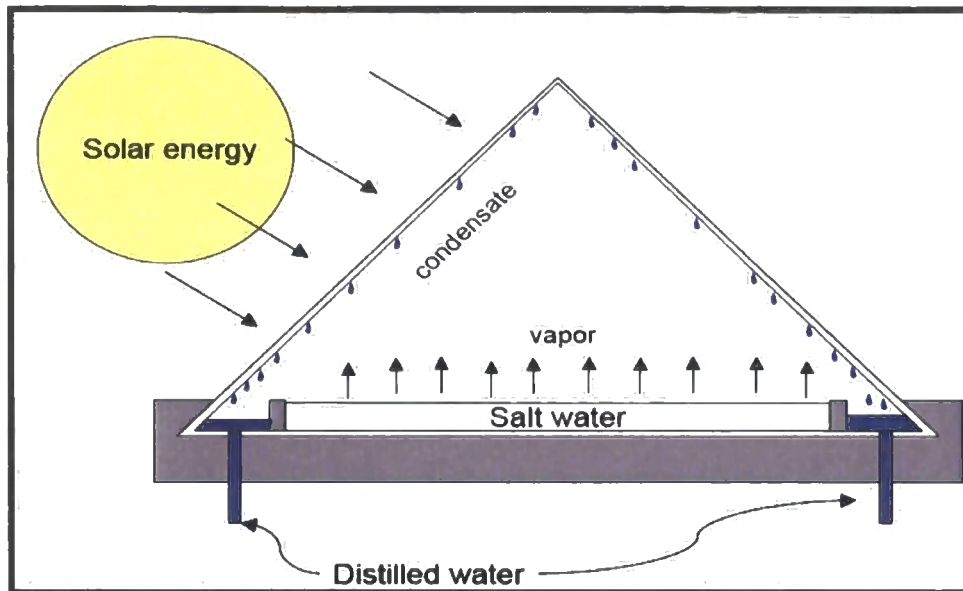
Figure 1-15: Solar Still Unit [64]

Advantages and disadvantages of solar still

Solar still technology requires a large area for solar collection so it is not viable for large-scale production, especially near a city where land is scarce and expensive.

The comparative installation costs tend to be considerably higher than those for other systems. They are also vulnerable to damage by weather.

Labour costs are likely be high for routine maintenance to prevent scale formation and to repair vapour leaks and damage to the still's glass. [14, 64]

However, they can be economically viable for small-scale production for households and small communities, especially where solar energy and low cost labour are abundant [14, 55].

1.5.1.4 Indirect systems

In these systems, the plant is separated into two subsystems, a solar collector and a desalination unit. The solar collector can be flat plate, evacuated tube or solar concentrator. and can be coupled with any of the distillation unit types described previously which use the evaporation and condensation principle. Systems that use photovoltaic (PV) devices tend to generate electricity to operate RO and ED desalination processes [64].

There are many factors that influence the selection of solar collectors for desalination processes. Flat plate and evacuated tube solar collectors are appropriate for low temperature processes which use heat to evaporate the saline water, often utilizing low pressure conditions created with vacuum pumps. Evacuated tube collectors ensure some energy even on cloudy days, and their efficiency at high operating temperatures or low insolation is significantly better than that of flat plate collectors.

Cylindrical tracking collectors can be more efficient than evacuated tube collectors, but have almost no output on cloudy days and collect only a small fraction of the diffuse radiation. Parabolic concentrating collectors require very accurate two-axis tracking mechanisms but they can produce temperatures of more than 120 °C, which is higher than the temperature needed for solar desalination [57].

In order to increase still productivity many researchers have experimented with coupling single still or multi effects stills with solar collectors as shown in Figure 1.16 and Figure 1.17 respectively. Coupling solar stills with such solar collector panels produces an increase in efficiency through utilizing the latent heat of condensation in each effect to deliver heat to the next stage.
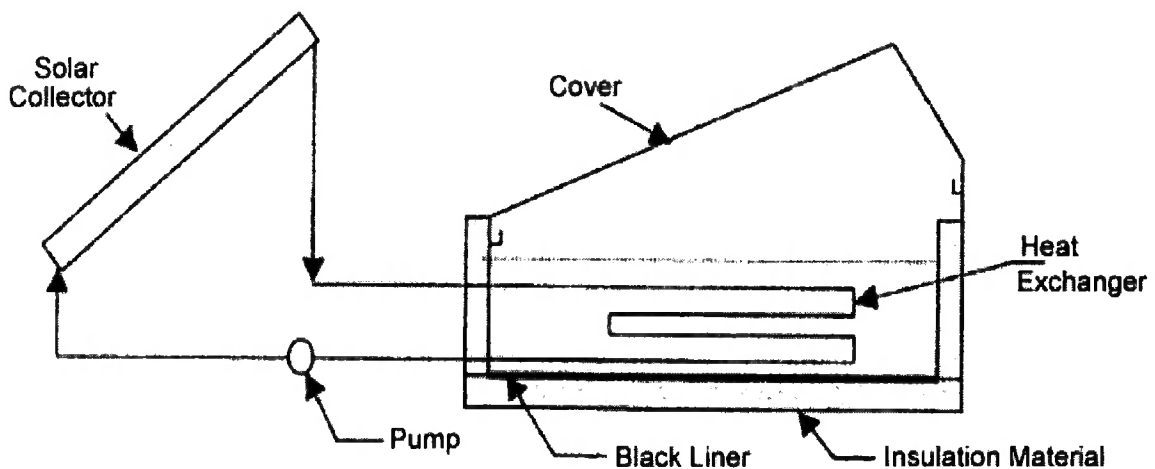
Figure 1-16: Schematic diagram of a single solar still coupled with solar collector [2]
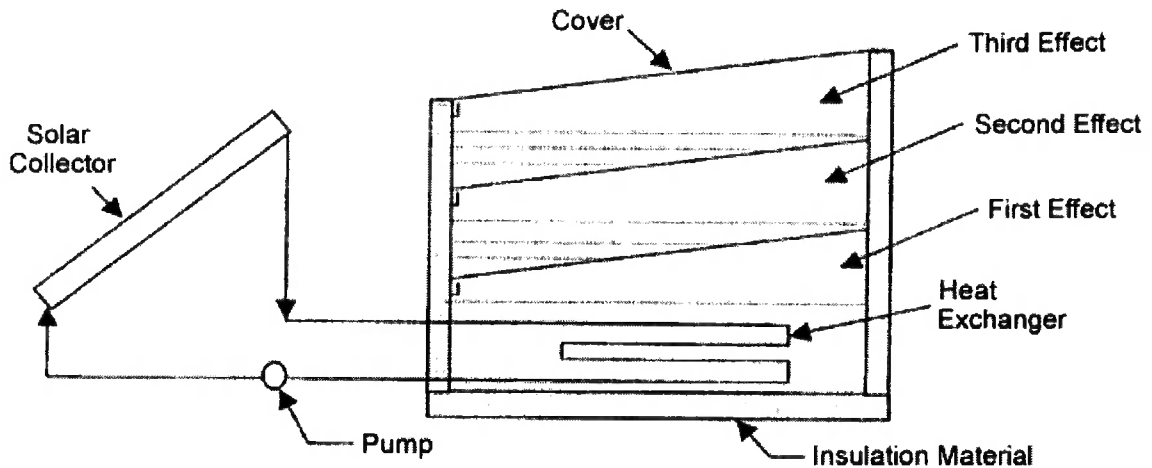
Figure 1-17: Schematic diagram of multi effect solar still coupled with solar collector [2]

1.5.1.4.1 Solar Humidification and Dehumidification

Potable water may be obtained from saline water through a humidification-dehumidification cycle. In this process, saline water is evaporated by thermal energy and the subsequent condensation of the generated humid air, usually at atmospheric pressure, produces freshwater [58]. Air has the capability to hold large quantities of water vapour and its vapour carrying capability increases with temperature [59].

Many studies on desalination with humidification–dehumidification have been conducted with a variety of fabricated devices [60].

- **Solar distillation method**

The principle of this desalination process is based on the evaporation of water and the condensation of steam from humid air. The humid air flows in a clockwise circuit driven by natural convection between condenser and evaporator, as shown in Figure 1.18. The evaporator and condenser are located in the same thermally insulated box. Seawater is heated in the evaporator and distributed slowly as trickles downwards. The air moves in a countercurrent flow to the brine through the evaporator and becomes saturated with humidity. Partial evaporation cools the brine that is left in the evaporation unit and it now has a higher salt concentration, while the saturated air condenses on a flat plate heat exchanger.
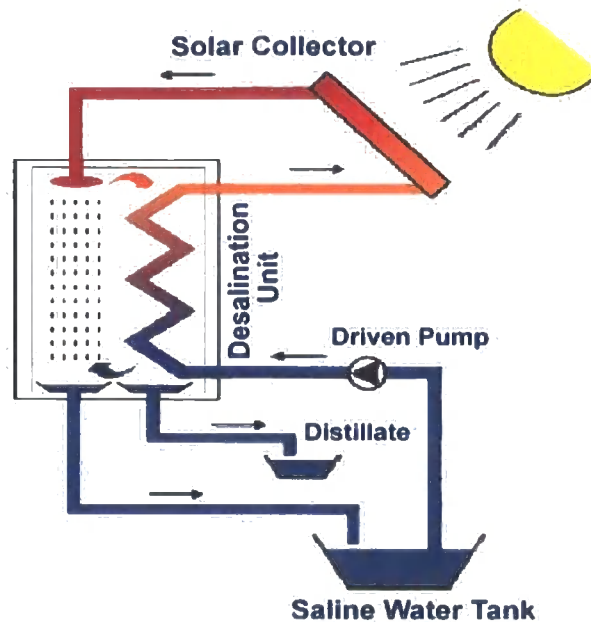
Figure 1-18: Schematic diagram of distillation system – adapted from [61]

The distillate runs down the plates and trickles into a collecting basin. The heat of condensation is mainly transferred to the cold seawater flowing upwards inside the flat plate heat exchanger. Thus the temperature of the brine in the condenser rises from 40°C to approximately 75°C. In the next step, the brine is heated to the evaporator inlet temperature, which is between 80-90 °C. The salt content of the brine as well as the condenser inlet temperature can be increased by a partial reflux from the evaporator outlet to the brine storage tank [61]. Then the distillate can be collected in a vessel whilst the brine goes to the saline water tank to recover a portion of its heat.

1.6 Alternative processes

A number of other processes have been used in water desalination but none has achieved as high a productive performance or reached the same level of commercial success as the MSF, ED and RO processes. They may prove valuable under special circumstances or after further research and development.

1.6.1 Freezing

Extensive commercial research was undertaken during the 1950s and 1960s to improve the performance of the freezing process. The basic principles of freezing

desalination are simple. During the process of freezing, dissolved salts are excluded during the formation of ice crystals. Seawater can be desalinated by cooling the water to form crystals under controlled conditions. Before the entire mass of water has been frozen, the mixture is usually washed and rinsed to remove the salts in the remaining water or adhering to the ice crystals. The ice is then melted to produce fresh water [14]. The main heat transfer processes, that is freezing and melting, are regenerative, resulting in very high-energy efficiency [62].

A small number of plants have been built over the past 40 years but the process has not been a commercial success in the production of fresh water for municipal purposes. The most recent significant example of desalting by freezing was an experimental solar-powered unit constructed in Saudi Arabia in the late 1980s but that plant has been disassembled. At present, freezing technology probably has better applications in the treatment of industrial wastes than in the production of municipal drinking water [14, 20].

1.6.1.1 Advantages and disadvantages

- The advantages include a lower theoretical energy requirement, minimal potential for corrosion, and little scaling or salt precipitation.

- It can produce very pure potable water and it has special advantages to produce water for irrigation [62].

- The disadvantage is that it involves handling ice and water mixtures that are mechanically complicated to move and process [14].

1.6.2 Ion exchange - solvent process.

In the last 50 years, ion exchange membranes have been moved from a laboratory tool to industrial products with significant technical and commercial impact. Today, ion exchange membranes are receiving considerable attention and are successfully applied in the desalination of sea and brackish water and in treating industrial effluents. They are efficient tools for the concentration or separation of food and pharmaceutical products containing ionic species as well as in the manufacture of basic chemical products [63].

Ion exchangers are organic or inorganic solids that are capable of exchanging one type of cation (or anion) immobilized in the solid for another type of cation (or anion) in solution. For example, Na^+ ions in solution can be replaced with H^+ by a cation exchanger and Cl^- can subsequently be replaced with OH^- by an anion exchanger resulting in the complete "demineralization" of a NaCl solution. The process can be reversed by regenerating the cation exchanger with an acid, and the anion exchanger with a base. In practice, ion exchange is a useful process for completely demineralizing water in applications where high purity is required, as in high-pressure boilers. Unfortunately, it is not suited to treat and desalinate brackish or sea water, simply because it is costs are prohibitive [64],65].

2   Overview of Water Situation in Gaza Strip

2.1   Introduction

The Gaza Strip covers an area of 365 km^2 and has one of the highest densities of population in the world at nearly 4,000 persons/km^2 [66]. Most of its people are refugees who fled their homes in areas now controlled by Israel in the 1948 and 1967 Arab–Israeli wars.

There is now a water crisis in Gaza Strip. According to one estimate, approximately 160 million cubic meters (MCM) of water is pumped from the coastal aquifer per year, but the sustainable yield of this subaquifer is about 100 MCM/year [67]. Moreover, most wells in the area produce nonpotable water by the standards of World Health Organization [67]. Because of the depletion of water and the declining economic situation, the Gaza Strip is now suffering from environmental problems such as salination of fresh water, contamination of underground water resources, lack of adequate sewage treatment, desertification, soil degradation and depletion, and water-borne diseases. Besides salts, which cause kidney disease, nitrates from solid waste and fertilizers are the most common water contaminants. The nitrates cause blue baby syndrome [67].

In spite of the fact that these problems are caused by the depletion of water, it should be noted that the Gazan people consume 70 litres per capita per day, while the World Health Organization and the United States Agency for International Development agree that the minimum human consumption for public health and hygiene purposes is 100 litres per capita per day [67]. As the population in Gaza Strip increases (population growth rate is 3.77% a year [71]), the consumption of water and energy will increase and the deficit in water supply and energy resources will also rise, leading to severe health and economic crises that will result in a significant rise in the probability of a health disaster and/or an outbreak of conflict.

Gaza enjoys sunny weather throughout the year, with an annual daily average solar insolation of 542W/m^2 [114], as shown in Figure 2.1. Solar thermal applications are widely used and the population is familiar with solar collectors for domestic purposes. However, solar power is not used in Gaza for water production, unlike most Middle East

countries where many desalination plants have been constructed to solve the water scarcity [3], Hence the use of solar power for the desalination of seawater could be considered to have great potential for tackling the water problems in Gaza.

Obviously, this critical water situation requires immediate and urgent action to improve the quality and quantity of the water supply[68]. The development and use of small-scale household solar desalination systems could prove a quick and feasible way to bring about some improvement.

Solar Radiation (W/m^2) for Year, 2004

	Jan	Feb	Mar	Apr	May	Jun	Jul	Aug	Sep	Oct	Nov	Dec
▣ Monthly Average Daily (W/m2)	360	427	568	603	613	687	717	659	593	513	395	373
▢ Monthly Max Average Daily (W/m2)	472	549	677	745	705	757	789	784	723	600	510	478
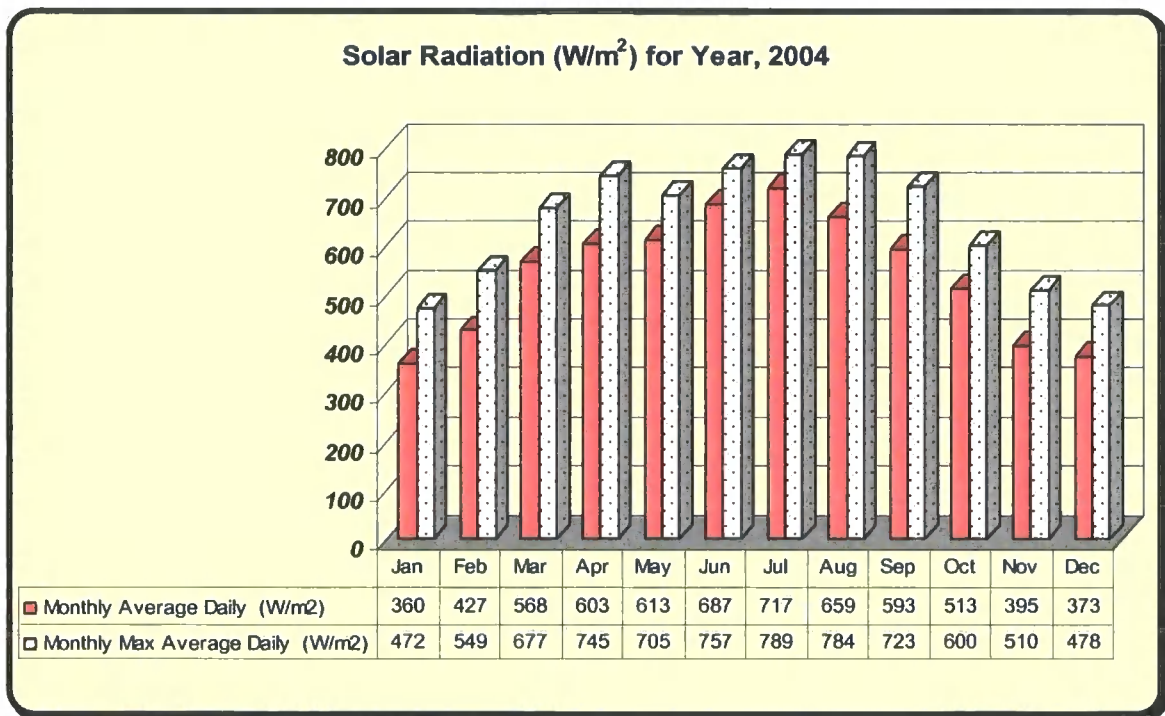
Figure 2-1: Average daily solar radiation for year 2004

2.2 Geographical location.

The Gaza Strip is a part of the coastal plain in the south west of Palestine, where it forms a long and narrow rectangle, approximately 45 km in length and about 8 km wide, giving an area of about 365 km^2. Its shows desert characteristics, bounded by the Negev Desert to the south east and the Sinai Desert to the south west. This information is illustrated in Figure 2.2.
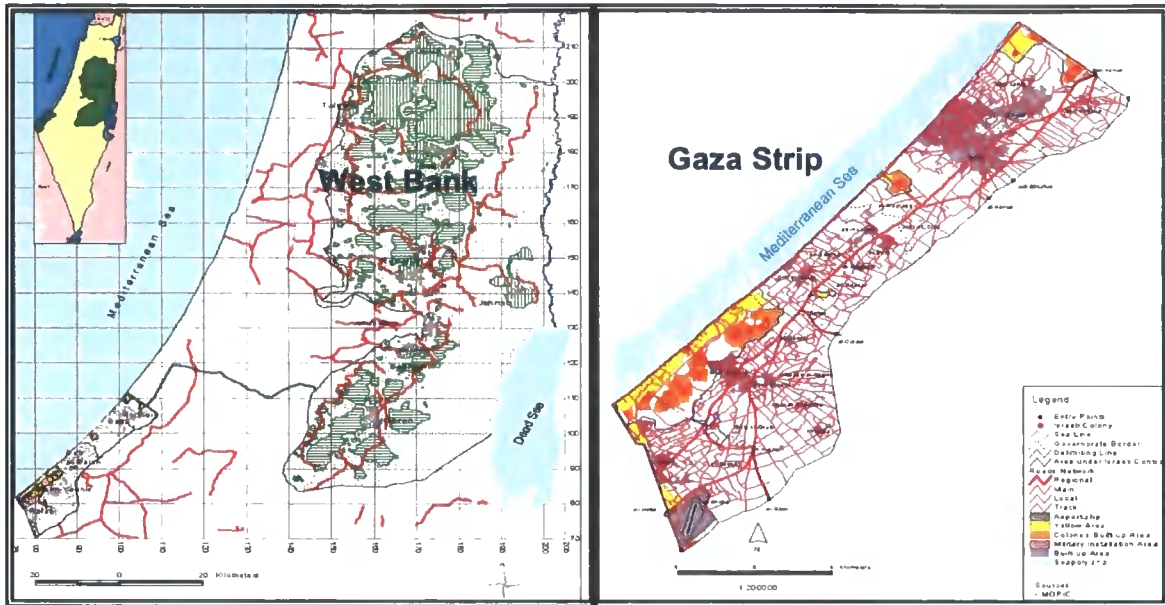
Figure 2-2: Gaza Strip Base Map

2.3   Climate and Rainfall

The Gaza Strip is located in the transitional zone between the arid desert climate of the Sinai Peninsula and the temperate and the semi-humid Mediterranean climate along the coast.

The average daily mean temperature ranges from 25°C in summer to 13°C in winter. Average daily maximum temperatures range from 29°C to 17°C and minimum temperatures from 21°C to 9°C in the summer and winter respectively, as shown in Figure 2.3.

The average annual rainfall varies from 450mm/year in the north to 200mm/year in the south. Most of the rainfall occurs in the period from October to March, with the rest of the year being almost completely dry. With regard to the evaporation of surface water, maximum values in the order of 140 mm/month are quoted for summer, while relatively low pan-evaporation values of around 70 mm/month were recorded during the months of December and January. The daily relative humidity fluctuates between 65% in the daytime and 85% at night in summer and between 60% and 80% in winter [69].
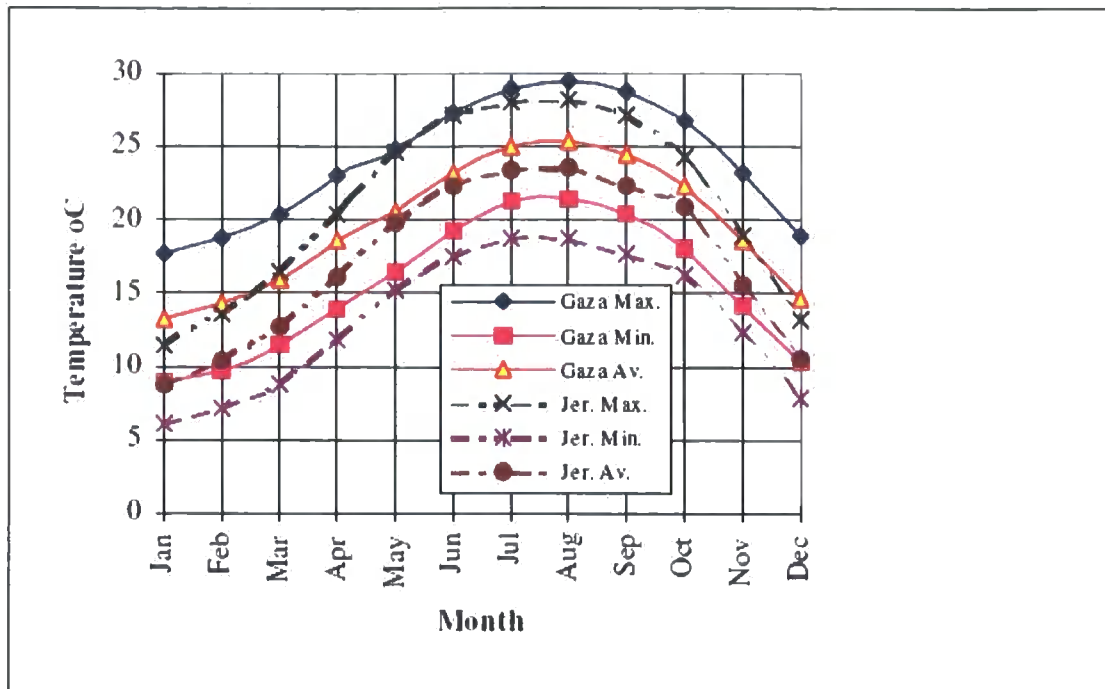
Figure 2-3: Annual monthly average variation in dry bulb temperature in both the Gaza and Jerusalem (1980 Minstry of Transport)

2.4   Water Situation

Gaza's water resources are essentially limited to that part of the coastal aquifer that underlies its $365km^2$ area. The coastal aquifer is the only aquifer in the Gaza Strip and is composed of Pleistocene marine sand and sandstone, intercalated with clayey layers. The maximum thickness of the different bearing horizons occurs in the northwest along the coast (150m) and decreases gradually toward the east and southeast along the eastern border of Gaza Strip to less that 10m, as shown in Figure 2.4.

The depth to the water level of the coastal aquifer varies between a few meters in the lowland area along the shoreline and about 70m along the eastern border. The coastal aquifer holds approximately $5x10^9m^3$ of groundwater of different quality. However, only $1.4 \times 10^9m^3$ of this is fresh water, with a chloride content of less than 500mg/L. This fresh groundwater typically occurs in the form of lenses that float on the top of the brackish and/or saline ground water. That means that approximately 70% of the aquifer is brackish or saline water and only 30% is fresh water [70].
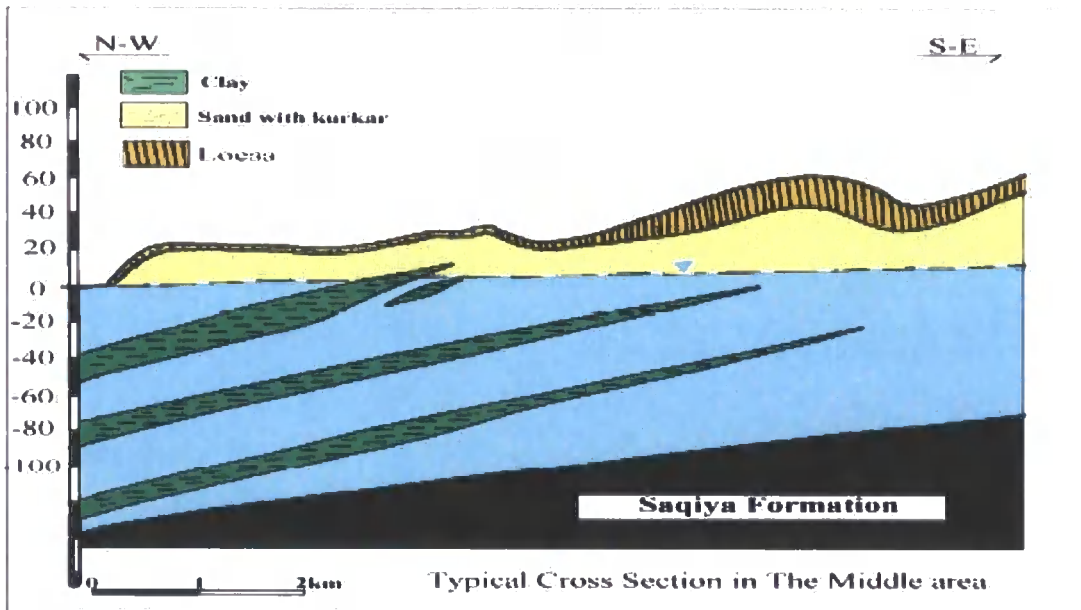
Figure 2-4: Typical hydrogeological cross section in the middle area of Gaza Strip

The quality of groundwater is as important as its quantity. All the groundwater contains salts in solution that are derived from the location and past movement of the water. In the last decades it has become clear that water resources are the most costly and vulnerable natural resources in the Middle East, especially in Gaza Strip with its extremely high population density. The estimated population in 2004 was around 1.30 million [71]. It is said to have the same population density as Manhattan, but without the skyscrapers.

There is no surface water (lakes or rivers) in the Gaza Strip so the only fresh water resource is ground water. At present, about 3,000 wells tap this water supply. Many years of over-pumping have resulted in seawater intrusion and upcoming of brine groundwater. Further human activities, like agriculture and industries have increased the pollution levels in the groundwater. The major environmental problem in the Gaza Strip is deteriorating water quality through salinization and pollution resulting from a deficit in the water balance. This problem covers the fresh groundwater in the shallow aquifer underlying the Gaza Strip. The major indicators for deterioration are increases in salinity (chloride) and nitrate concentration [72].

2.4.1 Brackish ground water in Gaza

The available fresh groundwater resources in the Gaza Coastal Aquifer that can be used for domestic uses and that comply with the recommended WHO guidelines in terms of water quality is in the range of 5-10% of the total aquifer capacity. At present, most of the domestic municipal water supply is far from the acceptable level. Figure 2.5 and Figure 2.6 show the chloride and nitrate concentration of the pumped water from the municipal wells [68].
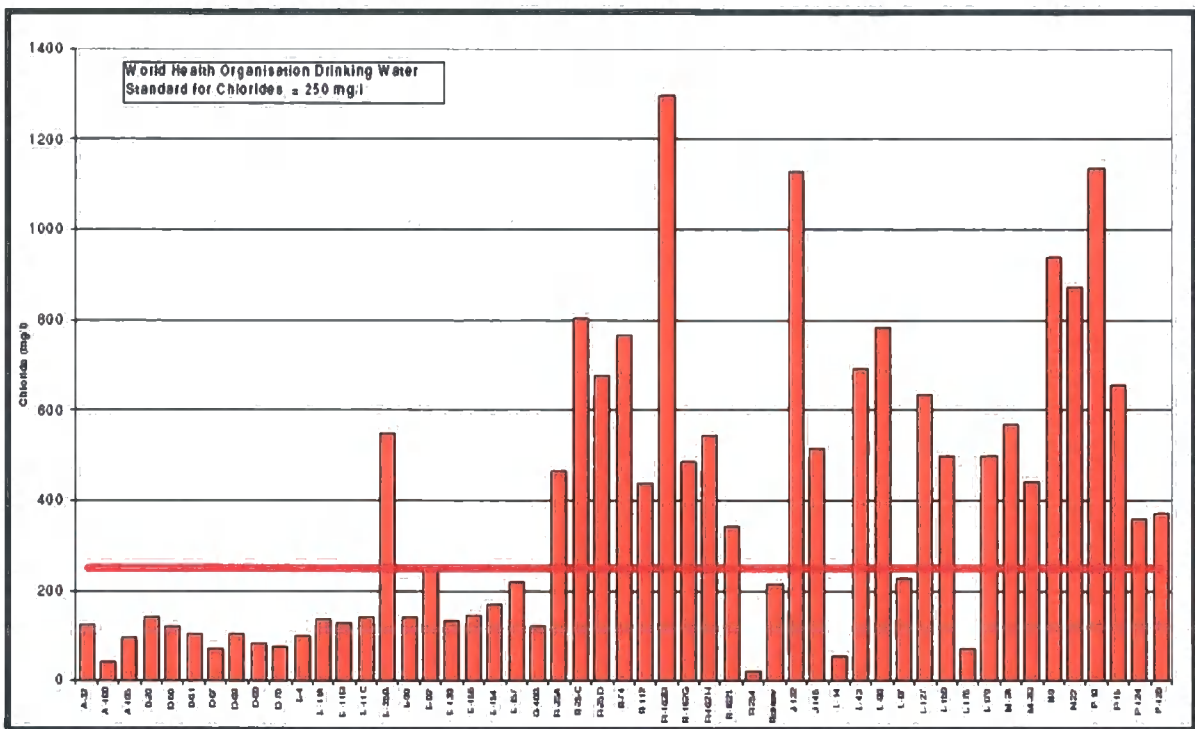
Figure 2-5: Chloride Concentration of Domestic Municipal Wells in Gaza
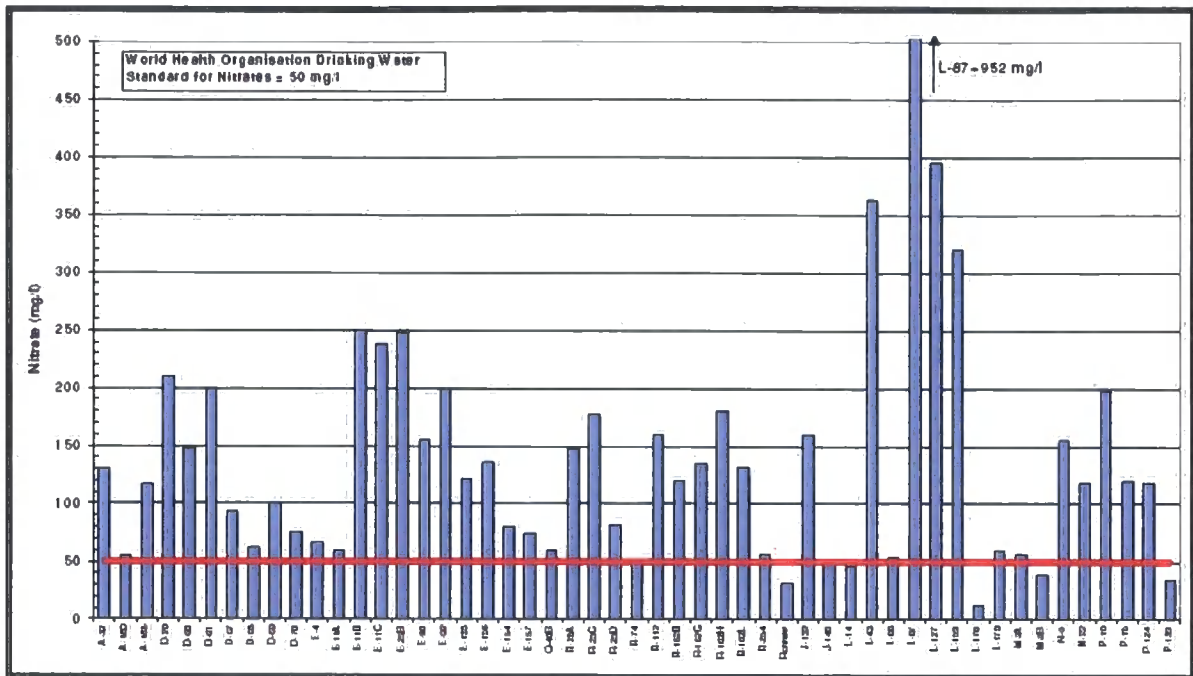
Figure 2-6: Nitrate Concentration of Domestic Municipal Wells in Gaza

2.4.2 Prospect of seawater desalination

In order to maintain the water balance and to fulfill the domestic water demand in terms of quality and quantity, new water resources need to be introduced into the Gaza Strip as soon as possible. Those new water resources would relieve stress on the aquifer and prevent further deterioration of its water quality. With the assumption of efficient comprehensive wastewater management in terms of the reuse of reclaimed wastewater for agriculture and recharging the surplus wastewater into the aquifer, the proposed water balance will be improved relatively and the total water deficit will be about 45 MCM/year in 2020 [68].

Many alternatives have been proposed to minimize the water deficit and fulfil domestic water demand in the Middle East region. Solar water desalination and the use of hydropower in desalination have been adopted in Jordan as the most feasible option to provide water for domestic and industrial sectors [73]. The decentralized small scale solar desalination units have been identified by the Palestinian Water Authority as the most realistic option [68]. This is especially true in politically unstable war regions with intermittent power and fuel supply like Gaza where there is water scarcity, and poverty but abundant solar radiation over the whole year.

3 Water Quality

3.1 Introduction

The composition of surface and ground waters is dependent on natural geological, hydrological and climatic influences in addition to human activity such as the recent dramatic expansion of industrial production. Increasing population density and urban expansion in many countries have led scientists and others to pay attention to the alarming pollution of water resources [74].

In the last few decades it has become clear that water resources are the most costly and vulnerable natural resource in the Middle East, and especially in the Gaza Strip where water resources have been depleted and water quality has deteriorated [69].

The major environmental problem in the Gaza Strip is deteriorating water quality through salinisation and pollution resulting from a deficit in the water balance in the shallow freshwater aquifer underlying the Gaza Strip. Human activities, like agriculture and industry, have increased the levels of pollution in this groundwater. The major indicators of deterioration are an increase in salinity, especially chloride and nitrate concentration. Other pollutants like hydrocarbons, heavy metals and pesticides may also be causing serious problems but little data are available on these.

At present about 3,000 wells tap this water supply. Many years of over-pumping have resulted in seawater intrusion and the upconing of brine groundwater. This means that approximately 70% of the Gaza aquifer is brackish or saline water and only 30% is fresh water [72].

Saline water may contain various pollutants such as biological, chemical and organic contaminants, though sodium and chloride make up the most of the total dissolved solids. For this reason, most of the desalination technologies would need pre-treatment and post-treatment based on the influent saline water characteristics and the nature of the desalination process. The influent water may be seawater or brackish ground water.

The importance of water quality depends on the actual and planned use of the water, such as for drinking, agricultural irrigation or industrial use. WHO, and other institutions worldwide, have established regulations and standards to protect human

health. For instance, drinking water should not contain any chemicals or micro organisms that could be hazardous to human heath or that could contribute to the outbreak of diseases.

Establishing water quality involves analyzing its physical, chemical and biological characteristics. These are usually expressed in terms of the concentration of organic and inorganic substances in the water [75].

This chapter looks at the physical and chemical contaminants and parameters of drinking water and possible biological contaminations, in addition to saline water classifications and the physical and chemical characteristics of seawater. It also discusses the water quality of various desalination processes by presenting some case studies for water quality from desalination plants.

3.2 Quality standards of drinking water

Water quality should satisfy the requirements or standards set for specific use. The main reason for monitoring water quality is to verify whether the observed water quality is suitable for its intended use, such as drinking [75]. There are many physical and chemical parameters but this research will focus on those adopted by WHO.

3.2.1 Alkalinity

Alkalinity in water is its capacity to neutralize acid, and the amount of strong acid needed to neutralize the alkalinity is called total alkalinity [75]. It can be defined as the sum of carbonates and bicarbonates, whilst the most convenient form in which to express alkalinity is in mg/L $CaCO_3$ equivalent, as in the following equation.

Alkalinity = $[HCO_3]$ + $2[CO_3^{2-}]$ (3-1)

In most natural water, pH ranges between 6 and 8. Hard water contains metal carbonates (mostly $CaCO_3$) and it is high in alkalinity.

High concentrations of sodium bicarbonate can cause taste problems and the level of alkalinity is also important in chemical coagulation because of the buffering capacity it imparts to the water [76, 82].

3.2.2 pH

pH can be defined as the concentration of hydrogen ions [H^+] in a solution and this can be expressed as:

pH = - log [H^+]   (3-2)

It is used as an indicator of the acidity or basic nature of a solution; the more acidic the solution, the lower the pH and the more basic, the higher the pH, [77]

The pH value of distilled water can be affected by the presence of carbon dioxide in the atmosphere and it can reach a slightly acidic pH-value within a couple of hours. It is worth mentioning that the pH of distilled water is difficult to measure. Not only does high-purity water rapidly pick up contaminants such as carbon dioxide (CO_2), as stated, but its low conductivity can affect the accuracy of pH meters. For instance, absorption of just a few ppm of CO_2 can cause the pH of ultra-pure water to drop to 4.5, although the water is still of essentially high quality

The most accurate estimation of the pH of ultra high quality (resistively = 1 − 18 $M\Omega.cm$) distilled water is obtained as a function of water resistively. Figure 3.1 shows the relationship between the resistance and pH which must lie between certain limits. For example, if the resistance is 10.0 $M\Omega cm$, the pH of distilled water must lie between 6.2 and 7.2 [78].
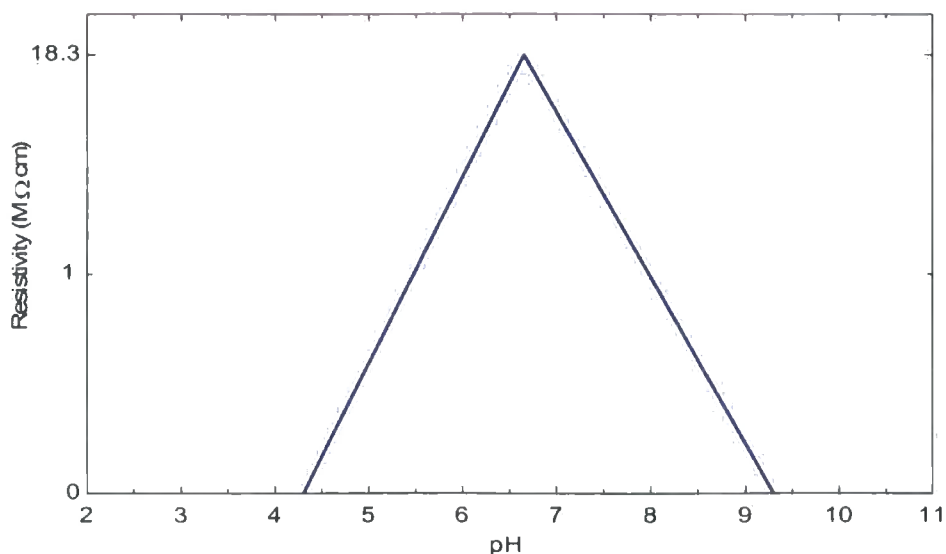
Figure 3-1: Electrical resistively versus pH of purified water

3.2.3 Electrical conductivity

Conductivity is the measurement of the ability of a solution to carry electric current. As this ability is dependent upon the presence of ions in solution, pure water, such as distilled water, has a very low specific conductance, and seawater has a high specific conductance. Thus a conductivity measurement of water is an indicator of its total dissolved solids. The unit of conductivity is μS/cm (micro-siemens per cm) [76]. According to Hem (1970), for most waters, a factor in the range 0.55-0.75 multiplied by conductivity gives a close approximation to the total dissolved solids in mg/L [79]

3.2.4 Hardness

Hardness can be defined mainly as the sum of calcium (Ca^{2+}) and magnesium (Mg^{2+}) ions present in water. These are the predominant cations in natural waters. Calcium usually enters the water either as calcium carbonate ($CaCO_3$) in the form of limestone and chalk, or calcium sulphate ($CaSO_4$), or in the form gypsum or anhydrate. The predominant source of magnesium is dolomite ($CaMg(CO_3)_2$). The sum of calcium and magnesium is called the total hardness, which is expressed in units of ppm (parts per million). Table 3.1 illustrates the classifications of hard water [75].

Description	Hardness range (equivalent mg/L CaCO₃)
Soft	0-75
Moderately Hard	75-100
Hard	100-300
Very hard	>300

Table 3-1: Hard water classifications [76]

Hardness poses many problems such as the difficulty in obtaining lather when washing with soap, and scaling where calcium and magnesium carbonates precipitate in tubes and heaters, causing equipment damage as a result of high temperatures. But hardness can be solved by softening processes [76, 82].

3.2.5 Total suspended solids

Suspended solids are solid materials, organic and inorganic, suspended in the water as a result of erosion from urban runoff and agricultural land, and industrial waste.

It is also the measurement of the dry-weight of particles trapped by a standard glass filter, typically of a specified pore size of 0.45 microns.

This problem can be solved and treated during the pre-treatment stage through sedimentation and filtration [80, 82].

3.2.6 Total Dissolved solids (TDS)

TDS in drinking-water originate from natural sources, sewage, urban run-off and industrial wastewater. It is an expression of all inorganic and organic substances contained in a liquid. It can also be defined as the substances remaining after evaporation and drying of a water sample minus the suspended solids, as defined above [81]. Meanwhile it can be calculated mathematically as shown in the following equation but it should be less than the measured TDS [75].

The calculated TDS = 0.60 (Alkalinity) + Na^+ + K^+ + Ca^{2+} + Mg^{2+} + Cl^+ + SO_4^{2+}
+ SiO_3 + NO_3^- + F^- + any other dissolved ions   (3-3)

TDS is used as an indication of the aesthetic characteristics of drinking water and as an aggregate indicator of the presence of a broad array of chemical contents in terms of salinity. A high TDS count is likely to cause technical problems such as scaling in pipes and damage to equipment [82].

3.2.7 Turbidity

Turbidity is the suspension of fine colloidal particles that do not readily settle out of solution and so can result in "cloudiness". It is determined by a nepholometer that measures the relative amount of light able to pass through a solution. Turbidity is reported as NTU (Nepholometric Turbidity Units). Typical reverse osmoses process element warranties list a maximum of 1.0 NTU for the feed water [82].

3.2.8 Chloride

Chlorides, compounds of chlorine with another element or radical, are present in nearly all natural waters. Concentrations can vary widely, but the highest concentrations are with sodium (NaCl) and, to a lesser extent, with calcium and magnesium.

Chlorides are one of the most stable components in water, and concentrations are unaffected by most of natural physiochemical or biological processes. In addition NaCl is a strong electrolyte and it has a high solubility in water [83]; in seawater, chlorides represent more than 55% of TDS. A high chloride concentration may indicate pollution from sewage or industrial wastes or the intrusion of seawater into an aquifer, as in the Gaza Strip. The WHO standard for chloride in drinking water is a maximum of 250 mg/L.

The salty taste of water is caused by the ions associated with chlorides. For sodium, the taste can be detected when the chloride concentration is at about 250mg/L while, for calcium and magnesium, the taste may be undetectable even at a chloride level of 1000mg/L. A high concentration of chloride has a corrosive effect on metal pipes and is harmful to plants [75].

3.2.9 Sodium

The sodium ion is ubiquitous in water owing to the high solubility of its salts and the abundance of mineral deposits. Concentrations vary from negligible in fresh water to high in seawater and brackish water. Seawater contains more than 10 g/L of sodium. The highest levels of sodium in fresh water are found in groundwater [75].

High levels of sodium are associated with groundwater in areas where there is an abundance of sodium mineral deposits or where there has been contamination from seawater intrusion, as is the case in Gaza [72].

3.2.10 Sulphate:

Sulphate is naturally abundant in the earth's crust and industrial wastes, mine drainage and the breakdown of sulphur compounds may contribute to high concentrations of sulphate in water. However, it is considered one of the least toxic anions in water, and consequently the UK and EU standard for sulphate concentrations is 250 mg/L, above which it can cause diarrhea [75].

3.2.11 Magnesium

Magnesium is one of the earth's most common elements and it forms highly soluble salts. It contributes to both carbonate and non-carbonate associated with granite

or silicates and it increases hardness in water [75].

Excessive concentrations of magnesium are undesirable in domestic water because of scale formation problems and also because magnesium has a cathartic and diuretic effect, especially when associated with high levels of sulphate. The maximum permissible value is 50mg/L according to the UK drinking water standards. Most drinking water from wells in the Gaza Strip contains varied magnesium concentrations less than 100 mg/L [72].

3.2.12 Calcium

Calcium is found in most natural waters and its level depends upon the type of rock through which the water has passed. Usually it is present as carbonate or bicarbonate and sulphate, although in waters of high salinity, calcium chloride and nitrate can also be found. Only $CaCO_3$ + $CaNO_3$ contribute to the hardness of water.

Calcium is an essential part of the human diet. However, the nutritional value from water is likely to be minimal compared to that from other food sources. There is no health objection to a high calcium content in water and the main limitations are made on the grounds of excessive scale formation [75]. The WHO recommends a maximum level of 200 mg/L as Ca (500 mg/L expressed as equivalent $CaCO_3$), above which deposition in water systems can cause major problems.

The calcium concentration in the most of the drinking wells in the Gaza Strip is less than 100 mg/L, which means that most of this water is suitable for drinking as far as the calcium compound is concerned [72].

3.2.13 Potassium

Potassium is a relatively common element in water. Concentrations are normally less than 20mg/L in most groundwater but in brine and seawater it is about 380 mg/L. The maximum permissible value is 12 mg/L according to the UK drinking water standards. It can be measured by the flame photometry method [75].

3.3   Microbiological contamination

An important aspect of drinking water is its microbiological quality. It is of particular significance because many types of disease can be transmitted to humans via

pathogenic microorganisms or parasites in drinking water. Pathogenic organisms are highly dangerous to human health [85].

The three types of micro-organisms that can be found in water are viruses, bacteria and protozoa and these are responsible for outbreaks of hazardous diseases, as shown in Table 3.2 [84]. In addition there can be fungi and algae.

Waterborne diseases	Bacterial	Salmonella (typhoid), Enterobacteria (E.coli, Campylobacter), Cholera, Leptospirosis, etc.
	Viral	Hepatitis A, Poliomylitis, Rotaviruses, Enteroviruses
	Parasitic	Amoebiasis, Giardiasis, Intestinal Protozoa, Balantidium coli.

Table 3-2: Water Borne Diseases [72]

Source: Linda and Briola, 1989

Furthermore, there are a huge number of microbial contaminants and types of pathogens that can cause water contamination, and it is difficult to set standards for individual pathogens [69]. Generally, around the world, faecal coliforms and coliforms groups are used as indicators of the presence of microbial contamination in water and they have been adopted by WHO, UK and EU standards bodies as the most effective indicator of microbiological contamination [85].

Since groundwater is the main source of drinking water in the Gaza Strip and since groundwater is protected from direct pollution from the land surface, it is unlikely that most pathogens and micro-organisms that cause diseases will be found there, especially in the deep aquifer supplying municipal wells. Moreover, all the Gazan municipal water wells are equipped with a disinfection system using the chlorination process [72].

3.4 Saline water classification

Saline water is water that contains significant concentrations of dissolved solids and especially sodium chloride. Nevertheless it can be utilized as fresh water for drinking and crop irrigation after treatment.

As shown in Table 3.3 [86], the United States Geological Survey (USGS) classifies saline water in three categories based on the concentration of total dissolved solids (TDS), expressed as (ppm)

Saline Water Type	TDS - Concentration (ppm)
Slightly saline water	1,000 to 3,000
Moderately saline water	3,000 to 10,000
Highly saline water	10,000 to 35,000

Table 3-3: Saline water classification

3.5 Physical and chemical characteristics of seawater

Seawater contains various dissolved solids that originate from natural sources, erosion of the earth's crust, sewage, urban run-off and industrial wastewater. All of these elements contribute to increasing the density of seawater, which is 1,030 kg/m^3 while fresh water is 1,000 kg/m^3.

The average seawater salinity is about 34,482 mg/L or may be slightly higher and the concentrations of the major salts in seawater are constant for the connected oceans and seas. 99.29% of seawater salts are made up of six elements and compounds: chlorine (Cl$^-$), sodium (Na$^+$), sulphate (SO$_4^{2-}$), magnesium (Mg^{2+}), calcium (Ca^{2+}), and potassium (K$^+$). Table 3.4 illustrates the chemical characteristics of seawater.

Parameter	Symbol	Concentration (ppm)
Chloride	Cl$^-$	18,980
Sulphate	SO$_4^{2-}$	2,649
Bicarbonate & Carbonate	HCO$_3$ + CO3^{2-}	140
Bromide	Br$^-$	65
Borate	H$_2$BO$_3^-$	26
Fluoride	F$^-$	1
Sodium	Na$^+$	10,556
Magnesium	Mg^{2+}	1,272
Calcium	Ca^{2+}	400
Potassium	K+	380
Strontium	Sr^{2+}	13
Overall total salinity		**34,482**

Table 3-4: Average concentration of major ions in sea water [87]

It is clear that chloride and sodium ions represent more than 85% of the total dissolved solids [87]. Moreover, seawater also contains various fine suspended materials such as sand, clay, microorganisms, viruses and colloidal materials and the size of these materials varies over the range of 0.05 to 0.150 μm [88].

3.6 Drinking water standard.

The chemical, physical and biological standards of drinking water are set to ensure human health. Standards show great differences in the permitted concentrations for various chemical substances; some, such as sulphate, are relatively harmless to health and can be tolerated up to 250 mg/L and are considered to have no long term health effect, while others, like mercury and cadmium, need low and stringent limits because of their toxicity and the tendency of the body to bio-accumulate them. Meanwhile, many of physical parameters such as pH, colour, turbidity, temperature and hardness, and aesthetic, physical and taste characteristics are still subject to much debate.

Many types of disease can be transmitted to humans through drinking water. which could be caused by pathogenic microorganisms and parasites, so stringent standards for drinking water have been adopted by water monitoring departments around the world [85] The standards of the main chemical and physical parameters for drinking water, adopted by the UK and the World Health Organization (WHO) in 1993 and by the European Union (EU) in 1998 can be found in Table 3.5.

Parameters	UK Standards (mg/L) (1993)	WHO Standards (mg/L) (1993)	EU Standards (mg/L) (1998)
Chloride	400	250	250
Nitrate	50	50	50
Fluoride	1.5	1.5	1.5
Sulfate	250	Not mentioned	250
Calcium	250	Not mentioned	Not mentioned
Magnesium	50	Not mentioned	Not mentioned
Sodium	150	200	200
Potassium	12	Not mentioned	Not mentioned
Hardness	60 as Ca/l	150-500	Not mentioned
Electrical conductivity	1500 μS/cm	2500 μS/cm	2500 μS/cm
Turbidity	< 4 NTU	< 5 NTU	Not mentioned

Table 3-5: Standards of drinking water adopted by (WHO) [4,85]
Adapted from the UK 1993, WHO 1993 and EU 1998 drinking water standards

3.7 Water quality and desalination processes.

Desalination is a process in which saline water is separated into two parts: one that has a low concentration of dissolved salts and which is called fresh water, and the other with a much higher concentration of dissolved salts than the original feed water, and which is usually referred to as brine concentrate [14].

Some desalination processes incorporate a pre-treatment stage for water influent. The main goal of pre-treatment is to reduce feed water pollution, such as turbidity, iron, silica, algae and microbial contamination, in order to improve the efficiency of the desalination plant and to reduce technical problems and equipment breakdown.

Thermal desalination processes, like multi-stage flashing (MSF) and multi-effect distillation (MED), do not require pre-treatment except for the addition of anti-scaling chemicals to prevent salt precipitation. However, in membrane processes like reverse osmosis (RO), pre-treatment is crucial because it protects membrane surfaces from fouling and also provides protection for the high-pressure pumps and avoids the clogging of the RO section.

In the pre-treatment stage, the saline water is filtered from debris, particles and suspended solids by a multimedia gravity filter that removes particles larger than 10 μm. The water is biologically disinfected by injecting chemicals like sodium hypochlorite to remove algae and bacteria and to prevent micro-organism growth. Also added are ferric chloride as a flocculant and sulphuric acid to adjust pH and to control scale formation [27].

Post-treatment for the desalinated water is carried out in all desalination processes because it is generally stabilizes the water to meet the potable water specifications. It may include chlorination for disinfection, carbonation and aeration to remove dissolved gases such as hydrogen sulphide and carbon dioxide [20].

The following section looks at case studies on pre-treatment and post-treatment for thermal and membrane water desalination processes.

3.7.1 Thermal desalination quality case study

Khawaji and Wie (1994) [16] presented pre- and post-treatment processes for two thermal multi-stage flashing desalination plants: a land-based plant and a barge-

mounted plant, both of which consisted of 8 units with an estimated total volume of 3,080 m^3/hr

The pre-treatment of seawater was carried out in the seawater supply system before the feedwater entered the MSF distillation system. The supply system consisted of an open intake channel, pump house, NaOCl generators and return piping. The pump house consisted of seawater pumps, screens and traversing trash rakes.

In the pre-treatment unit, the seawater passed through the screens and sedimentation tanks before the addition of anti-scale materials such as a scale inhibitor to avoid salt precipitation.

Post-treatment consisted of the injection of a mild caustic solution into the discharge of the product water pumps to maintain the pH of the water in the range of 8-8.5. This dosage minimized corrosion by the distillate of the product pipes. The caustic-dosed distillate became process water and contained few dissolved solids. Its conductivity was less than 10 μS/cm.

The desalinated water was stored in epoxy-coated steel storage tanks for distribution for industrial uses, while the processed water was used within the power plant to supplement boiler water and for closed loop cooling water systems.

For drinking water use, the stored caustic-dosed water received further post-treatment to produce potable water. This consisted of four unit operations: carbonation, liming, chlorination and aeration [16].

Carbonation and liming

Carbonation and liming, based on the addition of CO_2 gas and hydrated lime, were used to increase the hardness and alkalinity of the water to desirable levels. Thus the water became well buffered and non-aggressive.

Chlorination

In this process, chlorine was injected into the water for disinfection in two stages, the supply system and the desalinated product water, with chlorine dosage rates of 0.7 mg/L and 0.5 mg/L respectively.

Aeration

The dissolved oxygen content of the distillate was negligible because oxygen had been driven out for corrosion control by the MSF process. The water was aerated to replace oxygen and this improved its taste.

Results

The produced fresh water was of high purity and contained a very small amount of dissolved solids [16]. Table 3.6 presents the typical water quality of the fresh water product samples, all of which met the WHO standards for drinking water.

Quality parameter	Unit	Measured quality value
Temperature	°C	25-32
pH (at 25°C)		8.4
Residual chlorine	mg/L	1
Conductivity	μS/cm	90
Total alkalinity mg/L as equivalent $CaCO_3$	mg/L	40
PP alkalinity, mg/L as $CaCO_3$	mg/L	1
Carbonate alkalinity, mg/L as equivalent $CaCO_3$	mg/L	2
Bicarbonate alkalinity, mg/L as equivalent $CaCO_3$	mg/L	38
Total hardness, mg/L as equivalent $CaCO_3$	mg/L	40
Calcium hardness, mg/L as equivalent $CaCO_3$	mg/L	40
Dissolved oxygen, mg/L at 25 °C	mg/L	7
Turbidity	NTU	1

Table 3-6: Water quality analyses data

3.7.2 Solar stills quality case study #1

Samee, Mirza, et al. (2007) [55] studied a simple single-basin solar still for water desalination in rural areas to solve the big problem in the southern and south western arid regions of Pakistan where the underground water is usually brackish water and can not be used for drinking.

The production of fresh water varied directly with the amount of solar radiation and the ambient temperature. The maximum hourly production was in the afternoon

when the temperature was at its daily peak. The average daily output was found to be 1.7 litre/ day for a basin area of $0.54m^2$.

Three water samples from different sources were used in the experiment. One was drinking water coming from the Simly dam, the second was from brackish ground water with a highly turbidity and salinity, and the third sample was prepared in the laboratory. All the samples were tested before and after desalination for total dissolved solids (TDS), electrical conductivity (EC) and pH.

Table 3.7 shows the results of the tests on each sample, before and after desalination. and demonstrate that the quality of the desalinated water met the WHO drinking water standards on these parameters [55].

Sample No.	TDS (mg/L)		pH		Conductivity (μS/cm)	
	Before Desalination	After Desalination	Before Desalination	After Desalination	Before Desalination	After Desalination
1	370	30	6.72	6.50	1.291	0.041
2	544	84	6.78	5.74	1.668	0.031
3	17663	226	7.58	6.13	85.3	0.0885

Table 3-7: Tested water quality parameters

3.7.3 Solar stills quality case study #2

Hanson et al (2004) [89] presented a laboratory and field study for a single-basin solar still for desalination of contaminated raw water in southern New Mexico at New Mexico State University in the USA. They reported on the performance of solar stills in the removal of selected inorganic, bacteriological and organic contaminants.

Six solar stills were designed with modifications by the El Paso Solar Energy Association (EPSEA). Their dimensions were 2.47m x 0.94m; the high side wall was 0.15m and the low side wall was 0.05m, in addition to heat insulation.

Various types of feed water were used in order to test and evaluate the treatment efficiency of the stills. In stills Nos. 1 and 2, tap water from the municipal source was used as a control and the other four stills used water from contaminated wells and prepared samples in the laboratory.

Stills No.3 to No.6 were all used to test removal of salinity, hardness, pH, fluoride and nitrate. Only stills No. 3 and No. 4 were used for the bacteriological and pesticide tests.

In all cases, samples were taken from the input source and from the output water product and they were analyzed in the laboratory for the identified contaminants.

The results of laboratory analysis of water quality showed very high removal efficiencies of more than 99% for salinity, total hardness and fluoride and of more than 99.9% for bacteria, in addition to the successful removal of volatile organic compounds and pesticides [89].

These results confirm that solar still systems can produce high quality drinking water from a poor water source.

3.7.4 Membrane desalination quality case study

Abou Rayana and Khaled (2002) [90] presented a case study for a seawater desalination plant operated by reverse osmosis technology with a capacity of 2000 m^3/d located at Dahab city in the south of Sinai, Egypt.

The salinity (TDS) of the feed seawater was 44,000 ppm. The station consisted of 4 units with each unit having a maximum capacity of 500 m^3/d.

The plant was designed to operate in three stages: the pre-treatment system, the RO unit and the post-treatment stage. The chlorination and chemical systems were shared with the post-treatment system.

3.7.4.1 Pre treatment and RO unit

This stage consisted of a seawater disinfection unit, multi media filters and cartridge filters. In the disinfection unit, sodium hypo-chlorine solution was added to disinfect and kill micro-organisms and to protect the membrane against bio-fouling. Other chemicals, such as anti-scale materials, were added to prevent membrane clogging by salt precipitation.

The multi media filter unit consisted of two filters in series. The first filter was for sand and the second was for activated carbon filtration. The plant had one cartridge filter of 5 micron pore size so that particles larger than 5 micron could not enter the membranes.

3.7.4.2 Post-treatment

Post-treatment of the product water consisted of chlorination to disinfect the water put into the potable water network and chemical treatment for pH adjustment within the range of 7.5-8.5.

3.7.4.3 Results

It was concluded that pre-treatment is the most crucial stage in reverse osmoses plants because it protects membrane surfaces from fouling and also it provides protection to the high-pressure pumps and avoids the clogging of the RO section.

The produced fresh water was of acceptable dissolved solids content compared with the WHO guidelines for drinking water.

4   Overview of Recent Investigations of Small Scale Thermal Desalination Units

There have been numerous studies conducted on small scale solar water desalination to try to improve system efficiency and water productivity.

Zhang and Yuan (2007) [91] studied a closed circulation solar desalination unit based on the principles of humidification and dehumidification. This study focused on an analysis of water production and system performance by investigating the effect of the cooling water flow rate, the feed water rate and the structural dimensions. Similarly, Eames et al. (2007) described the theoretical and experimental investigation of a small scale solar powered barometric desalination system and, comparing the results with the given theory, they showed that the production rate of fresh water depended on three main factors, namely the heat exchanger effectiveness of the condenser, solar insolation and pressure [92].

A single solar still connected to a flat plate collector has been studied by various researchers. Voropoulos et al. (2001) carried out an experimental investigation of a basin still coupled with 24 flat plate solar collectors and a storage tank. They used the tank to increase the water distillation during the night and also to utilize the available waste heat coming from thermal processes nearby. The water in the tank could be heated either directly or indirectly through the heat exchanger. The system was investigated under two conditions. In the first case the distillation unit was coupled with the solar collectors only. In the second case tests were conducted incorporating the storage tank. The results demonstrate a maximum productivity of 35.29 kg/day in the first case and 47.77 kg/day in the second case, at a solar insolation of 18.5 MJ/m^2 [93].

Schwarzer et al. (2001) built a solar desalination plant consisting of a tower housing 6 stages and a heat recovery system with an area of 0.8m x 0.8m connected to a 2 m^2 flat plate solar collector. Its numerical simulation showed that the system could reach water productivity of 25 kg/m^2/day, with a variation of 4.8 kW/m^2/day. The water quality analysis also showed a high purity of produced water, achieving 99% of physical and chemical contaminant removal and 100% of biological contaminant removal [94].

Many researchers have tried to improve the thermal efficiency and water productivity performance of still technology by building new prototypes and through

experimental and theoretical analysis. The productivity of such systems remains low and limited in comparison with still systems coupled with solar collectors. Bouchekima (2002) [95] and Chaibi (2000) [96] performed a theoretical analysis and experimental study on a basin still and the results showed that efficiency increases with an increase in solar radiation and brine temperature and with recovery of the latent heat of condensation.

Badran et al. (2005) investigated a basin still of a $1m^2$ area coupled with a flat plate collector of a 1.34 m^2 area and found that the overall efficiency was 27 % with a maximum total daily productivity of 4.6 kg/day [97].

A multi-effect desalination system with air evacuation to allow the water to evaporate at low temperatures, coupled with a solar collector and photovoltaic cells, was designed by Abu Jabal et al. (2001) in the Gaza Strip. This system consisted of three effects made from transparent glass and utilizing the latent heat of evaporation and condensation in addition to a direct and indirect heating system. The dimensions of the system were 9 m in length, 3.2 m in width, and 2.3 m in height. The dry weight was approximately 5 tons and the operating weight was 11 tons. The area of the solar cells was about 5.1 m^2, and the evaporators were about 3.3 m-long cylinders with a heat exchanger. The highest production achieved was in July when 204.5 kg/day level was recorded and the lowest was on a day in December with no production at all [98]. Multi effect solar stills were investigated also by Toyama et al. (1987) [99].

Abakr and Ismail (2005) designed a theoretical and experimental investigation of a multi-stage evacuated solar still coupled with a flat plate solar collector working under atmospheric pressure and pressure evacuation [100] where the latent heat of the vapour condensate from the first stage was passed to the next stage. Their work proved that water productivity could be higher with pressure evacuation of 0.5 bar; this produced 14.2 kg/m^2 day compared to 9 kg/m^2 day under the atmospheric pressure condition. Numerical modeling of a multi stage solar still with an electrical heater instead of solar energy for power input was presented by Jubran and Ahmed et al. (2000) and this proved that 9 kg/m^2/day could be produced with a distillation efficiency of 87 % [101]. In the same context, Abdel Dayem and Adel (2006) investigated the performance efficiency of a multi stage condensation and evaporation solar water desalination unit coupled with a flat plate solar collector. Their field experiments and numerical simulation

demonstrated that the system could work continuously with fresh water production of 24 L/day [102].

Hou and Zhang (2008) proposed a hybrid desalination process using a multi-effect humidification–dehumidification system heated by solar collectors and concluded that the output ratio is increased by 2 - 3 when the rejected water is reused [103].

Garg and Adhikari et al. (2002) tested an MEH solar system to provide continuous hot water to a desalination unit over a 24 hour period by system modeling based on solving heat and mass transfer equations. The result showed that the rate of distilled water production varied linearly as a function of water temperature at the humidifier [104]. Muller-Holst et al. (1999) studied the same concept on a small scale thermal seawater desalination apparatus and showed that the water productivity depended on the magnitude of the thermal energy used in the evaporation process [61].

A numerical simulation study on a multi-stage stacked tray solar still for the steady state condition was conducted by Adhikari et al. (1995) [105] where the steady state model was developed and validated theoretical results experimentally on a three-stage unit with an immersion type electric heater used as a heating source. Multi-effect solar stills were also investigated by Toyama et al. (1987) [106] and a similar system was described by Abakr and Ismail (2005) [100].

A water desalination system using low grade solar heat was studied by Al Kharabsheh and Goswami (2003) [9]. Their system utilized gravity and atmospheric pressure to create a vacuum to evaporate the liquid rapidly with a lower temperature and with less energy than in conventional techniques. The experimental results illustrated the superior performance of this system since it produced twice the quantity of fresh water compared to a flat basin solar still.

Fernandez and Chargoy (1990) studied experimentally and theoretically a multi-stage indirectly heated solar still with a W-shape condensing surface and coupled with 32 flat plate collectors. Each of these collectors had an effective area of 1.59 m^2. During the experiment a maximum daily production of 77.2 kg was achieved. They concluded that multi-stage desalination of seawater was a sound and reliable technique, but the undesirable flow of steam that bypassed the condenser in the pan immediately above the evaporator was detrimental to the overall performance [107].

5   Aims and Objectives of Research

5.1   Conclusions from literature

From literature review, large scale thermal and reverse osmosis desalination processes operating on fossil fuels are one of the main technologies in the world playing a crucial role in providing fresh water. However, the use of such plants in remote coastal areas is not always economically viable despite the general commercial success of these technologies. Extensive Research and Development activities are still ongoing to find new feasible methods to produce drinking water. These include small scale systems using solar energy since very often people in developing countries also experience a shortage in fossil fuel and electricity supply.

In remote locations, conventional basin solar stills with a relatively large footprint area are an example of this simple technology. The disadvantages of basin solar stills include their relatively low performance due to excessive heat losses to the ambient surrounding, their generally low thermal efficiency and progressing reduction in efficiency over the exploitation period because of the scaling and accumulation of salt impurities.

Analysis of previously published papers shows that the possibility of using relatively compact multi-stage tray solar stills, coupled with flat-plate solar collectors, has been investigated by a number of researchers. But this study is concerned with the development of a novel small scale solar water desalination technology and includes experimental and theoretical investigations of the operation of a multi stage solar still desalination system coupled with a heat pipe evacuated tube solar collector.

It also can be concluded that most of the previous work shows that mainly lumped-parameter type models are used for the theoretical modeling of the operation of multi-stage tray solar stills. In addition, simulations are often restricted to just the steady state operation at a fixed value of insolation.

This work describes the mathematical model of a multistage tray solar still for transient numerical simulations when insolation varies over the whole daylight period. It also shows how the developed mathematical model can be used to determine the rational design parameters of the solar still for a given aperture of the evacuated tube

solar collector in addition to the simulation of number of stages as a function of water productivity.

Currently, carrying out the experimental investigations is no longer restricted to a specific solar insolation region because the presence of the light solar simulator at Durham University makes it possible to simulate any solar insolation condition available.

5.2   Research objectives

The main objectives of this research are:

- to develop a mathematical model of the still;
- to carry out the experimental study on the test rig in order to investigate the performance of a multi stage solar still coupled with an evacuated tube solar collector;
- to compare the theoretical calculations with the experimental results;
- to conduct a water quality analysis for the distillate product;
- to conduct an economic study to examine the feasibility of this system.

5.3   Scope of work

This research was carried out through several routes.

The literature for all desalination technologies has been thoroughly reviewed, with a particular concentration on the solar powered water desalination technologies.

The theoretical and experimental analysis has also been studied for the multi stage solar still through the following activities:

- A mathematical model based on a thermodynamic analysis for heat and mass transfer has been developed.
- The experimental work has been carried out to investigate the performance of water productivity of this system which includes the preparation of a synthetic saline water solution, data collection, system set up and its assemblage.
- Water quality analysis for each stage in the system has been performed for all distillate samples during the day.
- The developed model has been calibrated and validated by the experimental results obtained.

- MATLAB program code has been developed based on the transient numerical model to simulate the water productivity and temperatures inside the still stages and to use to still sizing.

- Engineering Equation Solver program code has also been developed to solve the experimental results.

- A computational fluid dynamic (CFD) simulation model using FLUENT 6.2 software has been developed to simulate the evaporation and condensation processes inside the stages of the solar still.

- The economic study has been performed for the desalination system by developing an economical model to simulate different design parameters so that the best option could be selected based on the lowest product cost.

- Conclusions and future work have been highlighted.

6 Lumped Parameter Mathematical Model

6.1 System description and operating principle.

A water desalination test rig was built at Durham University comprising a four-stage metallic still coupled with a 20 evacuated tube solar collector. This rig was built within the framework of investigations on the development and improvement of static still and, most importantly, dynamic solar water desalination methods. The major components of this test rig was described by Mahkamov et. al. (2007) [108]. Figure 6.1 presents a schematic diagram of the test rig with the multi-effect still. Each stage is made of steel and has a rectangular form with the length and width equal to 1200 mm and 400 mm, respectively,

The first (bottom) stage of the apparatus, with the largest volume, contained the main body of the saline water. The remaining stages of the still were identical in design and were open at the bottom but covered at their top by an angled water tray The water depth was about 40 mm and covered a serpentine copper tubular heat exchanger fixed to its base using plastic clippers.

Solar energy was utilized in the multi-effect still in several phases. First, the energy flux absorbed by the solar collector was used to increase the temperature of the liquid which was continuously circulated in the closed "solar collector manifold"–"heat exchanger" loop. The energy then was transferred to the brackish water in the first stage of the still via the above tubular heat exchanger. The temperature of the saline water in the bottom stage increased and this resulted in the production of water vapour which condensated on the slopping surface of the second stage tray since the temperature of the saline water in the tray was lower than that of the water in the bottom stage. Droplets of the condensate were formed on the slopping surface and these flowed under gravity towards the tray's edge and they were collected in the trough. From the trough, the condensate was taken out and collected in the metering cylinder. The latent heat of condensation was utilized to gradually increase the temperature of saline water in the tray of the second stage of the still and then the process of condensation was repeated between the second and third stages and the third and fourth stages, respectively.
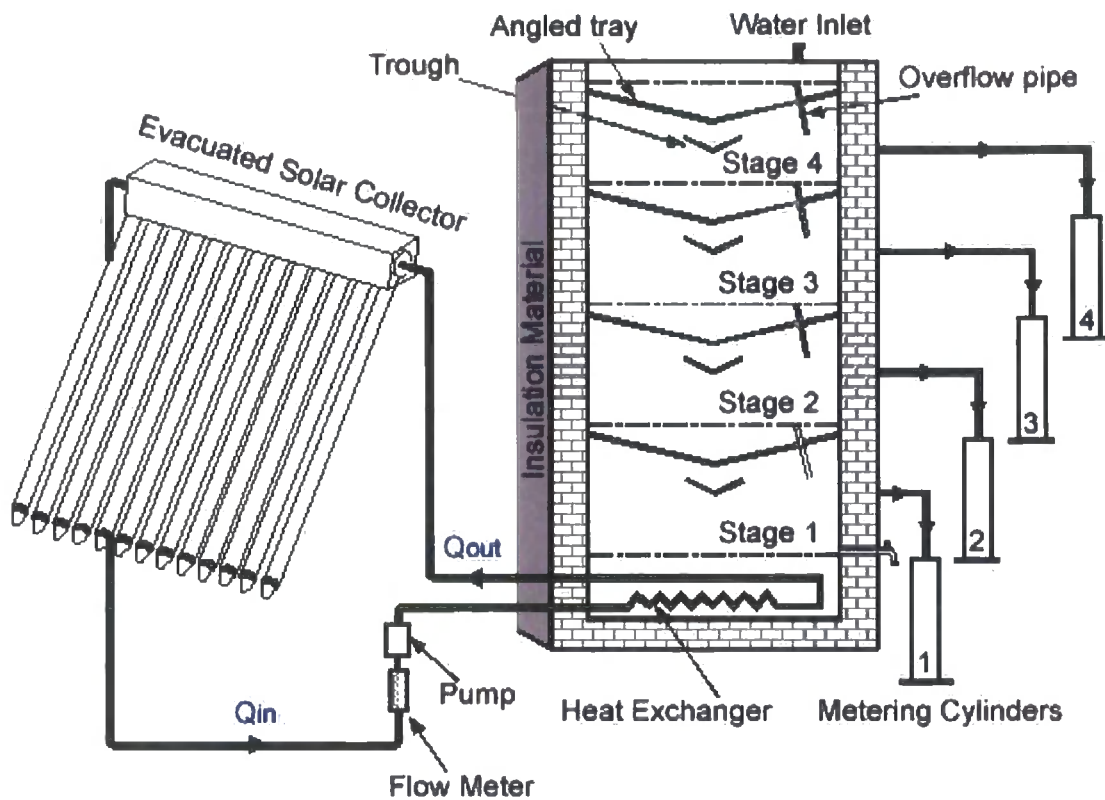
Figure 6-1: Schematic diagram of solar desalination system

6.2 Assumptions of the mathematical model

The theoretical analysis of a water desalination system using low grade heat solar energy was performed using the developed mathematical model that described the operation of the solar water still. Energy and mass balance equations were written for each stage and for the whole system. Several assumptions were made when developing the model as follows:

- The thermo-physical properties of brackish water are identical to those of pure water.

- The effect of non-condensable gases released from water when it is heated or expanded is neglected.

- The amount of water evaporated and the distillate output in the ith are equal.

- The distillate product leaves the desalination system with the temperature equal to that of the condensation surface T_{ci}.

- The system's heat losses to the ambient environment through the still walls and the mineral wool insulation were evaluated based on the insulation material's thermal properties.

- The model was designed to simulate and predict the water production of the desalination system over a 24 hours period, based on the heat supply during a light day with variable insolations (W/m^2).

6.2.1 Mathematical Model

The mathematical model derived here represents the system of energy and mass conservation equations written for each stage of the still in the form of ordinary differential equations. Figure 6.2 presents a calculation scheme of the still and its energy balance diagram

The energy conservation equations can be expressed as follows:

- The first stage of the still:

$$\dot{Q}_H - \dot{m}_{e1}(h^*_{fg1} + c_p T_{c1}) = M_{s1} C_p \frac{dT_{s1}}{dt} + \Delta \dot{Q}_{losses\ 1} ; \tag{6-1}$$

-The second stage:

$$\dot{m}_{e1} h^*_{fg1} - \dot{m}_{e2}(h^*_{fg2} + c_p T_{c2}) = M_{s2} C_p \frac{dT_{s2}}{dt} + \Delta \dot{Q}_{losses\ 2} ; \tag{6-2}$$

-The third stage:

$$\dot{m}_{e2} h^*_{fg2} - \dot{m}_{e3}(h^*_{fg3} + c_p T_{c3}) = M_{s3} C_p \frac{dT_{s3}}{dt} + \Delta \dot{Q}_{losses\ 3} ; \tag{6-3}$$

-The fourth stage:

$$\dot{m}_{e3} h^*_{fg3} - \dot{m}_{e4}(h^*_{fg4} + c_p T_{c4}) = M_{s4} C_p \frac{dT_{s4}}{dt} + \Delta \dot{Q}_{losses\ 4} ; \tag{6-4}$$

$\dot{Q}_H$ in equation 4-1 is heat input rate to the still:

$$\dot{Q}_H = \dot{m}_c C_p (T_{SCinlet} - T_{SCoutlet}) ; \tag{6-5}$$
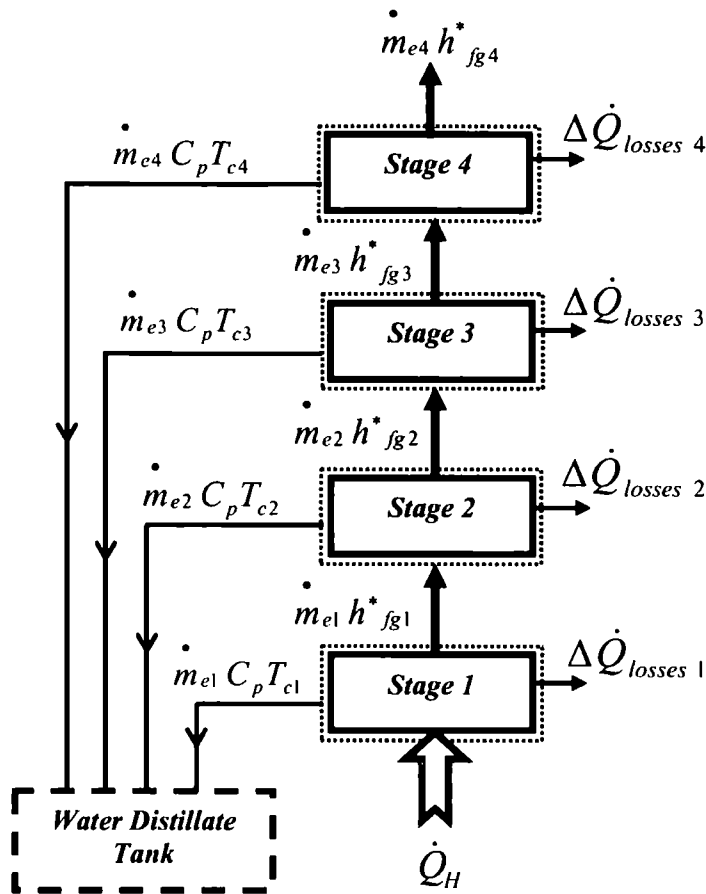
Figure 6-2: A calculation scheme of the still in the lumped-parameter model

Mass conservation equation for each stage can be written as:

$$\frac{dM_{si}}{dt} = -\dot{m}_{ei}.$$

(6-6)

During the experiments and after many repetitions of experiments it was observed that there was a difference in the temperature between the condensing surface and its next upper evaporation surface for each stage. Hence these differences in temperature were taken into consideration in the model. In the fourth stage the condensing surface temperature was determined as a function of water bed temperature based on the fitted experimental temperature results as follows:

$$T_{c1} = T_{s2} - 2K \ ; \tag{6-7}$$

$$T_{c2} = T_{s3} - 2.7K \ ; \tag{6-8}$$

$$T_{c3} = T_{s4} - 1.11K \ . \tag{6-9}$$

In the fourth stage the temperature of the condensing surface (°C) was determined as a function of the water bed temperature as:

$$T_{c4} = T_{s4} - \left(0.00007T_{s4}^{\ 3} - 0.015T_{s4}^{2} + 0.9763T_{s4} - 10.324\right). \tag{6-10}$$

The above empirical corrected equations. Equations 6.7 to Equation 6.10 are appropriate for the proposed multi stage still configuration and could be used in other design prototypes built on the same concept. The results of theoretical calculations based on the validated model demonstrated an acceptable level of accuracy in the predication of system water productivity and performance design parameters compared with the experimental results as shown in the next chapters.

The heat of evaporation is mainly dissipated from one stage to another through the condensation surface of each stage and the rest is used to increase the temperature of the produced fresh water.

During calculations the amount of heat losses $\Delta Q_{lossesi}$ in each stage was calculated and the amount of water evaporated and the distillate output in the ith were equal. The dependence of the magnitude of the latent heat and the refined latent heat of vaporization of water from current temperatures were determined as proposed by Cooper (1969) [109] and [110], relatively:

$$h_{f\,gi} (T_i) = 1000 * [(3161.5 - 2.40741 (T_i + 273)] \ ; \tag{6-11}$$

$$h_{f\,gi}^{\bullet} = h_{f\,gi} + 0.68 C_{pi} (T_{si} - T_{ci}) \ . \tag{6-12}$$

where T_S is the water bed temperature (°C) and T_c is the water condensation temperature (°C).

The heat capacity of water is defined as a function of its temperature as suggested by Eames et al. (2007) [92] as:

$$C_{pi} = 1000*[4.2101 - 0.0022 \times T_i + 5*10^{-5} \times T_i^2 - 3*10^{-7} \times T_i^3] \qquad . \qquad (6\text{-}13)$$

In these equations h_{fg} is in J /kg, T in (°C) and C_p in J/kg °C

6.2.2 Determination of heat transfer coefficients

Convective heat transfer coefficient

In convective loss coefficient the heat transfer occurs by free convection due to the temperature gradient in the fluid. Hence the rate of heat transfer coefficient from the water surface to the bottom surface of the next stage upward can be obtained according to Dunkle (1961) [111].

$$h_{sci} = 0.884 \times \left[(T_{si} - T_{ci}) + \frac{(p_{si} - p_{ci})(T_{si} + 273)}{268.9 \times 10^3 - P_{si}} \right]^{1/3} . \qquad (6\text{-}14)$$

and vapour pressures can be calculated as suggested by Fernandez and Chargoy (1990) [107].

$$p_i = e^{\left(25.317 - \frac{5144}{T_i + 273} \right)} . \qquad (6\text{-}15)$$

In these equations the temperature is in (°C) and pressure is in (*Pa*).

Evaporative heat transfer coefficient

The mass transfer coefficient h_{ew} as a function of the convective heat transfer coefficient h_{sc} can be calculated as proposed by Cooper (1973) [111].

$$h_{ewi} = 16.273 \times 10^{-3} h_{sci} \left(\frac{p_{si} - p_{ci}}{T_{si} - T_{ci}} \right) . \qquad (6\text{-}16)$$

6.2.3 Determination of distilled water

The distillate output rate in stages can be taken equal to the mass evaporation rate of brackish water in the corresponding stages as follows:

$$\dot{m}_{ei} = \frac{(T_{si} - T_{ci})h_{ewi} A_{si}}{h^{\bullet}_{fgi}}.$$

(6-17)

6.2.4 Solar collector efficiency

The solar collector efficiency can be defined in terms of inlet and outlet fluid temperatures of the collector manifold, the area of the collector, and mass flow rate. This was suggested by Yuan and Zhang (2007) [91] as follows:

$$\eta_i = \frac{\dot{m}_c C_p (T_{SCinlet} - T_{SCoutlet})}{\overline{G} A_{collect}}.$$

(6-18)

6.2.5 Distillation efficiency

The distillation efficiency for the still system was defined as:

$$\eta_{distill} = \frac{\sum_{i=1}^{4} m_{ei} h_{fgi}}{\dot{Q}_H}.$$

(6-19)

The overall efficiency of the system is calculated as:

$$\eta_{overall} = \frac{\sum_{i=1}^{4} m_{ei} h_{fgi}}{\overline{G} A_{collect}}.$$

(6-20)

The above mathematical model was used to develop a computer program in MATLAB software. In the first stage of numerical investigations the program was used to simulate the operation of the still using boundary and initial conditions identical to those in physical experiments. After experimental validation, the model was used in the second stage of investigations in order to determine rational design parameters and number of stages of the still for a given aperture of the evacuated solar collector.

7   Computational fluid dynamic – (CFD) simulation

CFD simulation was used to simulate the condensation and evaporation processes inside the first stage of the solar still. A 3D model was set up using FLUENT 6.2 CFD software. Segregated solver and multiphase VOF model were used to simulate the transient processes inside the first stage of the still.

Multiphase flow regimes can be grouped into four categories: gas-liquid or liquid-liquid flows, gas-solid flows, liquid-solid flows, and three-phase flows. In this case, the gas liquid regime has been considered [112].

7.1   Description of volume of fraction (VOF) model.

The VOF model can model processes in two or more immiscible fluids by solving a single set of momentum equations and tracking the volume fraction of each of the fluids throughout the domain. Typical applications include the prediction of jet breakup, the motion of large bubbles in a liquid, the motion of liquid after a dam break, and the steady or transient tracking of any liquid-gas interface.

The VOF formulation relies on the fact that two or more fluids (or phases) are not interpenetrating. For each additional phase that is added to the model, a variable is introduced which is the volume fraction of the phase in the computational cell. In each control volume, the volume fractions of all phases sum to unity. The fields for all variables and properties are shared by the phases and represent volume-averaged values, as long as the volume fraction of each of the phases is known at each location. Thus the variables and properties in any given cell are either purely representative of one of the phases, or representative of a mixture of the phases, depending upon the volume fraction values [112].

If the q_{th} fluid's volume fraction in the cell is denoted as α_q then the following three conditions are possible:

$\alpha_q = 0$ when cell is empty (of the q_{th} fluid);

$\alpha_q = 1$ when the cell is full (of the q_{th} fluid);

$0 < \alpha_q < 1$ when the cell contains the interface between the q_{th} fluid and one or more other fluids.

7.2   Continuity equation

The tracking of the interface(s) between the phases is accomplished by the solution of a continuity equation for the volume fraction of one (or more) of the phases as shown in the following equation:

$$\frac{1}{\rho_q}\left[\frac{\partial}{\partial t}(\alpha_q \rho_q) + \nabla \bullet (\alpha_q \rho_q \vec{\upsilon}_q) = S_{\alpha q} + \sum_{p=1}^{n}(\dot{m}_{pq} - \dot{m}_{qp})\right]; \tag{7-1}$$

where $\dot{m}_{qp}$ is the mass transfer from phase q to phase p. $\dot{m}_{pq}$ is the mass transfer from phase p to phase q. By default, the source term on the right-hand side of $S_{\alpha q}$ is zero, but it can be specified as constant or user-defined mass source for each phase.

The volume fraction equation will not be solved for the primary phase; the primary-phase volume fraction will be computed using the following condition:

$$\sum_{q=1}^{n}\alpha_q = 1. \tag{7-2}$$

7.3   Momentum equation

A single momentum equation is solved throughout the domain, and the resulting velocity field is shared among the phases. The momentum equation shown below is dependent on the volume fractions of all phases through the properties [112].

$$\frac{\partial}{\partial t}(\rho\vec{\upsilon}) + \nabla \bullet (\rho\vec{\upsilon}\vec{\upsilon}) = -\nabla_p + \nabla \bullet \left[\mu(\nabla\vec{\upsilon} + \nabla\vec{\upsilon}^T)\right] + \rho\vec{g} + \vec{F}. \tag{7-3}$$

7.4   Energy equation

The energy equation, also shared among the phases:

$$\frac{\partial}{\partial t}(\rho E) + \nabla \bullet (\vec{\upsilon}(\rho E + p)) = \nabla \bullet (k_{eff}\nabla T) + S_h. \tag{7-4}$$

The VOF model treats energy, E, and temperature, T as mass-averaged variables as in the following equation:

$$\frac{\sum\limits_{q=1}^{n}\alpha_q \rho E_q}{\sum\limits_{q=1}^{n}\alpha_q \rho_q} \cdot \tag{7-5}$$

where E_q for each phase is based on the specific heat of that phase and the shared temperature.

The properties ρ and k_{eff} (effective thermal conductivity) are shared by the phases. The source term, S_h contains contributions from radiation, as well as any other volumetric heat sources [112].

7.5 Mass and heat transfer user defined function

In calculations the mass and heat transfer has been simulated using external user defined function (UDF) for energy, liquid and vapour mass transfer (See Appendix C).

7.6 Evaporation and condensation mass transfer

For liquid temperatures greater or equal to the saturation temperature, the evaporation rate is determined as:

$$\dot{m}_v = \frac{r_v \alpha_l \rho_l \left(T_l - T_{sat}\right)}{T_{sat}} \cdot \tag{7-6}$$

For vapour temperatures less than the saturation temperature, the condensation rate can be calculated as:

$$\dot{m}_l = \frac{r_l \alpha_v \rho_v \left(T_{sat} - T_v\right)}{T_{sat}} \cdot \tag{7-7}$$

The user can specify saturation temperature and, if desired, "time relaxation parameters" r_l and r_v (Wen Ho Lee (1979)).

Unidirectional mass transfer r is constant: $\dot{m}_{12} = r\alpha_2 \rho_1$ [113].

7.7 Results of CFD simulations of the still

It was found to be unfeasible to use the CFD technique for modeling the heat transfer and flow in all four stages of the still and therefore FLUENT 6.2 CFD software was used to simulate the condensation and evaporation processes only inside the first stage.

Figure 7.1 shows the schematic diagram of the simulated case where the water body and upper condensing surface temperatures were assumed to be 368 K and 363 K respectively and the external walls were assumed to be thermally insulated. It was also assumed that the distillate leaves the still with a temperature equal to the condensing surface, as assumed in the aforementioned numerical model.

T = 363K

Collection Trough

Distillate Outlet
T=363K

16.0 cm

Water - Bottom temperature T = 368K

120cm
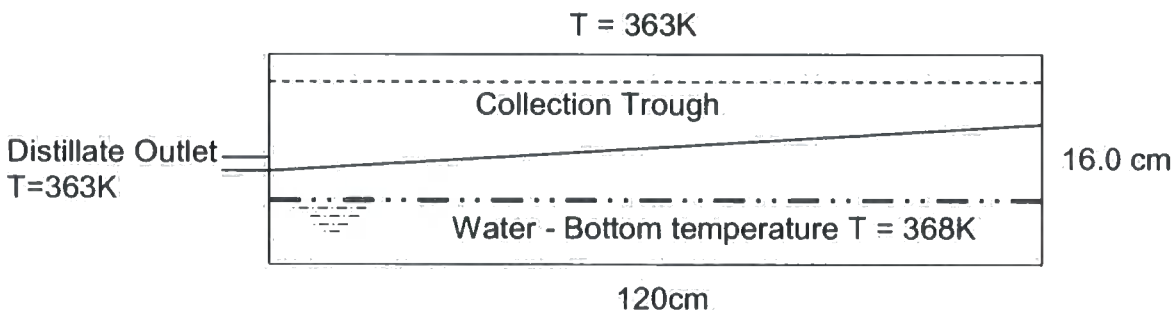
Figure 7-1: Still model case schematic diagram

Figure 7.2 represents the computational mesh with about seventy thousand cells used in numerical investigations
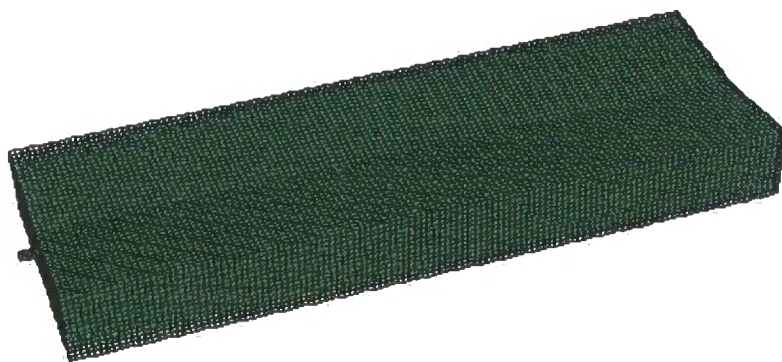
Figure 7-2: 3 D Solar still mesh diagram

A multiphase flow volume-of-fraction (VOF) model [112] was used to simulate and solve the time-dependant governing equations of mass, momentum and energy

conservation describing heat transfer and flow inside the first stage of the still and to track the volume fraction of both fluid and vapour throughout the computational domain.

Figure 7.3 show the temperature distribution inside the still stage for a certain time of the heating-up process. Computational results demonstrate that the temperature gradually increases in the first stage from its bottom to the top with some fluctuations due to convection flows and eventually the temperature distribution reaches some quasi-steady state for specified boundary conditions. Figure 7.4 illustrates the distribution of the volume of the liquid fraction and it can be seen that the bottom part of the tray is fully covered by water with vapour filling its upper part. Droplets of water can be observed forming on the condensing surface of the tray and over time the amount of droplets decreases.

The obtained CFD results do not correlate well with the experimental information and therefore can be used only for qualitative analysis of certain details of heat transfer processes taking place inside the distillation still. At this stage the computational time and PC recourses requirements restricted the intensive application of CFD technique for analysis and design of the distillation stills and a lumped parameter model was preferred for this purpose.
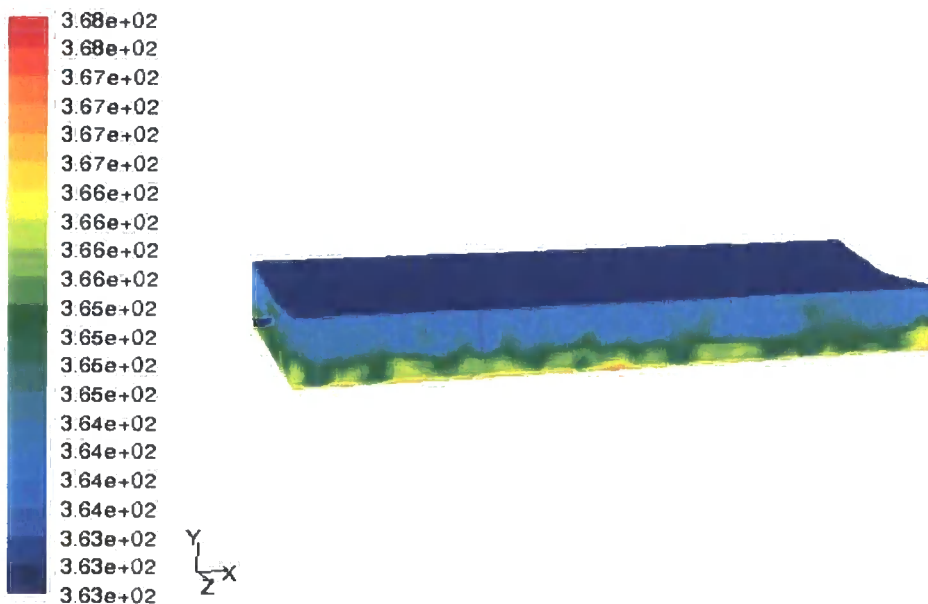
Figure 7-3: The temperature distribution in the first stage
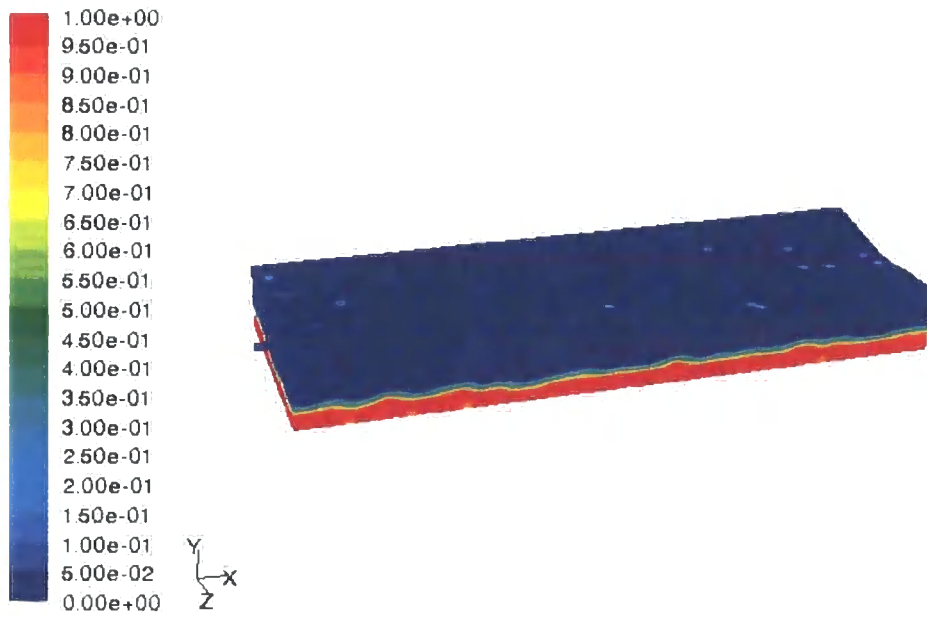
Figure 7-4: Volume of liquid fraction in the first stage

8 Experimental Study

The main objectives of the experimental study were to investigate the performance of the multi stage solar stills technology coupled with evacuated solar collectors in terms of fresh water productivity and to compare the theoretical results with the experimental ones.

8.1 Experimental setup

A water desalination system consisting of a four stage still, a 20 evacuated tube solar collector, a heat exchanger and a circulation pump, was created in the thermo fluids laboratory at Durham University. the schematic diagram of its main components is described above in Figure 6.1.

8.1.1 Evacuated tube solar collector

The 20 evacuated tube solar collector with heat pipes inside each tube has the aperture area and absorbance surface of about $1.7m^2$ and $2.20m^2$ respectively. The condensing zone of the heat pipes is in contact with fluid in the header of the solar collector. In order to extend the testing range, the rig was equipped with an artificial source of radiation, which consisted of 110 halogen floodlights and with area of approximately $1.8\ m^2$ simulates the solar radiation (insolation). The maximum electrical power of each floodlight is 150W. The array of floodlights was divided into three groups and connected to the grid via a 3-phase transformer which allowed the level of heat flux to be varied to simulate change in solar radiation over the day. Figure 8.1 shows the array of flood lights installed in the test rig. Table 8.1 shows the main specifications of the solar collector.

Figure 8-1: Evacuated tube solar collector panel and light flux

Model Type	Specification
Construction	Vacuum Tube Collector
No. of Collector Pipes	20
Tube Diameter (OD)	47mm
Panel area	$2.25m^2$
Absorber Surface	$2.20 \ m^2$
L x W x H (mm)	1760x1500x130
Weight	55kg
Fluid Content	1.5 l
Pressure Drop@100 l hr-1	10mBar
Max. Temp (°C)	190°C
Stagnation Temp (°C)	247°C
Heat exchanger material	Copper
Permissible Operating Pressure	6bar

Table 8-1: Main specifications of the evacuated tube solar collector panel

The copper manifold header pipe of the collector is a long horizontal cylinder with a volume of approximately 1 litre. The header pipe also contains twenty small cylindrical heat pipe housing ports. Figure 8.2 shows an example of a header pipe with four housing ports. The axis of each housing port is perpendicular to the flow direction in the header pipe. In the solar collector the head of each evacuated tube heat pipe is inserted into a separate housing port and the heat from the heater pipes is transferred to the flow inside the header pipe through the walls of the housing ports. The thermal contact

between the heads of the heat pipes and the housing ports is provided using a special metallic glue compound.
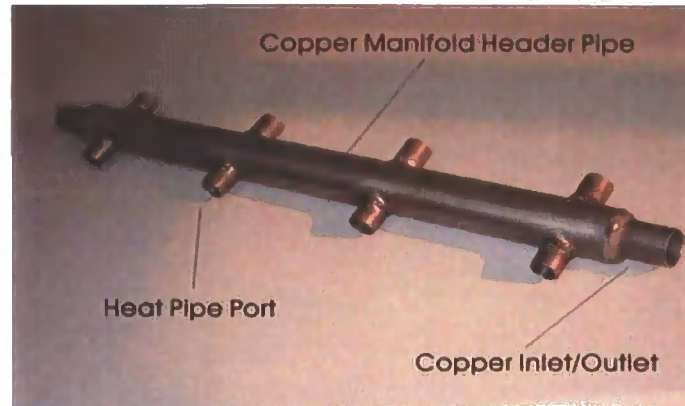
Figure 8-2: The design of the copper manifold header pipe with four heat pipe housing ports

8.1.2 Multi stage still

A solar still consisting of four stages mounted on top of each. Each stage of the still has a rectangular form steel casing of length and width 1200 and 400 mm, respectively, containing an angled tray, see Figures 8.3 and 8.4. The heights of the first and following stages are 160 and 125 mm, respectively. Initially all the casings and trays were brush painted using "HUMMERITE", a smooth black solvent based metal paint. During the test trials, when exposed to the temperature levels of 90-100 0C for several hours, the paint reached its melting point and started to peel from the metallic surface in the form of flakes which disrupted the flow of droplets on the angled condensation surface of trays. Therefore a polyolefin based alloy PLASCOAT PPA 567 was used for coating the trays. This was first sprayed on the undercoating of all the components and then exposed to a high temperature by placing the casings and trays in an electrical thermal furnace. At high temperatures the alloy forms a protective film which is not prone to cracks in the hot water and steam environment.

The first (bottom) stage is in fact a rectangular box with the open top covered with one of angled trays. This box has the largest volume and contains the main body of the saline water. The water depth in the case is about 40 mm and it covers a horizontally installed
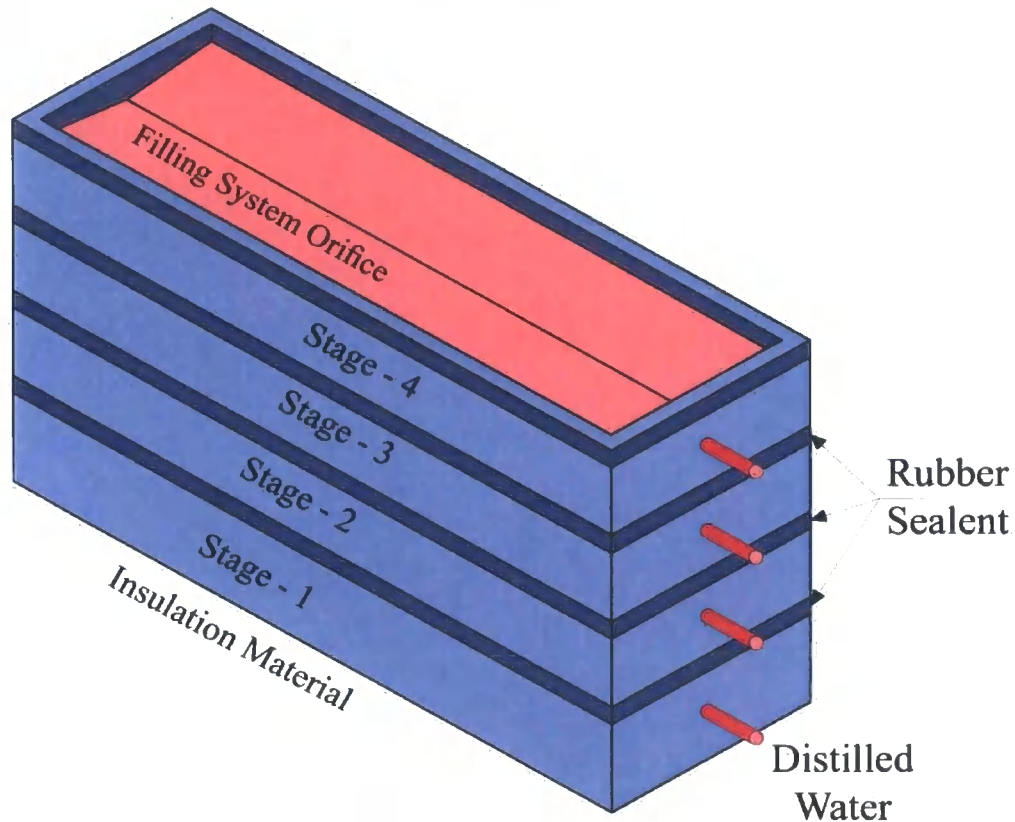
Figure 8-3:Multi stage stills (assembled)

The design of the tray is identical for all the stages and it is formed by two steel sheets inclined at angle of 8° and welded to the side walls of the rectangular box. A simple long triangular trough is installed in all four stage cases just below the ridge of the slopping tray and runs along the full length of the tray. Both ends of the trough are welded to the corresponding opposite side walls of the case at different levels and the lower end is connected to the pipe outlet from the stage box so that the distillate collected in the trough flows out to a metering cylinder.

All stages of the still are mounted on the top of each other and special rubber sealant strips are placed between the installation surfaces in order to prevent the escape of the water vapour from the system.
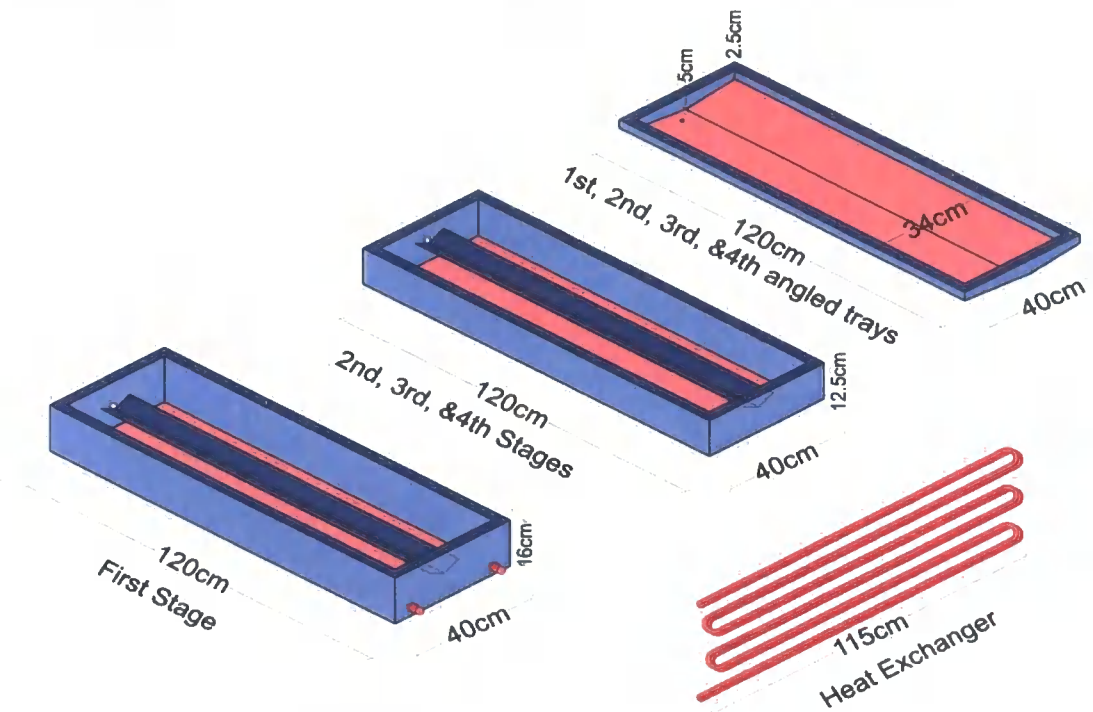
Figure 8-4: Multi stage still components and heat exchanger
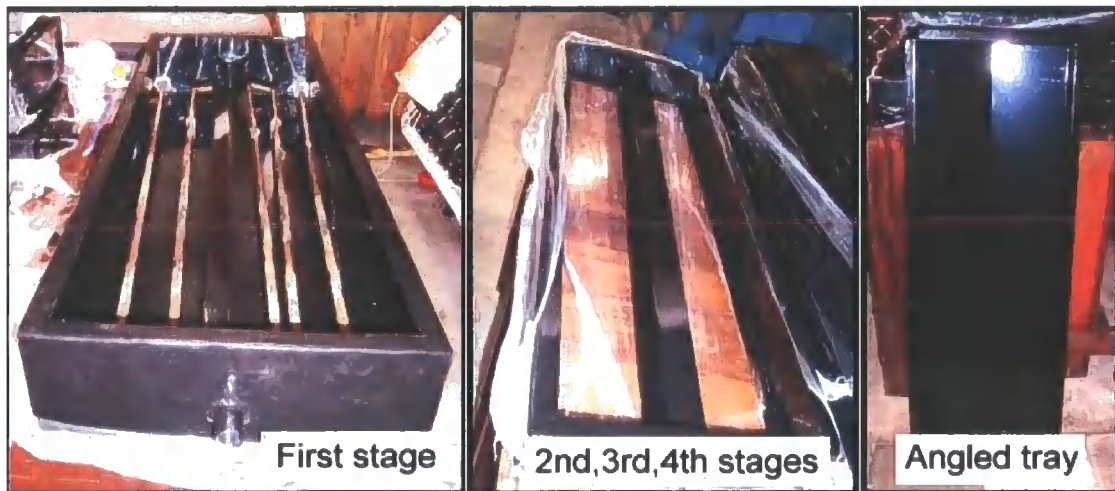
Figure 8-5: Multi stage still components

8.1.3 Heat exchanger

A serpentine heat exchanger with length of 7 m made of a copper tube with an outer diameter of 15 mm was fixed at the bottom of the first stage using plastic clips, as shown in Figure 8.4. The fresh water passes the heat exchanger and is heated by the

solar collector. Heat is transferred to the brackish water through the walls of the heat exchanger.

The inlet and outlet of the heat exchanger are connected to the outlet and inlet, respectively, of the copper manifold header pipe of the solar collector so these form a closed circuit, where clean water or antifreeze type fluid is circulated by an electrical pump.

8.1.4 Circulation pump

A GRUNDFOS - UPS 15-50 Selectric circulation pump was used to pump the hot fresh water from the solar collector to the heat exchanger.

This pump was selected to withstand the high temperature of the circulated water up to 100°C when heated by the evacuated tube solar panel and a maximum pressure of 10 bar. It also had to work under water, operating at an ambient temperature of 40 °C. Figure 8.6 depicts the pump performance curves.
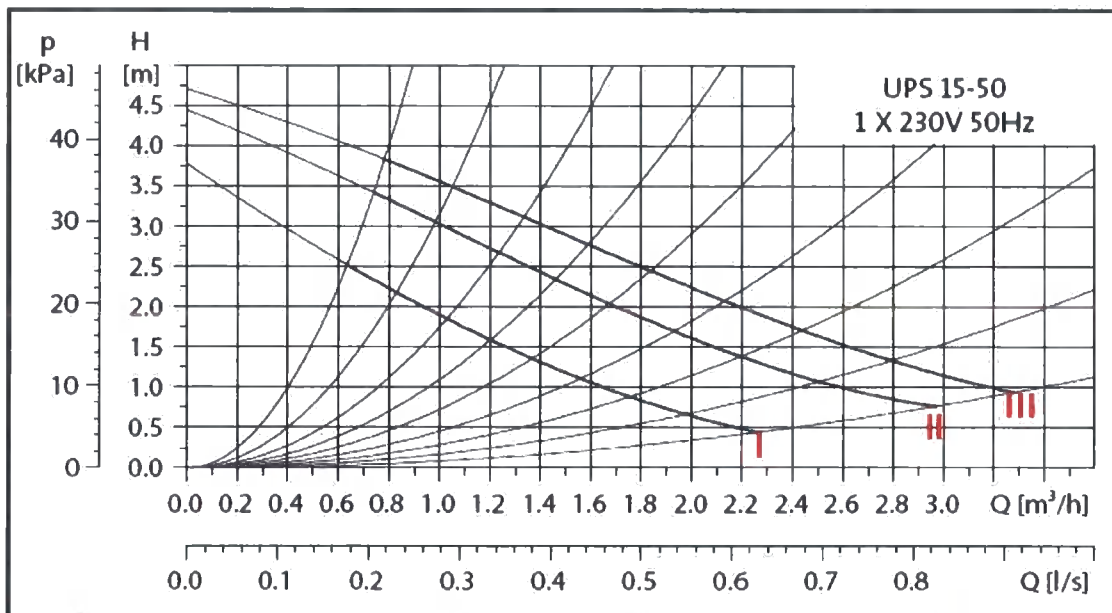
Figure 8-6: Pump curves for flow rate versus head pressure - A GRUNDFOS - UPS 15-50 Selectric circulation pump

8.1.5 Insulation Material and metering cylinders

Strips of glass mineral wool insulation material of thickness 15 cm and thermal conductivity of 0.044 W/m.K were used for the thermal insulation of the still. All tubes and pipe connections were also insulated using a polyethylene foam insulation material.

Four graduated metering cylinders were used to collect and measure the fresh water distillate from each stage, as shown in Figure 6.1.

8.2   Experimental test procedure

Prior to the experiments, the solar still was assembled so that all sections were horizontal and covered by thermo-insulation made from mineral wool.

The still was filled with synthetic brackish water from a single inlet point at the top of the still. The level of the water in each stage is controlled by adjusting the height of the special overflow pipe. When the level of the saline water reaches the desirable height in the angled tray then the water overflows to the next stage. The bottom stage is also equipped with overflow pipe which maintains a 40 mm water depth. When the system is full then the overflow pipe valve is closed. The volumes of the water in the first, second, third and fourth stages were 18.4, 4.2, 4.8 and 4.3 litres, respectively. The water depth in the angled trays varied from 0 to 25 mm.

The system was tested in conditions simulating a typical mid-summer day in the Middle East region. Thus the information on the variation of the solar radiation on 15 July 2004 [114] in this region was used and this is illustrated in Figure 8.7. The voltage of electrical power supplied to floodlights was adjusted every 20 minutes in order to simulate the insolation profile in accordance with the calibration diagram presented in Figure 8.8. This calibration was conducted at variable voltage using a pyronometer to measure the insolation for different locations on the light solar panel. Then the measured data was averaged and analyzed to produce the insolation voltage diagram as shown in Figure 8.8. The array of flood lights installed in the test rig replace the solar flux by heat flux and these lights cannot reproduce the sun's UV radiation. There are special bulbs which reproduce a UV band but they are extremely expensive. However the measured solar collector efficiency was found to be within the range of the manufacturer's solar panel efficiency as shown in the experimental results. Hence the error of calibration was slightly small.

The mass flow rate of water through the collector was kept at 5.8 litres/min as recommended by a manufacturer. The tests were repeated several times and the water condensed during experiments was collected into four separate metering cylinders and

then the amount of the condensate was measured after a 24 hour period. An analysis of water quality was also performed at the end of the experiment.
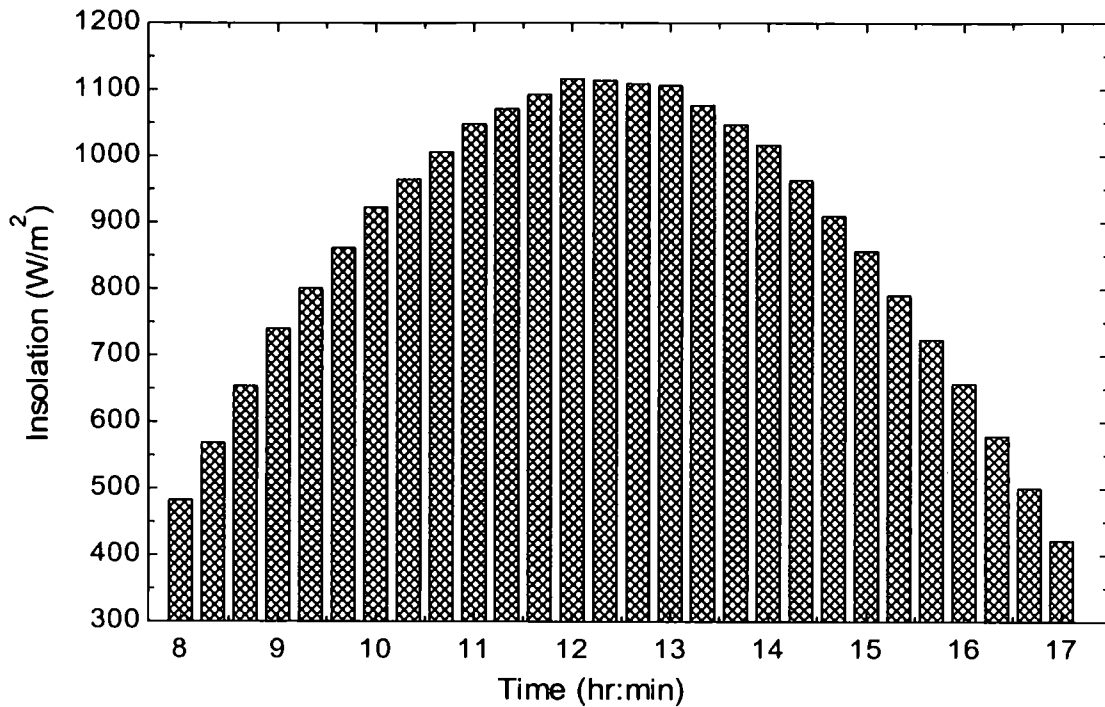
Figure 8-7: The mid-summer insolation variation in the Middle East region

$$G = 0.00152125 \cdot (V)^{3.09756}$$
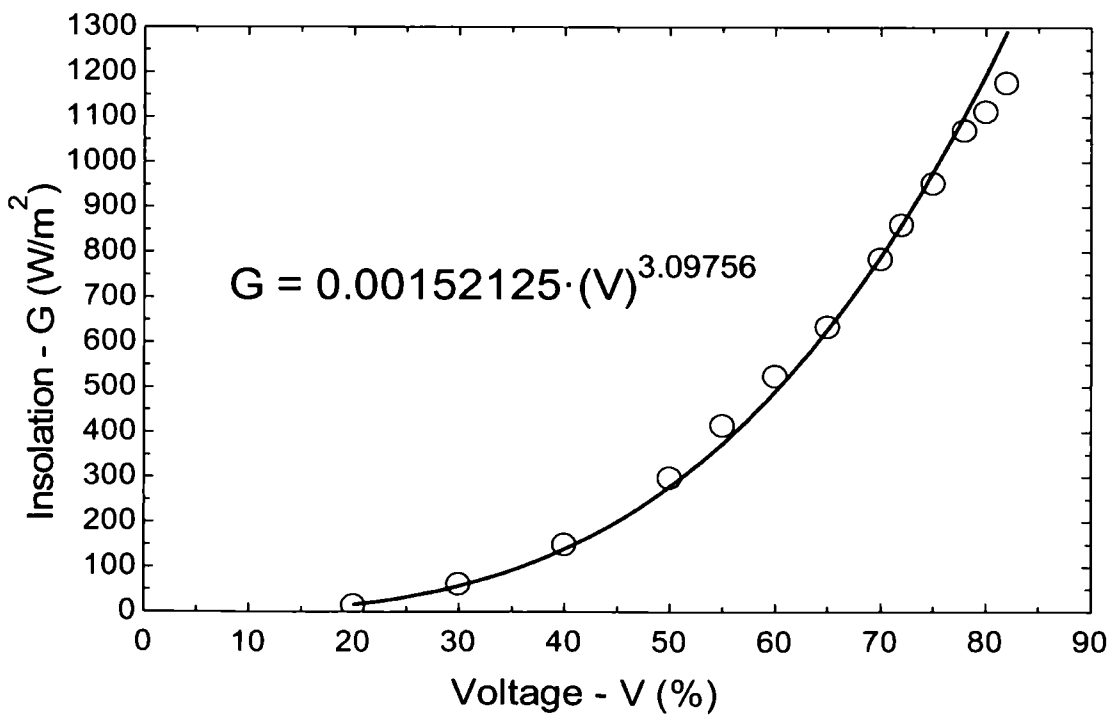
Figure 8-8: Radiation level versus transformer voltage calibration results

8.3 Measurements

The experimental measurements includes data from thermocouples at various locations in the rig including the inlet and outlet of the evacuated solar collector, the heat exchanger, the water body and the condenser surfaces in each still stage. In addition, the average ambient temperature variation was recorded. All these values were measured using K-type thermocouples connected to a multiple data logger acquisition system with a laptop computer to record and store continuously the averaged values at one minute intervals with the use of Picolog recorder software as shown in Figure 8.9.

The mass flow rate through the solar collector and heat exchanger was recorded and kept within the range of the solar collector manufacture's recommendation. In addition, the solar radiation (insolations) were measured using a pyronometer.

The distilled fresh water was collected from all four still stages separately using metering cylinders. Readings were taken every hour from 08:00 to 17:00 and the system was left working during the night after switching off the heating lights and the circulation pump.
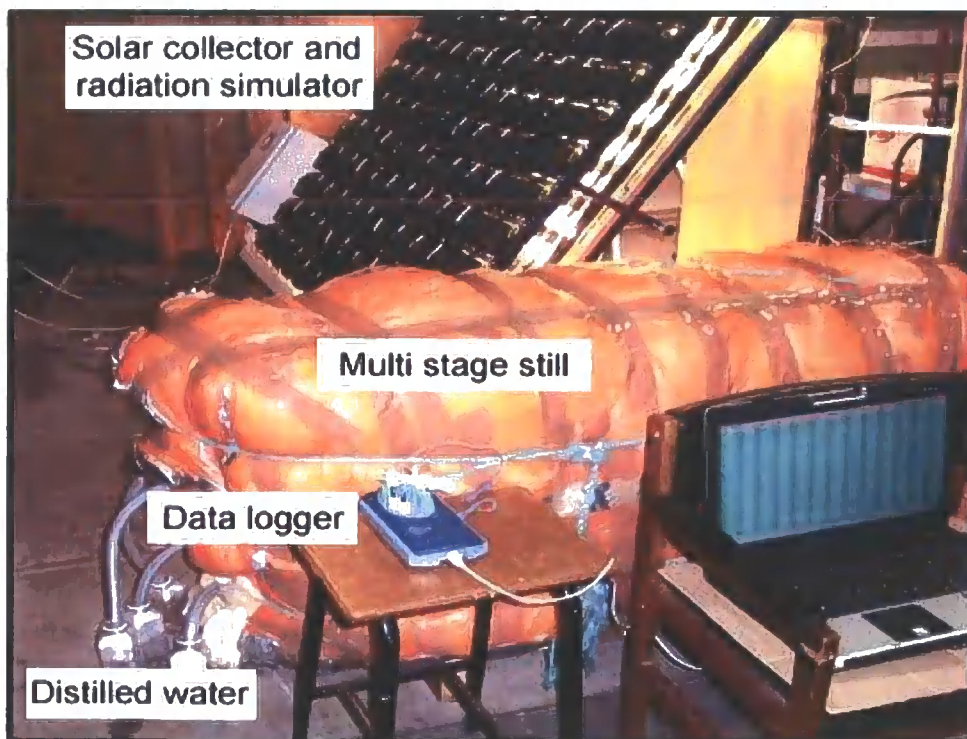
Figure 8-9: Photograph of the experimental desalination plant

8.4 Results and Analysis

To study the productivity of water distillation and the system performance, the system was investigated under two conditions namely when the system was fully insulated and when it was partially insulated. Hence two sets of data were collected for the conducted experiments and the Engineering Equation Solver software [115] was used to perform the theoretical calculations.

8.4.1 Fully insulated system

The experimental investigations made when the system was fully insulated showed that the system reached the steady-state condition 40 minutes earlier than the system with the partial thermal insulation. As it can be seen from the diagrams in Figure 8.11, the system operated for approximately 420 minutes, from 08.00 to 17.00 hours. At the end of this time period, the temperature in each stage reached the same level of about 96 °C. Following the corresponding reduction in the insolation level the temperature in all stages reduced but the temperature in the upper stages dropped more slowly. It was observed, that the insulated system gradually reached the thermal damage condition in which the temperature of the condensing surfaces exceeds that of the evaporation surface and therefore the distillation process stops.
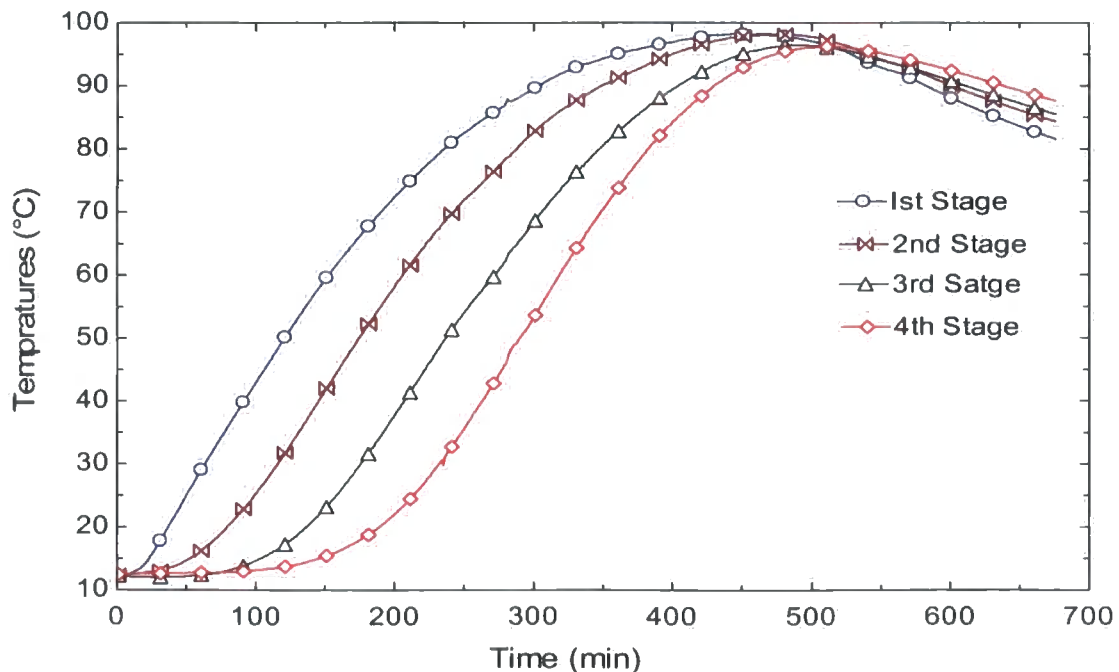
Figure 8-10 The variation of temperatures in the still with full thermal insolation

The amount of water produced in the 24-hour period was about 3.1 kg/day, as shown in Figure 8.11. The theoretical water productivity values showed a correlation with the experimental ones, as shown in Figure 8.12. The array of light bulbs was switched off at 17.00 hours but the recording of temperatures inside the still was continued and, 14 hours later, the temperature of the water in all the stages was equal at about 60 °C.

These results show that, for the given insolation conditions, the evaporation area of the still should be considerably increased in order to take advantage of the high radiation level. Consequently, the still should be filled up by a large amount of brackish water. In order to reduce the water temperature in all the stages by the start of the next day's operation, the still or a part of it should be freed from the thermal insulation.

See Appendix B for EES program code and Appendix C for experimental results and theoretical calculations.
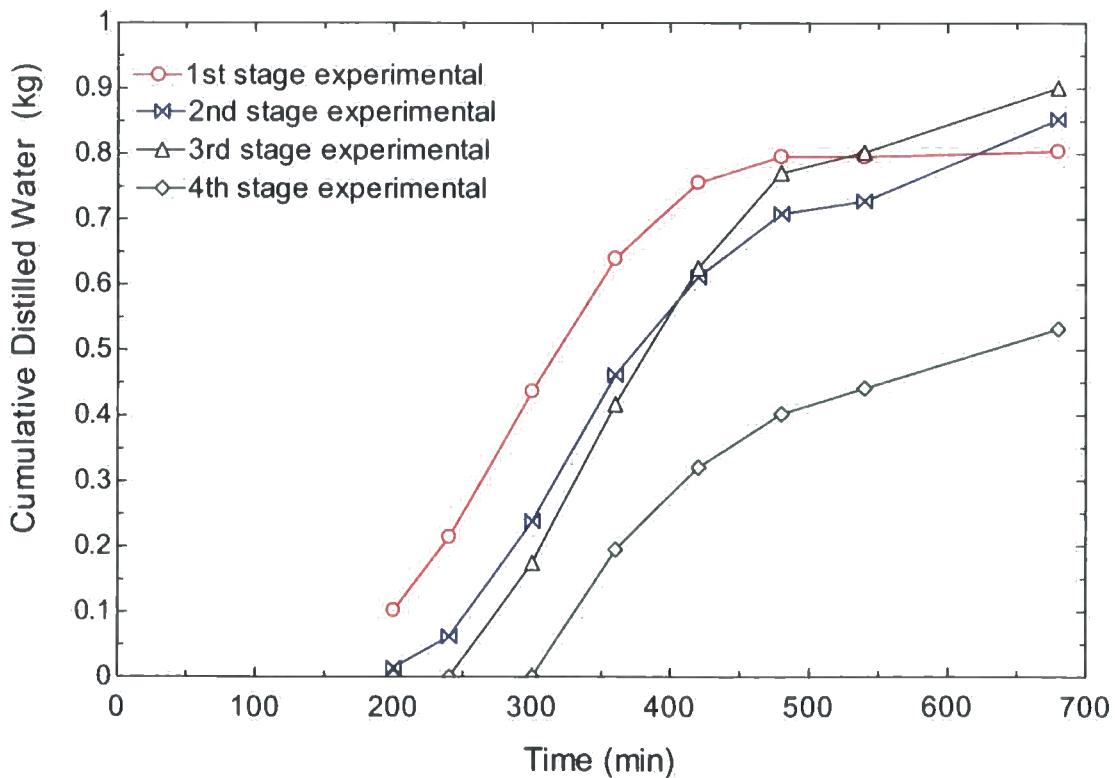
Figure 8-11: Experimental cumulative distillate output as function of time
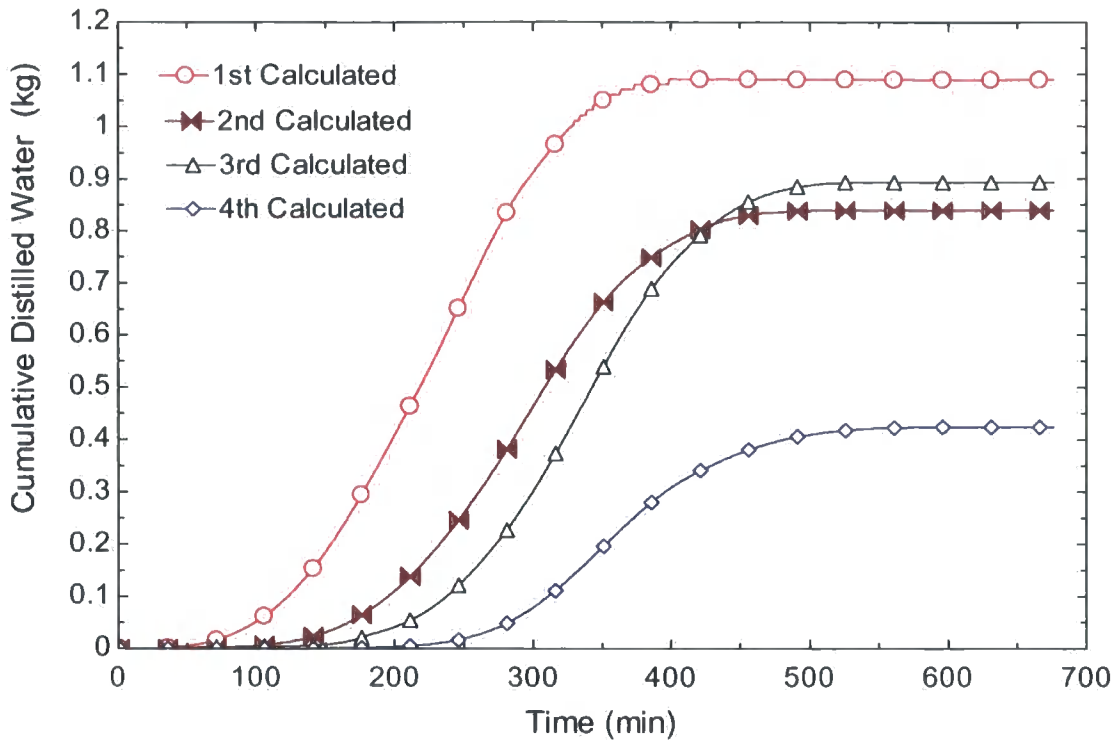
Figure 8-12: Theoretical cumulative distillate output as function of time

8.4.2 Partially insulated – (top uncovered) .

In this case, the bottom and the sides of the still were insulated and the upper tray of the still was left uncovered, as such conditions provided a continuous distillation process over 24 hour period. It can be seen in Figure 8.13 that during a typical summer day the desalination system can be heated up for approximately 540 minutes (from 8.00 am to 17.00). The array of floodlights was switched off at 17.00 but the temperature variations inside the still were recorded for the complete 24 hour cycle. It can be observed that that temperature of the water in the trays gradually decreased once the floodlights were switched off.

It also can be seen that, due to the relatively large heat losses from the upper open tray, the temperature of water in the final stage (maximum 80 $^{\circ}$C) is significantly lower than that in the first and second stages (maximum 99-100 $^{\circ}$C) and this allows the continuous condensation to be maintained. At the end of the 24 hour cycle the temperature of the water in the still is between 30 $^{\circ}$C and 40°C.
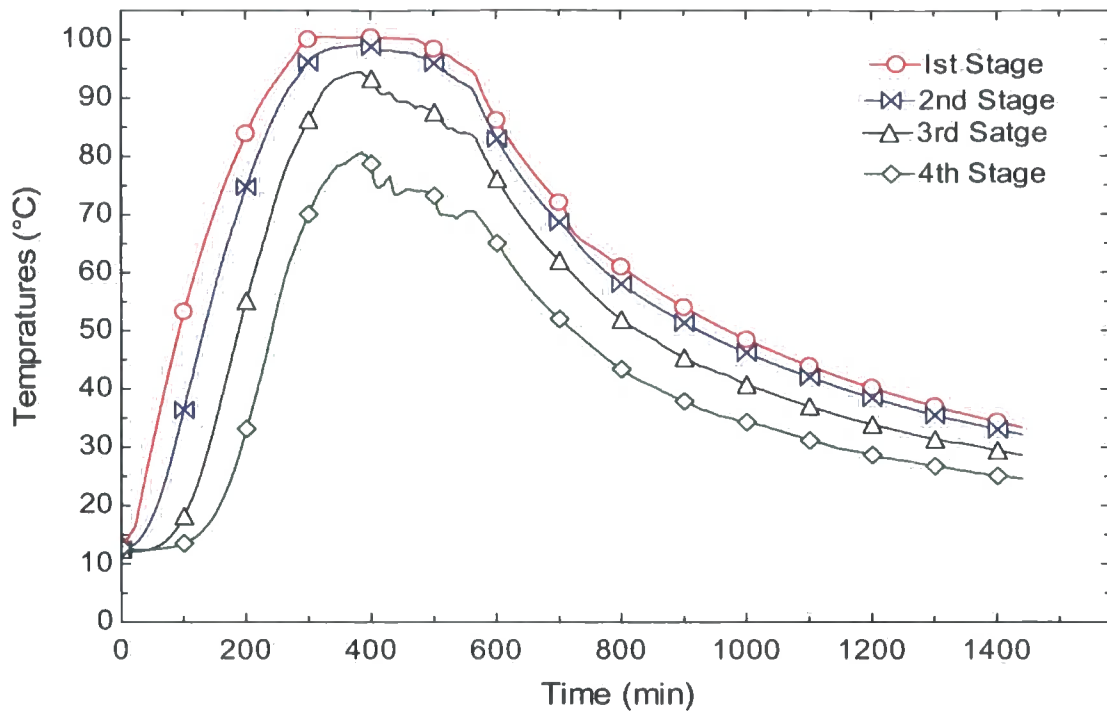
Figure 8-13: The variation of temperatures in the still with full thermal insolation

Recharging the still at the start of the next day with a new supply of brackish water reduces the temperature of the water in all the stages to approximately the same level as at the start of the initial experiment.

Figure 8.14 presents the predicted temperature variations in the stages and it can be seen that the character of the temperature curves corresponds to that of the experimental data, although the predicted temperatures are lower than the experimental ones by approximately 10 °C. The possible explanation for this discrepancy is the inaccuracies in the determination of the input heat and the magnitude of heat losses.

The rate of condensation of water in each stage is determined mainly by two factors, namely, the temperature of the water in the trays and the temperature differences between the stages.
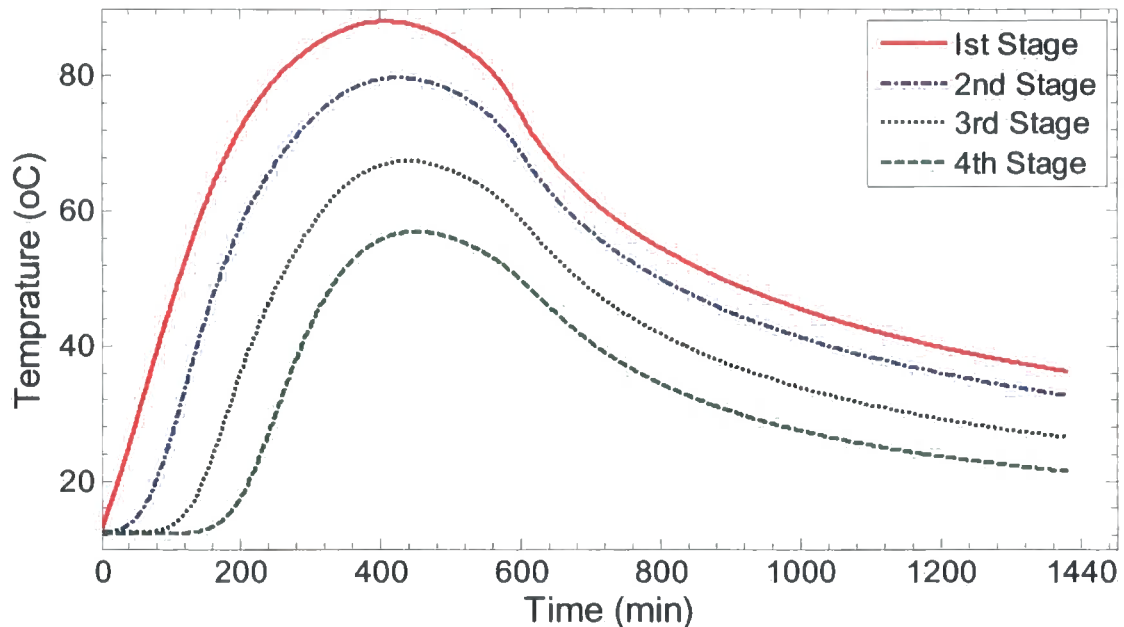
Figure 8-14: Simulation of variation of water bed temperatures in the still with partial thermal insulation

The maximum temperature difference of 14-21 °C is achieved between the stages during the heating up period. During the daylight period the first stage initially produces most of the distilled water, but then gradually the amount of the water coming out of the second stage becomes considerably greater. Finally, the third stage produces most of the condensate. The fourth stage produces the least water during the first 8 hours of the operation due to the low temperature of the water in the tray, but its distillate accumulated over the 24 hour period is less only than of that produced in the third stage. Overall, about 9 kg of the distillate was produced over the 24 hour period, with more than 7.7 kg produced during the solar test over the 10-11 hour period, see Figure 8.15.
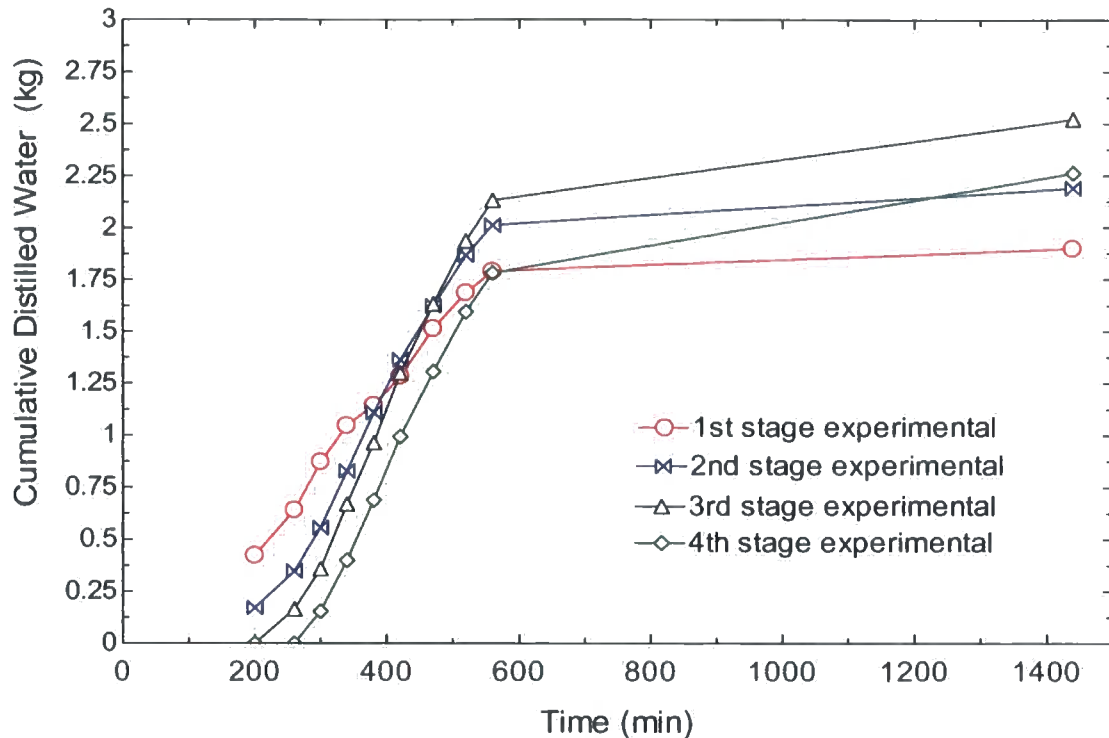
Figure 8-15: Experimental distillate output as function of time

Figure 8.16 shows the calculated distillate production curve for each stage over 24 hours. From Figure 8.17 it can be seen that there is a noticeable difference in the dynamics and quantity of the distilled water produced between experimental measurements and theoretical data obtained for each stage. Numerical data shows that the model noticeably over-estimates the production of water in the third (about 3.5 kg instead of 2.7 kg from experiments) and fourth (about 2.75 kg instead of 2.25 kg from experiments) stages but data for other two stages is in good agreement with information obtained from tests. Inaccuracies in theoretical estimations can be accounted for by the fact that not all the vapour generated was captured due to leakages from the system, errors in the estimation of heat losses and also in the horizontal positioning of the still and measurements of amount of water in each stage.

In experiments it was recorded that the highest distillation rate occurred when the solar radiation reached its maximum and this was then maintained for some period of the day. The average temperature differences recorded for all the stages, from the first

to the fourth, were 2.9, 5.6, 8.3 and 10.8 $^{\circ}$C, respectively, as shown in Figure 8.17.
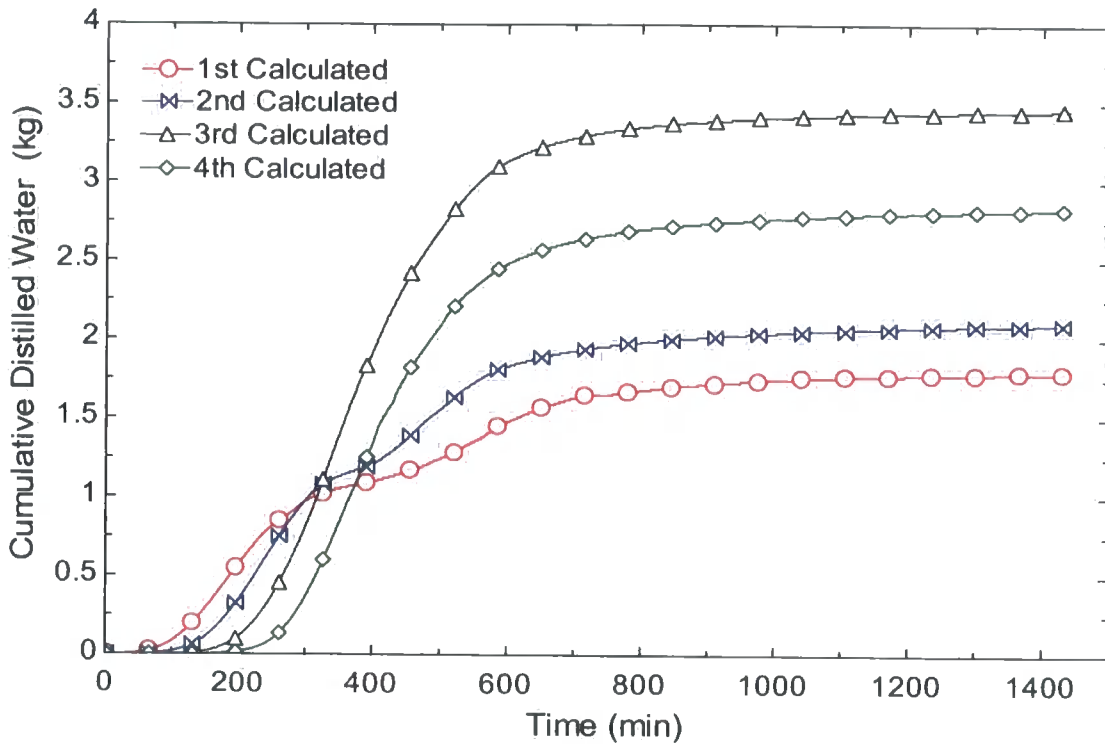
Figure 8-16: Theoretical distillate output as a function of time
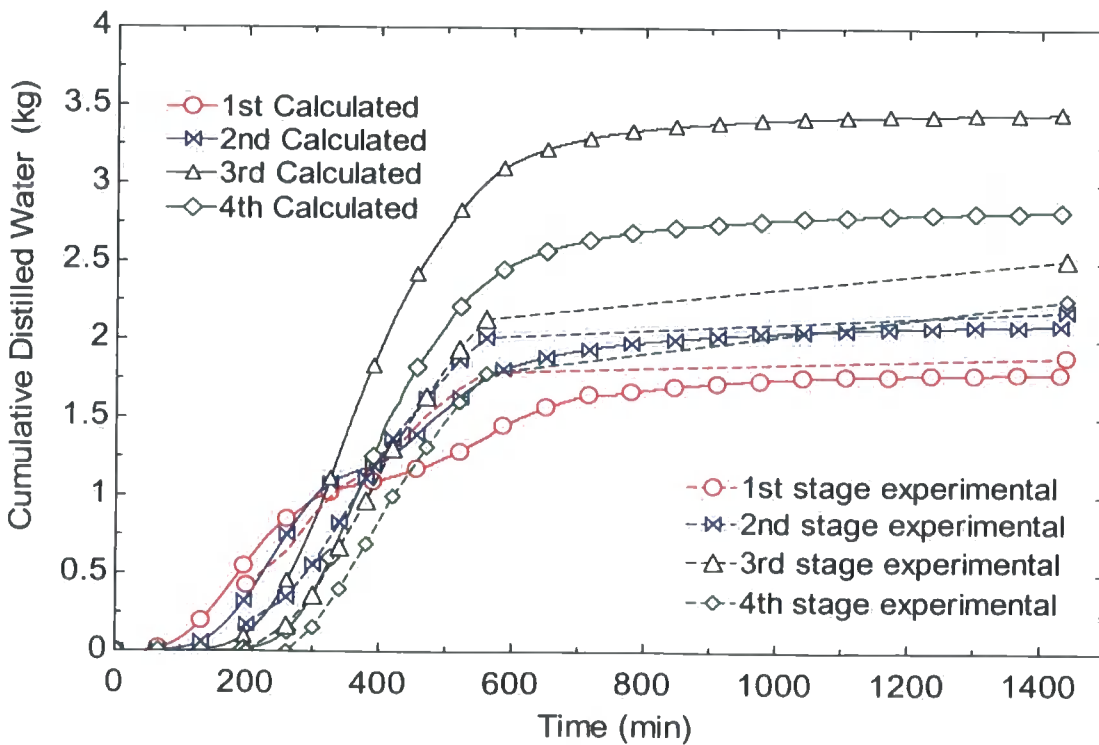
Figure 8-17: Theoretical and experimental distillate output as a function of time

Therefore the third and the fourth stages produced the largest quantities of water. Adding cold water to the upper surface of the fourth stage after 400 minutes of the operation resulted in a sudden decrease in the temperature of the condensing surface and a sharp jump increase in the temperature differences between the evaporative and condensing surfaces as well as a corresponding rise in the distilled water production as shown in Figure 8.18. This confirms the theoretical analysis.

Figure 8.19 compares experimental and theoretical results on the dynamics of the overall water distillation process in the still. The calculated total amount of the distilled water produced (about 9.7 kg/day) differs from the experimental value (about 9 kg/day) but these results show that the developed mathematical model describes performance of the installation within an acceptable level of tolerance and hence it can be used in the design process.
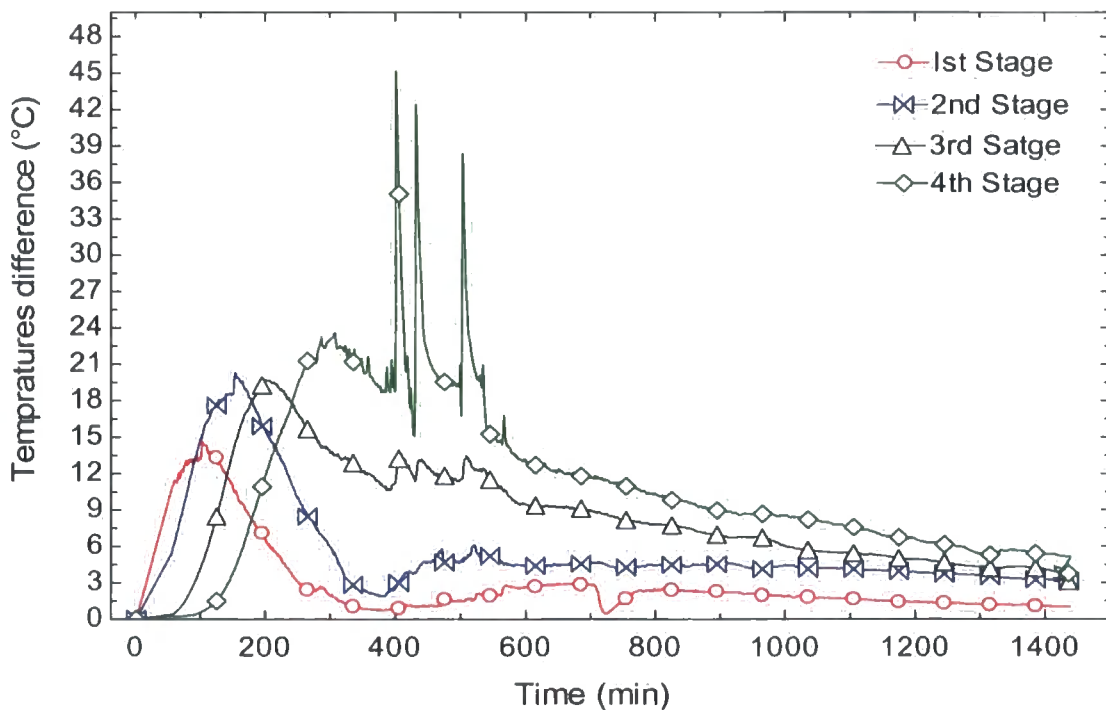
Figure 8-18: Differences in evaporation and condensing surface temperatures in the still
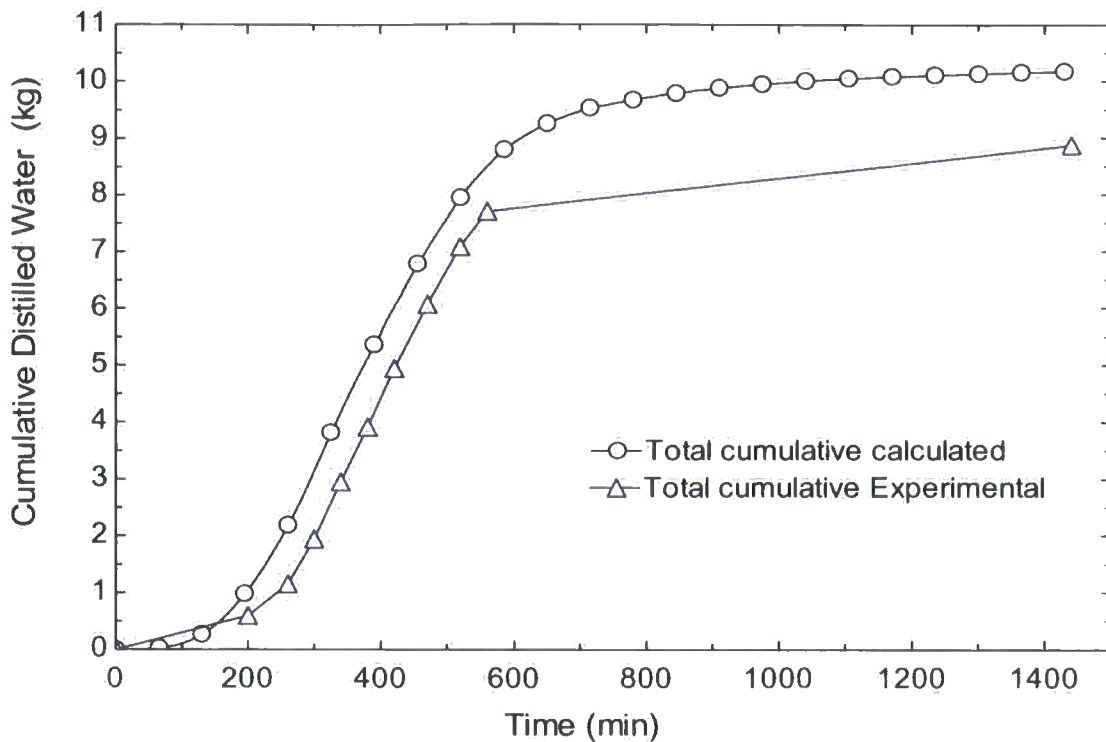
Figure 8-19: Theoretical and experimental values of the total cumulative distillate output

The experimental results demonstrate the comparatively high distillation efficiency of 90%. The solar collector efficiency is about 68% with the overall efficiency being about 33%. The low overall efficiency is the result of significant heat losses in the system.

8.4.3 Water body depth effect

An increase of water depth in the still stages was found to have a clear influence on water productivity. In this condition the system was investigated under the same circumstances while the depth at the second, third, and fourth stages changed linearly from 0 to 0.03 m respectively

The output varied between day and night, as the night time output was the result of energy being stored in the system during the initial hours of operation. It was found that the higher the depth of the water body, the higher was the night time water output, as seen in Figure 8.20. In this condition the peak temperature and the steady state were reached more slowly than in the case of smaller depth. As the depth of water increased

from 0.025 to 0.03m, the nighttime distilled water output increased by 0.123 kg but the day time output decreased by 1.18 kg.

For the case of depth equal to 0.03 m, the total accumulated water productivity was 5.22 kg, a decrease of 20 % on the output when the depth was 0.025 m. Also, the temperature at each stage decreased by 5 $^{\circ}$C compared with the 0.025 m depth case. Therefore, it was found that operating the system with a depth 0.025 m was more efficient than operating with a 0.03m depth.

Water productivity as a function of water depth in the first stage was also simulated with different water body depths ranging from 3 cm to 7 cm, as shown in Figure 8.21. It can be seen that the distilled water output decreases linearly with increasing the water depth; this demonstrates good consistency between the simulated results and the experimental ones.
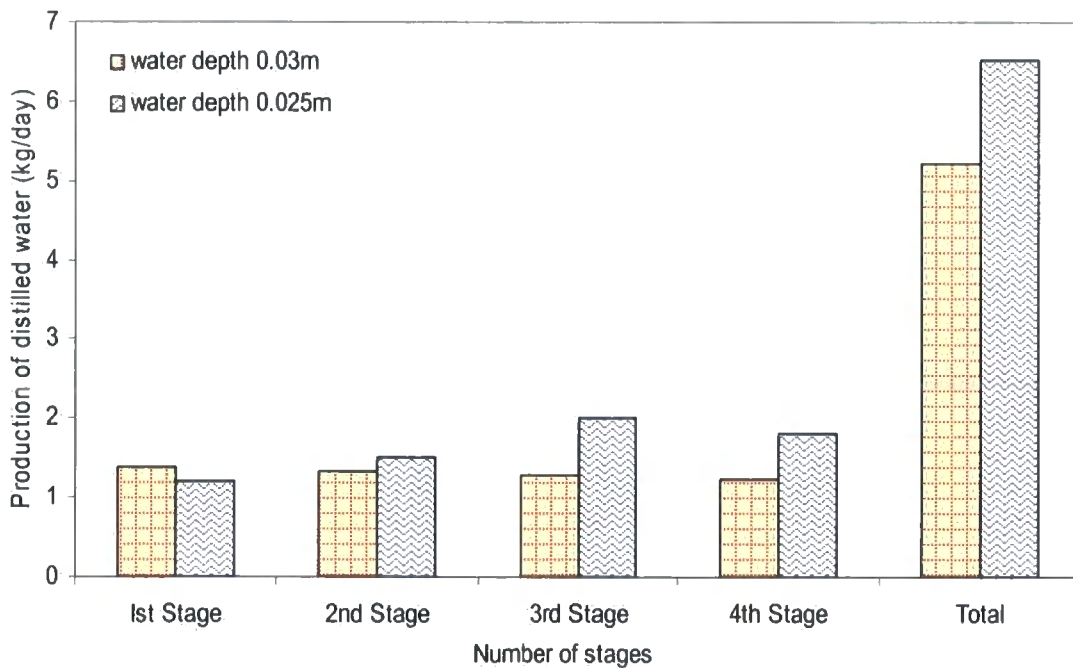
Figure 8-20: Experimental water distillate output as a function of water bed depth
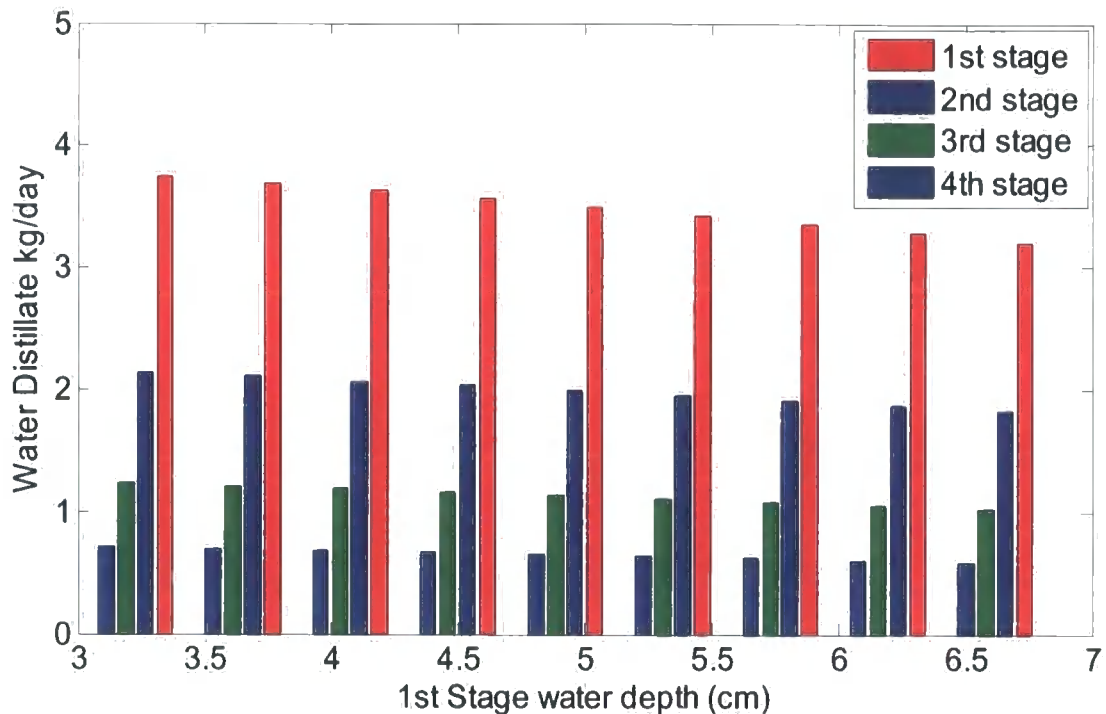
Figure 8-21: Simulated water distillate output as a function of water bed depth

To sum up, both the experimental results and theoretical analysis confirmed that the surface of water evaporated as a function of its temperature, irrespective of whether it was heated by the sun or by another source of energy. It was also shown that the rate of production of distillate water was proportional to the area of the evaporative surface, which confirmed the conclusion of Fernandez, (1990) [107] that a small distillation area at the first stage results in a very high temperature and therefore considerable loss of steam at the first condensation. This is responsible for the low water production (the amount of distillate water divided by the total collector area). To overcome this problem, it is necessary either to increase the distillate area by installing more distillation units whilst preserving the existing evacuated tube solar collector area or to resize the solar collector heating system.

In order to keep the system working, the latent heat of condensation in the last stage should be mainly dissipated to the environment via its upper surface. Alternatively, the fourth still could be coupled with the saline water storage tank used to recharge the stills and keep their water depths constant, thus utilizing the latent heat of condensation produced at the fourth stage.

Irrespective of the lower overall desalination efficiency in terms of solar collector input heat, the overall production of distilled water as an expression of the total evaporative surface was found to be in accordance with the literature. This said that the overall all basin still efficiency should be about 25%, with a daily production 2 to 3 litre/m^2/day and rarely would it reach 4 litre/m^2/day. Fernandez (1990) argued that the highest water production of a multi stage still coupled with flat plate collector was 1.6 litre/m^2/day. Coupling the desalination system with evacuated tube solar collectors achieved a higher distilled water production of 4.94 litre/m^2/day.

Eventually the water productivity performance of the partially insulated condition proved to be the most feasible scenario for operating this desalination system

9   Modeling Simulation and determination of rational design parameters

9.1   Model simulation

A computer program for the proposed lumped parameter mathematical model was developed on Matlab language 2007a to simulate the design parameters and the water productivity inside multi stage stills, as illustrated in Figure 9.1

```
                        ┌──────────────┐
                        (    START     )
                        └──────────────┘
                               │
                               ▼
                    ╱─────────────────────╲
                   ╱    Read Input Data     ╲
                   ╲     Lᵢ, Wᵢ,,hᵢ  Still   ╱
                    ╲─────────────────────╱
                               │
                               ▼
                    ┌─────────────────────┐
                    │ Specify initial      │
                    │ parameters           │
                    │ Ts1, Ts2, Ts3, Ts4, Qc│
                    └─────────────────────┘
                               │
                               ▼
                      ╱─────────────────╲
                     ╱  Read Time (t=0)  ╱
                    ╱─────────────────╱
                               │
                               ▼
                    ┌─────────────────────┐
                    │ Calculate convective │
                    │ and evaporative heat │
                    │ transfer coefficients│
                    └─────────────────────┘
                               │
                               ▼
                    ┌─────────────────────┐
                    │ Determination of     │
                    │ predicted Temperature│
                    │ and water production │
                    └─────────────────────┘
                               │
                               ▼
                        ┌───────────┐
                        │  t = t+1  │
                        └───────────┘
                               │
                               ▼
                          ╱─────────╲
               ┌─────┐   ╱    If     ╲
               │ Yes │◄──┤  t < time   │
               └─────┘   ╲           ╱
                          ╲─────────╱
                               │
                               ▼
                          ┌───────┐
                          │  No   │
                          └───────┘
                               │
                               ▼
                    ┌─────────────────────┐
                    │   Print  Results     │
                    │   Tₛ, Tc, mₑ, ......etc│
                    └─────────────────────┘
                               │
                               ▼
                        ┌──────────────┐
                        (     END      )
                        └──────────────┘
```

L_i, $W_{i,}$, h_i Still

T_{s1}, T_{s2}, T_{s3}, T_{s4}, Q_c

T_s, T_c, m_e, ...etc
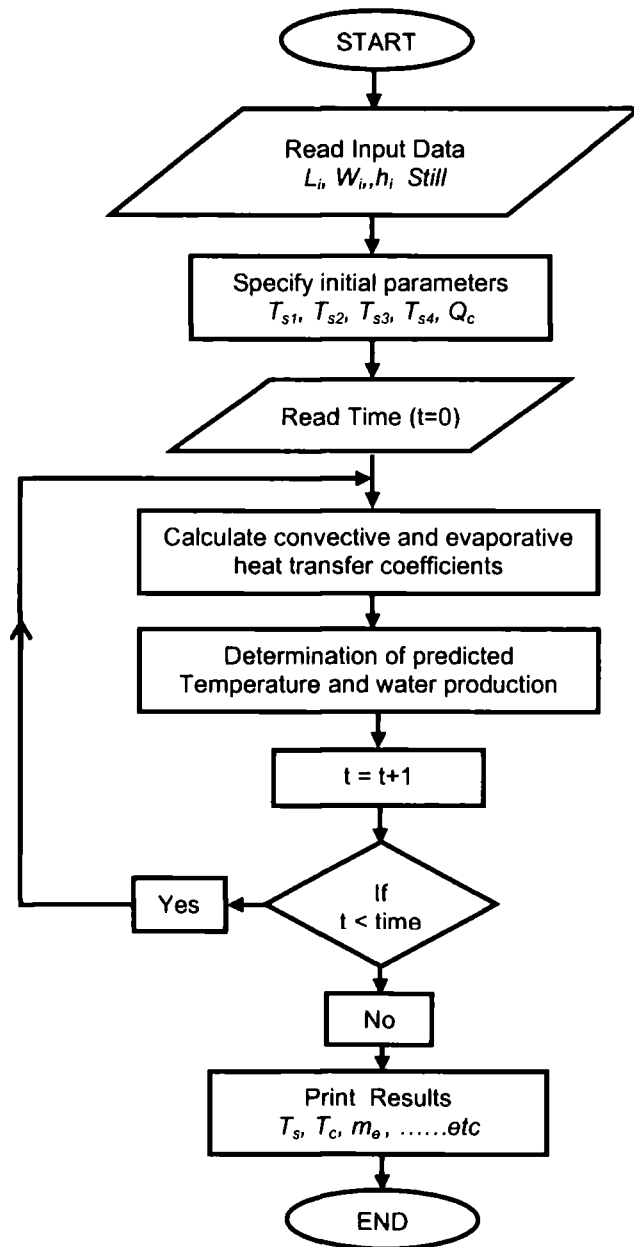
Figure 9-1: Computer simulation program flowchart

All thermo-physical parameters, including the various heat transfer coefficients and water productivity, were calculated for each stage. The corresponding temperatures and water productivity were also simulated and determined.

In this case, the four stages solar still was simulated for 24 hours for the same experimental conditions with a dynamic variation of Middle East summer insolation

Figure 9.2 shows the predicted water distillate productivity in each stage. It can be seen that there were acceptable differences between the amount of distilled water produced experimentally and the predicted amount. Hence it can be seen that there was a good correlection between the total experimental, total theoretical and the total predicted water distillate quantities of 9 kg/day, 10.18 kg/day, and 9.7 kg/day respectively, as shown in the previous corresponding figures.
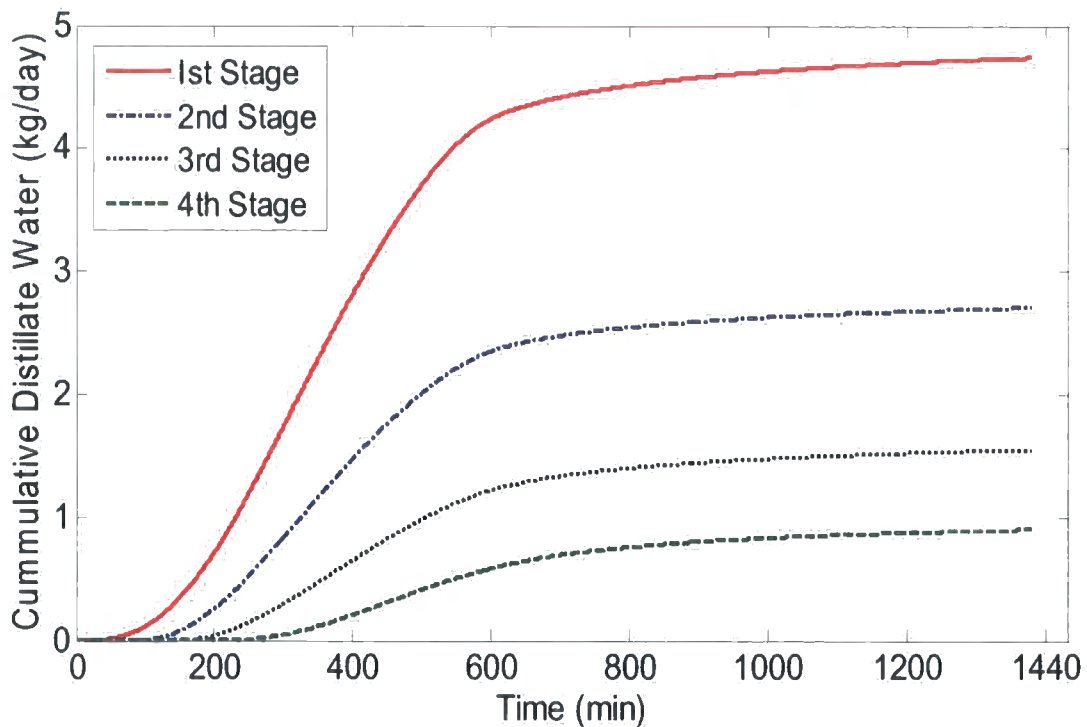
Figure 9-2: Prediction of water distillate output

9.2   Determination of rational design parameters of the still

After the experimental validation, the mathematical model was used to find rational design parameters of the still. In the first phase the four-stage still with a 40 mm water depth in the first stage was modelled in order to find the value of the evaporation area of each stage which provides the highest distillate production in a typical Middle East region summer day. The restriction which was imposed during simulations was that the depth of water in the first stage should not drop below the 3 cm level so that the heat exchanger was always submersed in the saline water. Figure 9.3 presents results of such calculations and it can be seen that the minimum value of the evaporation area equal to 1 m^2 satisfies the above requirement with the highest distillate production of about 21 kg/day.
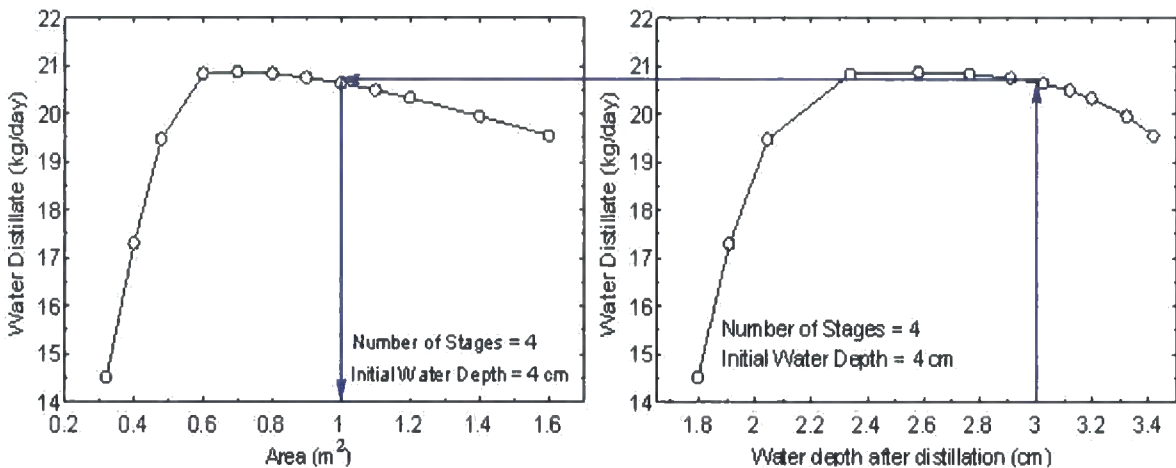
Figure 9-3: Determination of the rational evaporation area of the stages

In the second phase, the dependence of water productivity from a number of stages was investigated for a still with an evaporation area of 1 m^2 in each stage. Results of the calculations are shown in Figure 9.4 and it can be observed that the increase in the number of stages results in a rise in the amount of the distillate from the initial seven stages but then the increase becomes very small, with a virtually stagnant line, due to the fact that, after seven stages, most of the input heat is utilized and consumed in the evaporation process.
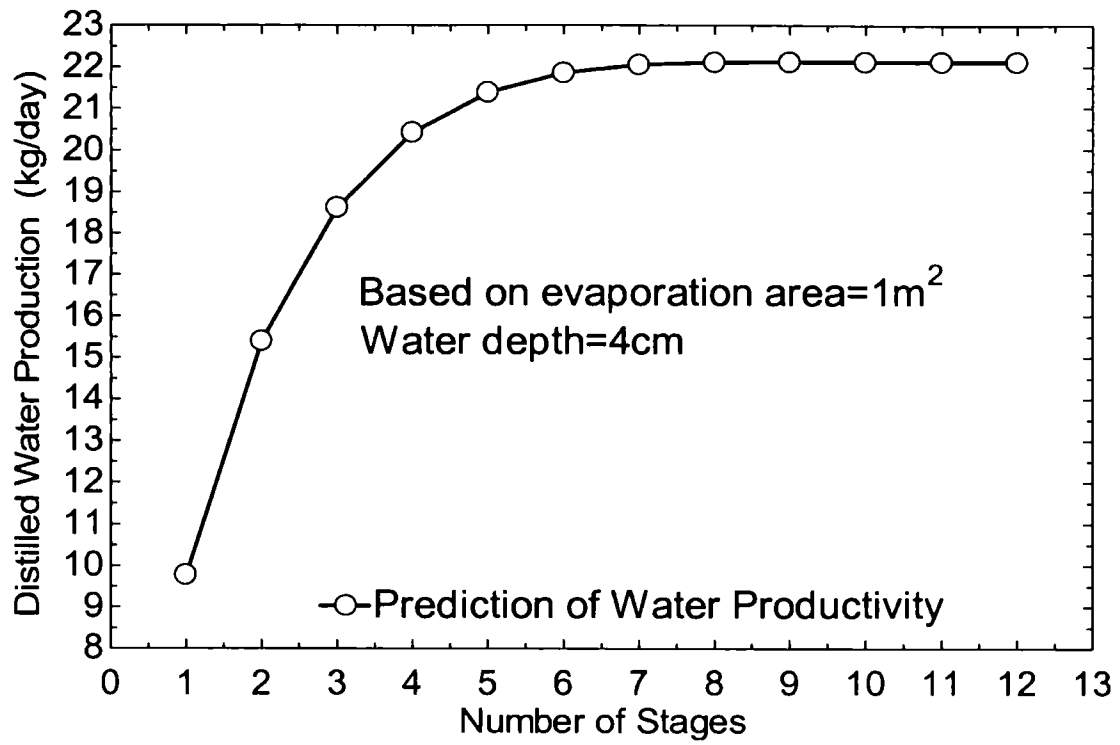
Figure 9-4: Determination of rational number of stages

10 Water Quality Results and Analysis

The most crucial aspect which needed attention is the distillate water quality. Generally, thermal water evaporation processes provide high quality condensate and this was confirmed during experiments in this study. In order to evaluate the water quality treatment efficiency of the proposed multi stage still desalination system, three parameters, namely total dissolved solids (TDS), electrical conductivity (μS/cm) and pH, were measured for each stage for the input saline water and desalinated output water, using a MYRON L Ultrameter II instrument with an accuracy of +/- 0.01 pH and conductivity in the laboratory, as shown in Figure 10.1

Figure 10-1: Photo for Ultrameter II instrument

Synthetic brackish water with total dissolved solids concentrations similar to that of brackish water found in the Gaza Strip was prepared in a Durham University laboratory for use in the multi stage stills

Figure 10.2 shows the composition of Gazan brackish water. It is clear that sodium and chloride represent the greatest contaminant concentrations.
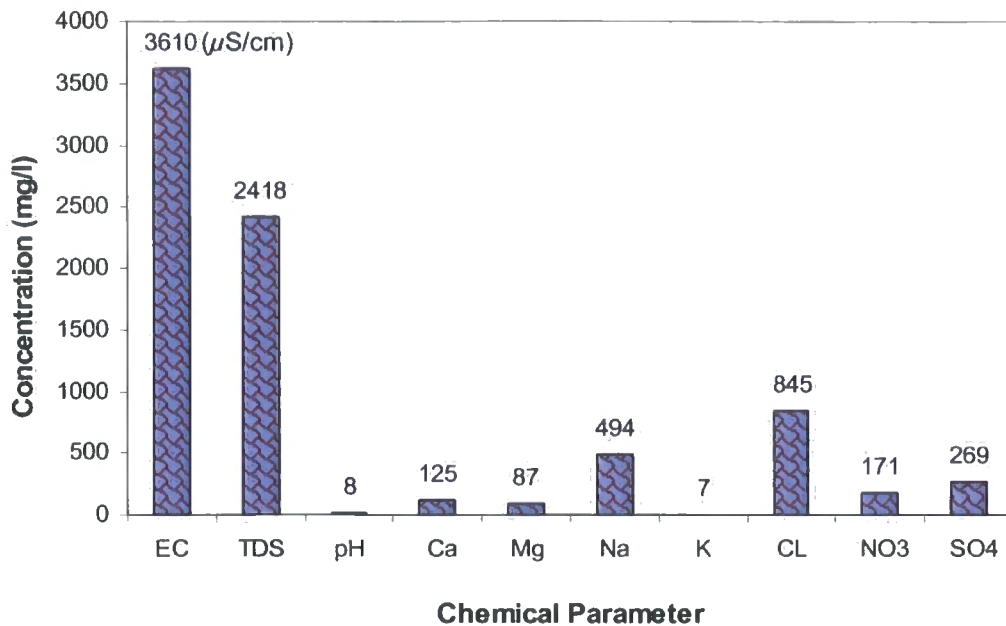
Figure 10-2: Brackish water composition at Gaza strip

10.1 Preparation of synthetic solution

An analysis of Durham University tap water showed that it had chloride and sodium ions concentrations of 8.65 mg/L and 12.83 mg/L respectively. In order to simulate the concentrations of sodium and chloride found in Gaza, 1500 mg/L sodium chloride salt was added to the tap water so that the concentrations of these parameters become as follows.

1 mole of sodium chloride NaCl = 1 mole sodium + 1 mole chloride

1 mole of sodium chloride NaCl = 23 + 35.5 = 58.5 g

Chloride concentration = 12.83+(1500*35.5/(23+35.5)) = <u>923.1 mg/L</u>

Sodium concentration = 8.65+(1500*23/(23+35.5)) = <u>598.39 mg/L</u>

10.2 Water quality laboratory analysis results

The distilled fresh water collected separately from all four still stages using metering cylinders was analyzed every hour for each stage from the starting time of water distillation until 17.00 hours. Then the system was left working during the night for 24 hours and the fresh water produced during that time was analyzed the next day.

Table 10.1 presents the average water quality measurements for electrical conductivity, total dissolved solids and pH under the three thermal conditions (fully insulated and partially insulated as described in chapter 8. Appendix E provides the data for all hourly water quality analysis in all conditions.

Condition	Still	Before Distillation			After Distillation		
	Stages	Conductivity (μS/cm)	TDS (mg/L),	pH	Conductivity (μS/cm)	TDS (mg/L),	pH
Partially Insulated	1	3056.62	2323.34	7.07	38.85	24.58	7.13
	2	3056.62	2323.34	7.07	31.57	19.15	7.63
	3	3056.62	2323.34	7.07	29.38	18.33	7.9
	4	3056.62	2323.34	7.07	38.32	24.13	7.77
Average values		3056.62	2323.34.	7.07	34.53	21.55	7.61
Fully Insulated	1	3136.43	2407.75	7.30	29.46	18.86	6.01
	2	3136.43	2407.75	7.30	30.17	19.03	7.00
	3	3136.43	2407.75	7.30	39.41	24.71	7.47
	4	3136.43	2407.75	7.30	51.41	32.45	7.23
Average values		3136.43	2407.75	7.30	37.61	23.76	6.93

Table 10-1: The average of water quality parameters measurements before and after distillation

Figures 10.3, 10.4 and 10.5 show the TDS, pH and electrical conductivity values respectively. All the hourly samples, and particularly those from the partially insulated scenario, showed that the system produced very pure water with average TDS of less than 24mg/L, an average electrical conductivity of 37.61 μS/cm and a pH of between 6 to 8.

According to the WHO drinking water quality guidelines, water with sodium and chloride concentrations of less than 200 mg/L and 250mg/L respectively and with TDS of less than 600mg/L are considered good, and water becomes unpotable at an electrical conductivity greater than 2500 μS/cm [4]. This desalination system produced distilled water with TDS concentrations of less than the upper limit for both sodium or chloride. From the literature review of water quality [4, 55] it was seen that WHO does not propose any limits for pH values but, according to EPA regulations, a pH level of 6-9 has no direct impact on human health.
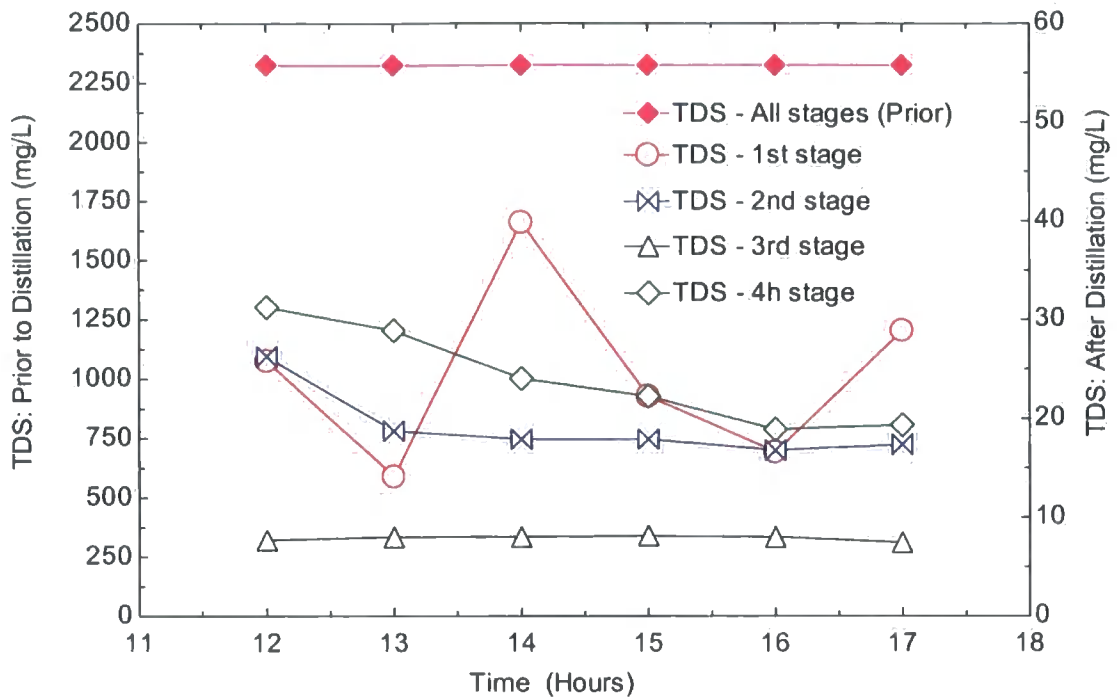
Figure 10-3: Results of total dissolved solids analysis for one day
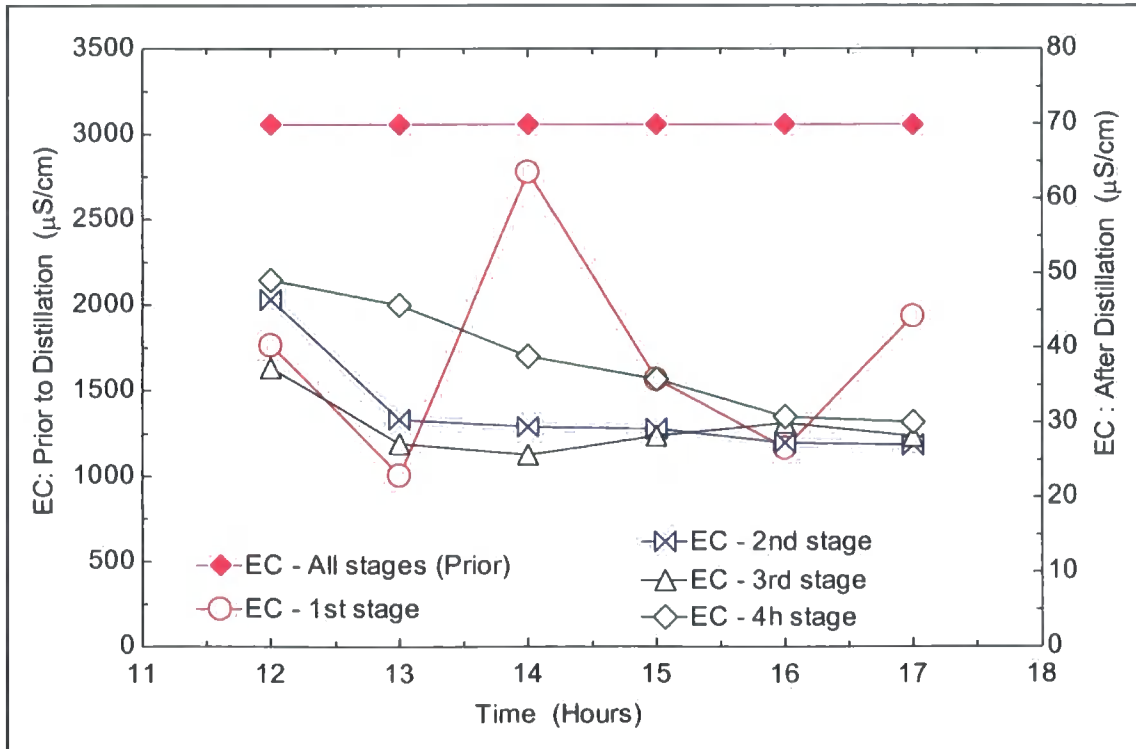
Figure 10-4: Results of electrical conductivity analysis for one day
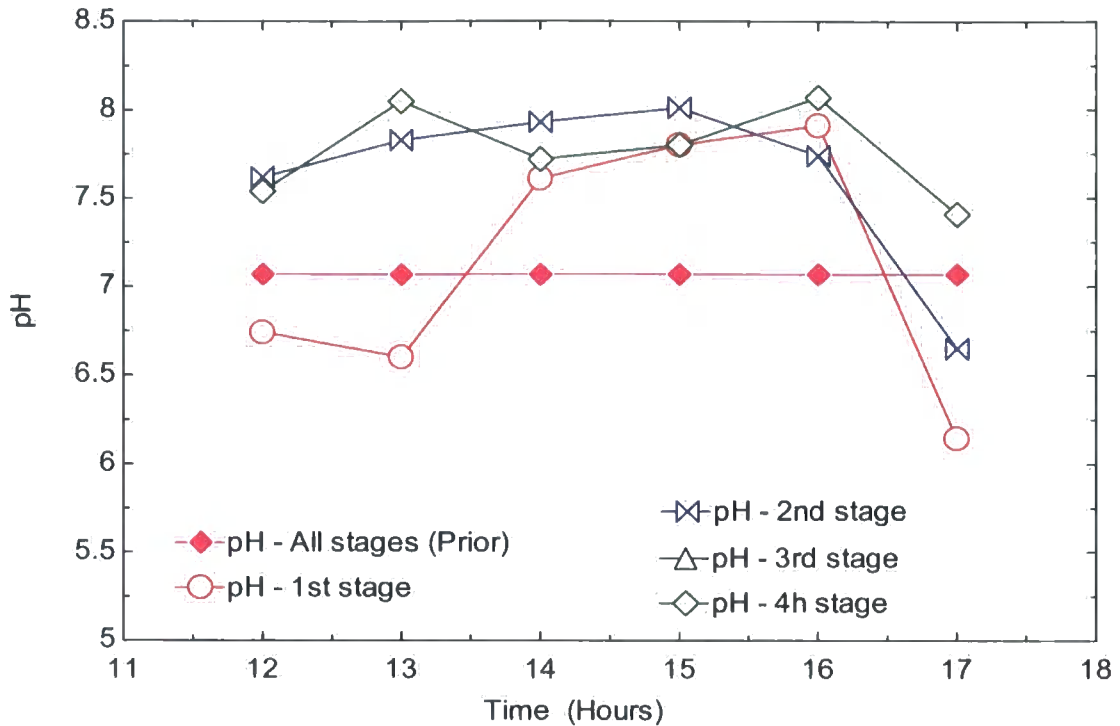
Figure 10-5: Results of pH analysis for one day

10.3 Significance t – test.

The significance test is a widely used statistical technique used in the evaluation of experimental results. It is used to decide whether the difference between the two measured results or the measured and standards values is significant or whether it can be accounted merely by random variations. In this analysis a t-test has been conducted to examine the significance of pH values for three days water analysis results as shown in Appendix E. [116]

10.3.1 Comparison of two sets of experimental results

To apply the t- test we have to test the truth of a hypothesis which is known as a null hypothesis and this means that there is no difference between the values of two observed data sets other than that which can be attributed to random variations. It is assumed that the null hypothesis is true when the means of two sets of data are equal. And usually the null hypothesis is rejected when the probability of such a difference is less than 5% then the difference is said to be significant at the 5% level.

In this case we have two sets of pH experimental analysis results with means of $\bar{x}_1$ and $\bar{x}_2$ and we need to test whether $(\bar{x}_1 - \bar{x}_2)$ differs significantly from zero. The statistical parameter t and the arithmetic mean $\bar{x}$ can be obtained as follows: [116]

$$t = \frac{(\bar{x}_1 - \bar{x}_2)}{s\sqrt{\dfrac{1}{n_1} + \dfrac{1}{n_2}}} \; ; \qquad\qquad\qquad (10\text{-}1)$$

$$\bar{x} = \frac{\displaystyle\sum_{i=1}^{n} x_i}{n} \; . \qquad\qquad\qquad (10\text{-}2)$$

where s is the standard deviation and can be calculated for each set of data as shown in the following equations :

$$s_{1or2} = \sqrt{\frac{\displaystyle\sum_{i=1}^{n}(x_i - \bar{x})^2}{(n-1)}} \; ; \qquad\qquad\qquad (10\text{-}3)$$

$$s = \sqrt{\frac{(n_1 - 1)s_1^2 + (n_2 - 1)s_2^2}{(n_1 + n_2 - 2)}} \; . \qquad\qquad\qquad (10\text{-}4)$$

To determine whether the difference is significant or not, the absolute value of $|t|$ should be compared to the critical value t_{df} with degrees of freedom equal to $(n_1 + n_2 - 2)$ for a particular significance level, which is recommended to be 5% and can be obtained from the statistical tables or by using Excel statistical analysis package.

If $|t|$ value is greater than the critical t_{df} value, the null hypothesis will be rejected and the difference is significant at a level of 5%.

A t – test was conducted to test the significance of the differences between three sets of pH analysis values for three days. The calculations were carried out using the statistical analysis package in the Excel software. Table 8.2 shows the results of calculations between the first and the second sets of data, the first and the third sets of data and the second and the third sets of data respectively.

Based on the statistical analysis results for data set1 and set 2, it can be seen that the critical two tails value of t_{37} = 2.03 at ($P=0.05$) is greater than the statistical value t = 0.52 which indicates that the test is not significant at this stage while the second and the third tests showed that the critical values of t are less than the statistical ones hence the differences in the pH analysis between the first day and the third day results and the second day and the third day results are significant. This could be due to the accuracy of pH meter or to the difficulties in measuring the pH of distilled water during the experiments because of its low conductivity.

Statistical Parameters	T - Test (1)		T - Test (2)		T - Test (3)	
	Data Set 1	Data Set 2	Data Set 1	Data Set 3	Data Set2	Data Set 3
Mean	6.98	6.87	6.98	7.61	6.87	7.61
Variance	0.38	0.42	0.38	0.29	0.42	0.29
Standard Deviation (s)	0.62	0.65	0.62	0.54	0.65	0.54
Observations	18	21	18	24	21	24
Pooled Variance	0.40		0.33		0.35	
Hypothesized Mean Difference	0.00		0.00		0.00	
Degrees of Freedom (df)	37.00		40.00		43.00	
t Statistical	**0.52**		**-3.51**		**-4.16**	
P(T<=t) one-tail	0.30		0.00		0.00	
t Critical one-tail	1.69		1.68		1.68	
P(T<=t) two-tail	0.61		0.00		0.00	
t Critical two-tail	**2.03**		**2.02**		**2.02**	

Table 10-2: Results of three T– Test calculations

From Figure 10.5 it can be observed that the pH values of the distilled water normally range between 6 to 8 but sometimes it reached 5.2. The lowest values of pH are due to absorbtion by the distilled water of carbon dioxide from the atmosphere. Distillation temporarily removes dissolved CO_2 from the water but, during condensation, the water can reabsorb CO_2, again resulting in a lower values of pH [78]. But the only reason that pH is lowered that carbonate HCO_3 is no longer there to buffer it.

Based on these water quality analysis results, it can be positively concluded that the multi stage solar desalination still proved to be very successful in removing contaminants from the brackish water and that it had a removal efficiency of 98.8%.

11 Economic Study

11.1 Cost analysis

There are many ways to analyze the economics of solar desalination systems. In this study, the method proposed by Mattheus F. A. et al. (2000) [117] was applied. This suggests that, in order to determine the unit cost of distilled water produced by the desalination system, it is necessary to calculate the total amount of fresh water produced and the total cost of the system, including capital, operating and maintenance costs over a certain period of time. In addition to these parameters, salvage value, product cost and the payback period should be considered.

11.1.1 Water distillate product

The daily distillate output for the system for 24 hours working can be calculated as follows:

$$m_d = \int_{t=0}^{24hr} \dot{m}_e dt .$$
(11-1)

The average annual distillate output can be calculated using the following equation:

$$m_y = \left(\frac{1}{365}\right)\sum_{i=0}^{365} m_{d.i} .$$
(11-2)

11.1.2 Solar desalination plant cost

The total cost of the desalination system in terms of the actual annual cost can be expressed as:

Actual annual cost (AC) = The first annual cost (M)+ Annual maintenance cost (AMC) − Salvage value (N)

In order to make an assessment of the cost effectiveness of the proposed system, the following cost analysis method should be conducted.

If P is the capital cost of the system and CRF is the capital recovery factor, the first annual cost of system M can be determined as.

$$M = P * CRF ; \tag{11-3}$$

with

$$CRF = \frac{r(1+r)^n}{(1+r)^n - 1} . \tag{11-4}$$

where r is the interest rate (%) of the lending bank and n is the life of the system (in years). The latter is the expected lifetime of the system without loss of efficiency.

11.1.3 Salvage value of the system

The salvage value (S) of the system is the expected market value at the end of useful life of the desalination plant. This was considered to be 40% of the usable material cost. Hence the annual salvage value (N) of the system can be obtained in the following equation

$$N = S * SFF ; \tag{11-5}$$

where SFF is the sinking fund factor:

$$SFF = \frac{r}{(1+r)^n - 1} . \tag{11-6}$$

11.1.4 Running cost

Maintenance is very important to keep the system in a proper working condition and the annual maintenance cost is the expenditure necessary to replace broken parts, and to clean and protect the system from corrosion and scaling.

The Annual Maintenance Cost (AMC) is taken as a percentage of the first annual cost (M) according to Goosen et al. (2000) [117]

11.1.5 Product cost

If the annual yield of the system is taken as Y, then the product cost per litre (PC) can be determined as:

$$PC = \frac{AC}{Y}.$$ (11-7)

and the yield per US\$ dollars *(y)* can be calculated as follows

$$y = \frac{Y}{AC}.$$ (11-8)

11.1.6 Payback period

The main purpose of calculating the pay back period is to determine the time point at which the capital invested in the project will be recovered by annual returns, and this can be obtained as:

$$Payback - Period = \frac{PC}{AC} * Y.$$ (11-9)

11.2 Multi stage still system

11.2.1 Capital cost of the distillation unit

The capital cost of a water desalination system coupled to an evacuated tube solar collector to produce a potable drinking water from seawater or underground brackish water can be expressed as follows:

$$P_{Total} = P_{Multi-Stills} + P_{Solar-Collector} + P_{Heat-Exchanger} + P_{Pump} + P_{Piping}.$$ (11-10)

The capital cost of the unit includes the initial cost of the metal sheets required for the fabrication and construction of the distillation unit, insulation materials, other required components and materials such as gasket, clamps and adhesive, and labour. It can be calculated as:

$$P_{Multi-Stills} = P_{SM} + P_{SI} + P_{SL} + P_{SA}.$$ (11-11)

The quantity of metal sheets required for fabrication of the distillation unit shown in Figure 6.1 can be determined as:

$$P_{SM} = A_M \rho_M t_m C_M.$$ (11-12)

where A_M, ρ_M, t_m are the total area, the density, and thickness of metal sheets respectively and C_M is the cost price per kg.

It is necessary to fully insulate the multi stage still unit, except for the top tray, using 150 mm mineral wool insulation. Therefore the cost of insulation can be calculated as:

$$P_{SI} = A_I C_I .$$
(11-13)

11.2.2 Solar panel cost

The cost of the evacuated tube solar collector depends on its area and can be calculated as:

$$P_{Solar-Collector} = A_C C_C .$$
(11-14)

11.2.3 Heat exchanger cost

It was assumed that the heat exchanger is made of the parallel copper tubes connected in serpentine pattern. The quantity of required pipes and the cost can be determined as:

$$A_h = \pi \left[\left(\frac{D_h}{2} + t_h \right)^2 - \left(\frac{D_h}{2} \right)^2 \right] ;$$
(11-15)

$$P_h = A_h \rho_h l_h C_h .$$
(11-16)

11.2.4 Results of economic and analysis

According to the results of the mathematical simulation and experimental investigations, we have designed a multi stage solar still that produces higher quantities of distillate than the conventional basin still, and with the added advantage of using clean energy. Technologically, it is a promising sustainable water resource. However, it is also necessary to investigate the economics of its construction and operation. Hence an economic model has been developed to calculate the economic parameters mentioned above.

Figure 11.1 shows the simulation results of water productivity for a multiple desalination plant with an evaporation area of 1 m^2 coupled with an evacuated tube solar panel. The optimization was conducted by varying the number of stages N and the ratio between the solar panel and the evaporation area R ($A_c/A_{Evaporation}$). Results show that the water distillate increases with the number of stages and with rise in the solar panel area.
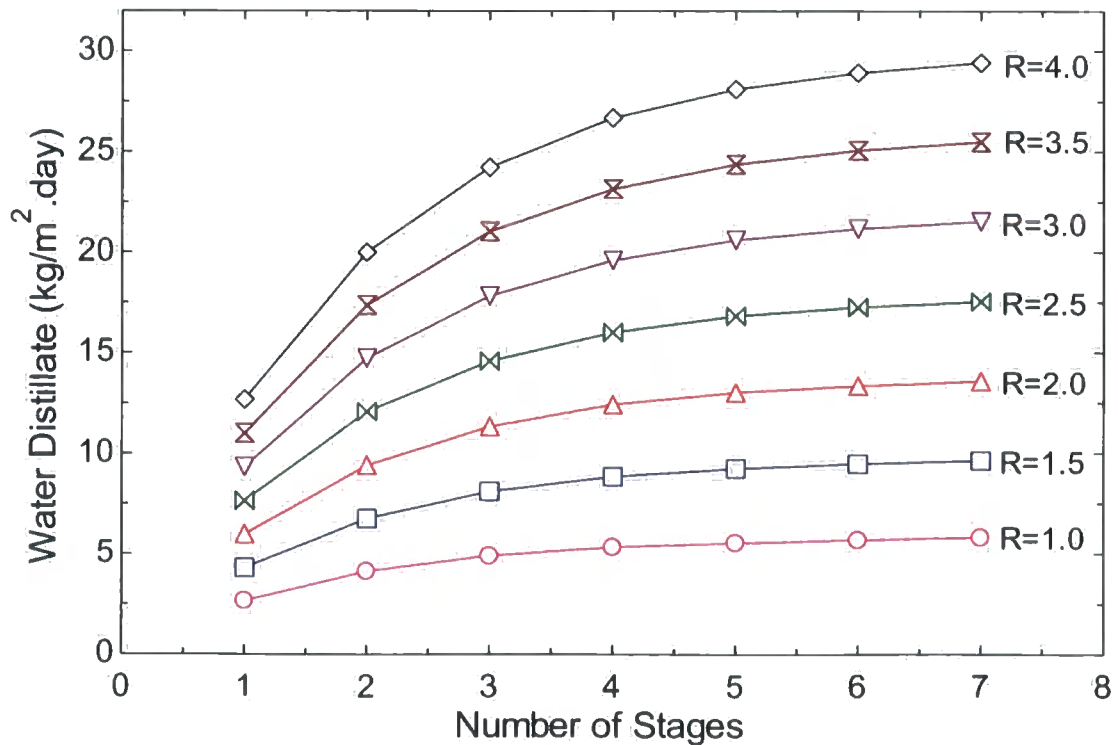
Figure 11-1: Variation of average daily distillate yield as a function of R and N

In the design process, it is necessary to take into account that saline water is very corrosive towards metallic alloys. Additionally materials should be carefully selected to have no adverse health impacts. There are some alloys such as titanium, stainless steel and aluminum alloys which satisfy the above requirements.

The capital cost of the desalination unit has been calculated for different design combinations and for different N and R values according to the proposed economic model and results for cases when stainless steel type material and aluminum alloys were used are presented in Table 11.1 and 11.2, respectively.

Calculations of capital cost of a desalination unit with an evaporation area of 1 .m²
Material: Stainless Steel type material.

Item	Unit	Quantity	Price per unit (US$)	One stage	Two stages	Three stages	Four stages	Five stages	Six stages	Seven stages
Evacuated solar collector panel	m²	1	225	225	225	225	225	225	225	225
Still Stainless Steel Metal Sheets										
First stage	m²	2.24	83	186	186	186	186	186	186	186
Middle stage	m²	1.13	83	0	94	187	281	374	468	562
Angled tray	m²	1.08	83	89	178	268	357	446	535	625
Sub total				275	458	641	824	1007	1190	1373
Insulation Material										
First stage	m²	1.93	8	15	15	15	15	15	15	15
Middle stage	m²	0.73	8	0	6	12	17	23	29	35
Angled tray	m²	0.00	8	0	0	0	0	0	0	0
Sub total				15	21	27	33	39	44	50
Heat exchanger	m	15	5	75	75	75	75	75	75	75
Circulation pump	unit	1	60	60	60	60	60	60	60	60
Piping, fittings system	L,S	1	50	50	50	50	50	50	50	50
Storage tank 50 liter	unit	10	10	10	10	10	10	10	10	10
Labour and assembling	unit	3	20	60	60	60	90	90	90	90
All sub totals				771	960	1148	1367	1555	1744	1933
Profit and additional material as a percentage of the initial capital cost	(%)	10%		77	96	115	137	156	174	193
Total cost				848	1056	1263	1504	1711	1919	2126

Table 11-1: Desalination system components made of stainless steel type of material and its capital cost breakdown

Calculations of capital cost of a desalination unit with an evaporation area of 1 m^2

Material: Aluminum alloy

Item	Unit	Quantity	Price per unit (US$)	One stage	Two stages	Three stages	Four stages	Five stages	Six stages	Seven stages
Evacuated solar collector panel	m^2	1	225	225	225	225	225	225	225	225
Still Aluminium Metal Sheets										
First stage	m^2	2.24	45	101	101	101	101	101	101	101
Middle stage	m^2	1.13	45	0	51	102	152	203	254	305
Angled tray	m^2	1.08	45	48	97	145	194	242	290	339
Sub total				149	248	348	447	546	645	744
Insulation Material										
First stage	m^2	1.93	8	15	15	15	15	15	15	15
Middle stage	m^2	0.73	8	0	6	12	17	23	29	35
Angled tray	m^2	0.00	8	0	0	0	0	0	0	0
Sub total				15	21	27	33	39	44	50
Heat exchanger	m	15	5	75	75	75	75	75	75	75
Circulation pump	unit	1	60	60	60	60	60	60	60	60
Piping, fittings system	L,S	1	50	50	50	50	50	50	50	50
Storage tank 50 liter	unit	10	10	10	10	10	10	10	10	10
Labour and assembling	unit	3	20	60	60	60	90	90	90	90
All sub totals				645	750	855	990	1095	1199	1304
Profit and additional material as a percentage of the initial capital cost	(%)	10%		64	75	85	99	109	120	130
Total cost				709	825	940	1089	1204	1319	1435

Table 11-2: Desalination system components made of aluminium alloy and its capital cost breakdown

In order to perform the economic simulation, some parameters have to be set initially. Thus the operational lifetime of the system was estimated to be 15 years, based on the recommendations of the evacuated tube solar collector manufacturer.

The estimated cost of a cubic meter of desalinated water was determined by the economic analysis model for cost prediction, as shown above. It was assumed that the annual maintenance cost would be 5% of the initial capital cost, and the lending bank interest would be 5%. The salvage value was taken to be 40% of the initial capital cost

The annual operating days of the desalination system was assumed to be 350.

The average yearly water distillate production for the various combinations of the number of stages with different R values has been simulated and results are shown in Figure 11.2 and (Appendix F)
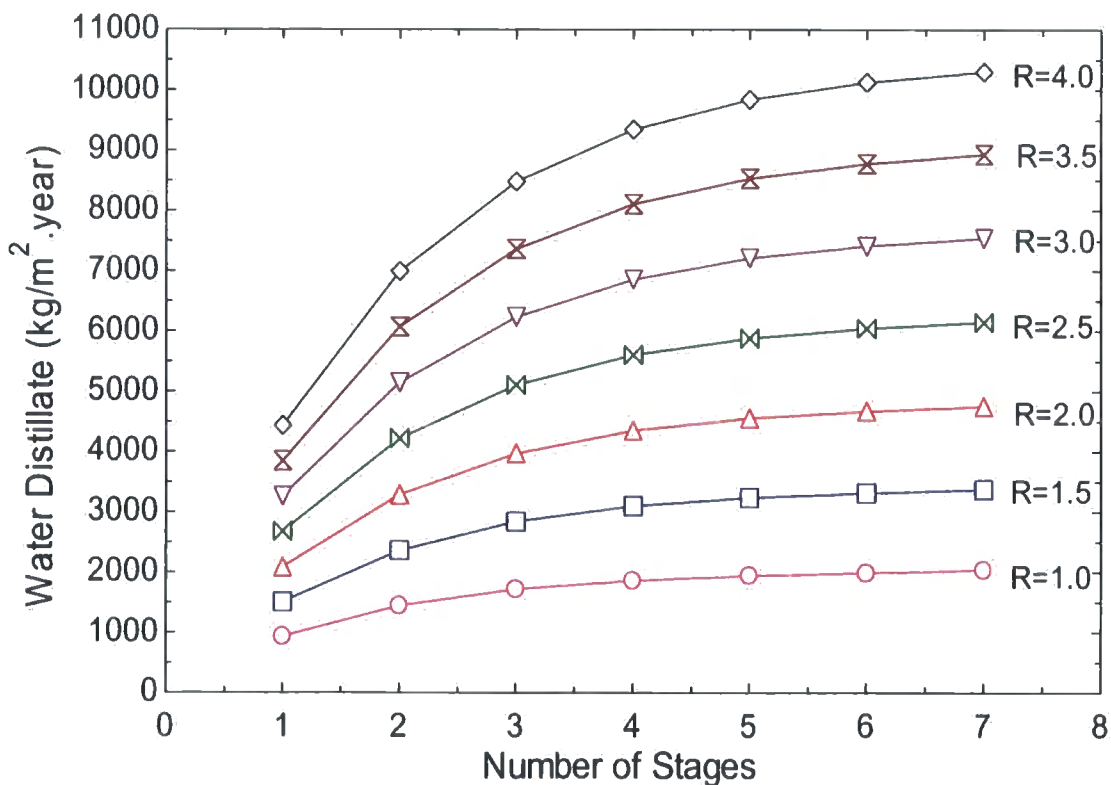
Figure 11-2: Variation of average annual distillate yield as a function of R and N

An economic optimization has been carried out where the product cost (*PC*) was used as an optimization parameter as a function of number of stages (*N*) and the (*R*)

ratio for stainless steel and aluminum alloys, as shown in Figure 11.3 and Figure 11.4 respectively.

From the diagrams it can be seen that the lowest product price of 0.016 US$/kg is achieved with a desalination plant made of aluminum alloys and consisting of 5 stages with an R ratio of 4, as shown in Figure 11.4. The minimum product cost of 0.022 US$/kg is achieved for stainless steel desalination plant composed from 4 stages with a R ratio of 4.

It can also be seen that an annual total production of distilled water of 9,343 litres can be achieved and that this can produce a useful annual energy saving of about 6,073 KW. The payback period of the system, was calculated to be 0.5 year based on the cost of bottled water in Palestine which is 0.35 US$/litre (See Appendix F).
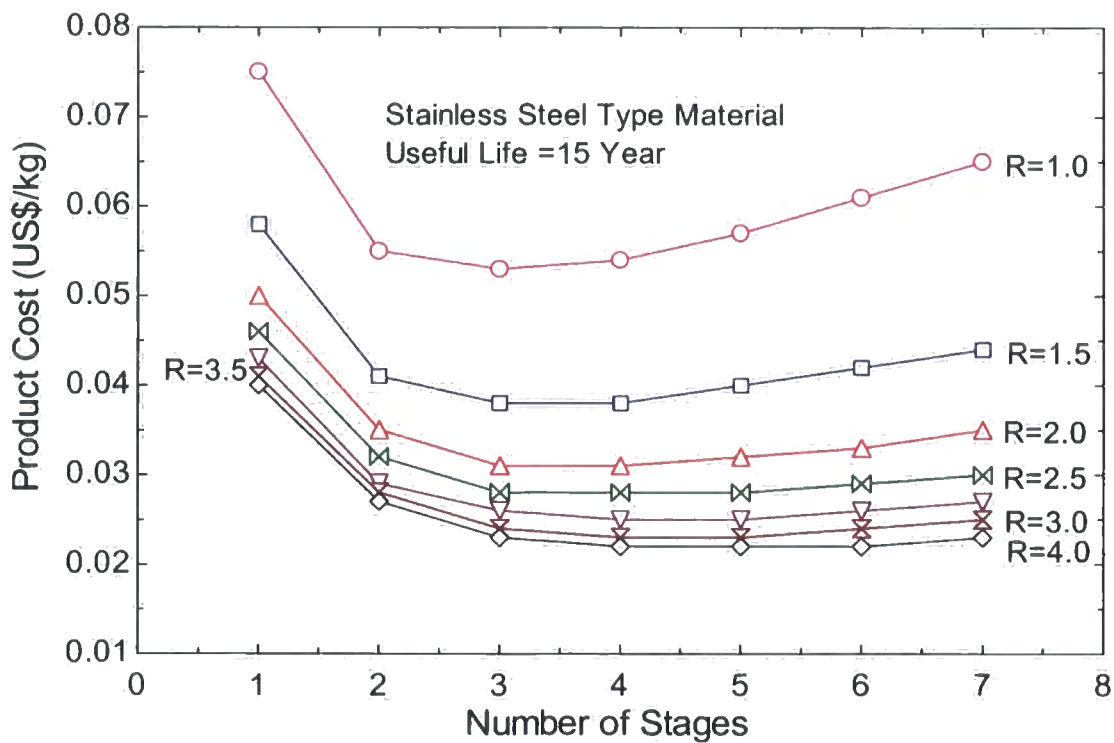
Figure 11-3: Variation of product cost versus the number of stages as a function of different values of R ($A_c/A_{Evaporation}$) for stainless steel material
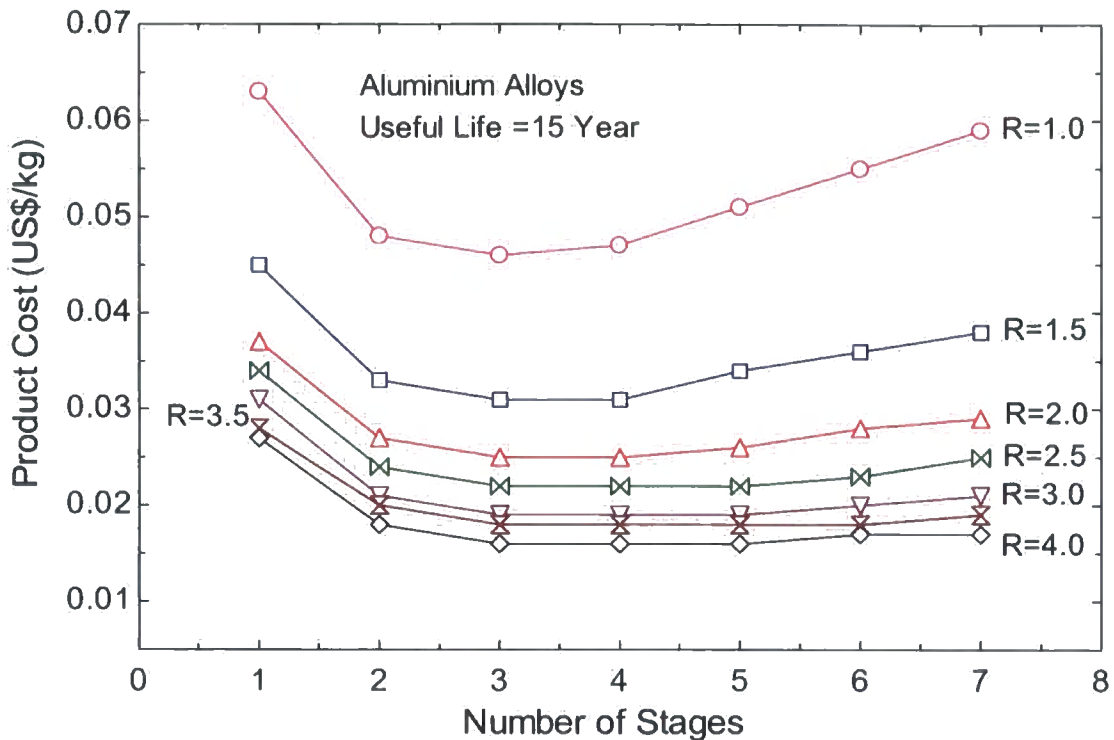
Figure 11-4: Variation of product cost versus the number of stages as a function of different values of R ($A_c/A_{Evaporation}$) for Aluminium material

To obtain a wider picture, a series of calculations were performed with sensitivity analysis for various rates of interest and different annual maintenance percentages. But it was demonstrated that such variations had a very small affect on the product cost and therefore can be ignored.

It is obvious that the capital cost is high, based on the Palestinian market. But this cost could be considerably reduced if the rig was manufactured in other regions where the raw materials and labour are less expensive and then exported to Palestine. For example, the cost of an evacuated tube solar collector panel in China is about 100 US$/m², which is half the cost used in this study.

However, even with such reduced costs, the cost of fresh water produced by this plant is still higher than that produced by other thermal technologies powered by fossil fuel. From the literature it is found that multi effect desalting systems can produce desalinated water from brackish water at cost of $ 2.5 – to $10 per m³ in systems which have capacities of less than 100 m³ per day [45]. However, when renewable energy sources are used to operate the RO plants, the cost was found to dramatically increase to (10.32$/m³) [48].

But the proposed system could prove viable for remote and rural areas and in politically unstable areas with intermittent electricity supply like the Gaza Strip, especially if they were funded by the United Nations or other forms of international aid. The vast majority of Palestinian families living in Gaza suffer from dire poverty and many are refugees. The UN Relief and Works Agency (for refugees) has undertaken other infrastructure projects in Gaza, as have several European countries. It is well known that there is a water scarcity of even poor water quality in the Gaza Strip, and this is one of reasons for social unrest in the area.

11.3 Reverse osmosis desalination system coupled with photovoltaics (PV).

11.3.1 System description

A reverse osmosis (RO) desalination plant is composed of a photovoltaic generator with multi PV modules to produce electricity, a charge controller to protect the battery block from deep discharge and overcharge [119], a set of battery blocks to stabilize the energy input to the RO unit and to compensate for solar radiation variations, and a RO unit to desalinate the water. All these components are as shown in Figure 11.5

To carry out an economical analysis for a RO desalination system, the design and sizing of the proposed desalination system is conducted as follows.
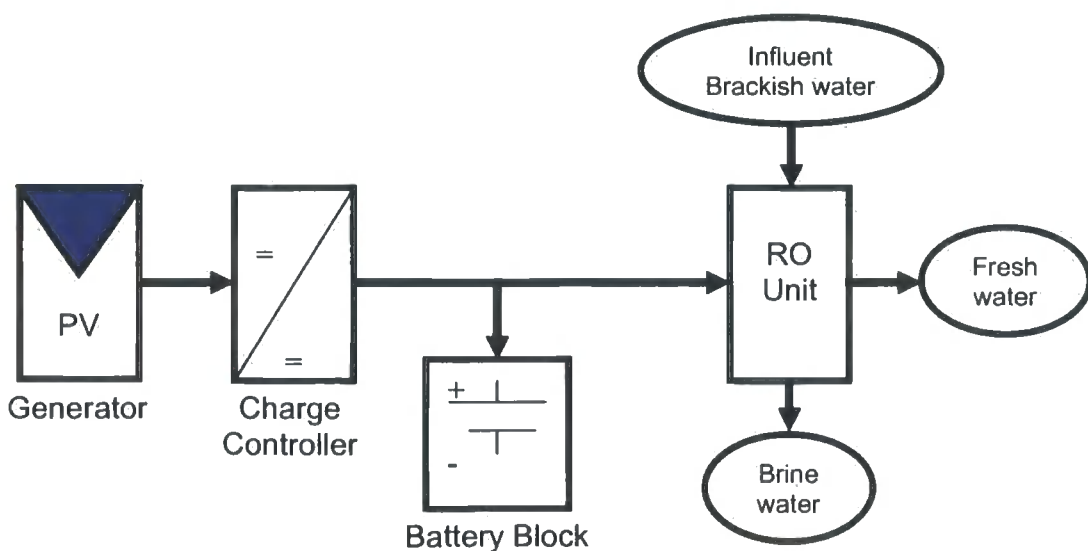
Figure 11-5: Schematic diagram of RO desalination unit coupled with PV generator

11.3.2 Design of desalination system

Sizing of RO unit

Based on the Palestinian Census, the average number of family members in the Gaza Strip is six [71]. Hence the RO unit was selected to cover the daily demand of a family of 6 persons. From the literature, the average water demand for drinking and food use is 30 litre per capita per day [92], hence the water demand for family is 6x30 = 180 litres per day. Therefore a residential RO unit with a daily production of 50 GPD (189L/day) was selected. This unit is shown in Figure 11.6 and its specification is presented in Table 11.3.
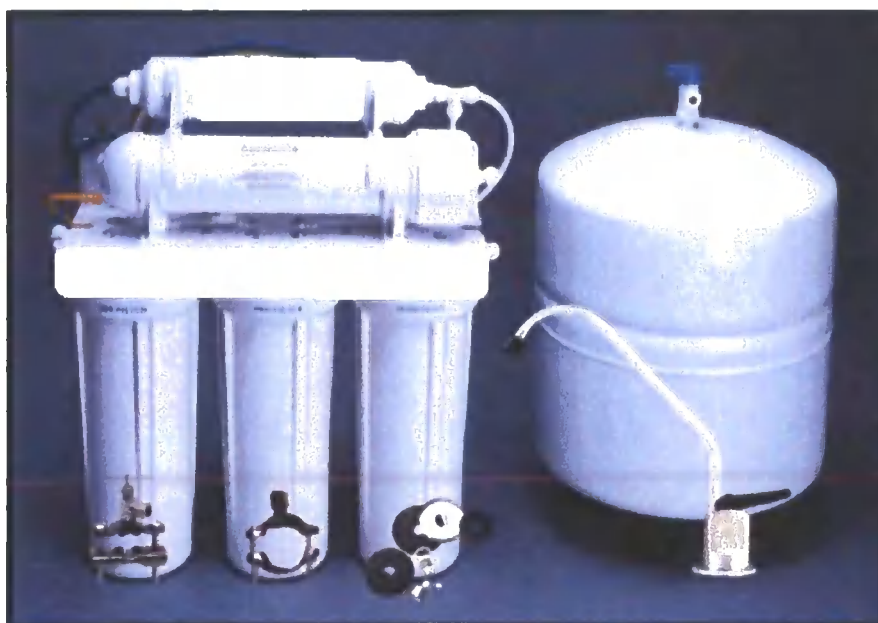
Figure 11-6: Photo of the reverse osmosis (RO) Unit

No.	Item	Unit	Quantity
1	Influent brackish water salinity	mg/L	2500
2	Effluent desalinated water production	Litre/day	189
3	Maximum recovery rate	%	50
4	Total daily power	Watt	518.40
6	DC voltage	Volts	24
7	TDS removal efficiency	%	95
8	Organics and bacteria removal efficiency	%	+99

Table 11-3: Specification of reverse osmosis (RO) unit

Calculation of the RO load power

The total power load required to operate the RO during 24 hours is 518.40 W/day = 21.6 Wh/day. RO units normally use the DC type motors; hence an inverter is not required and the PV arrays can be connected directly to the charge controller, the battery and to the RO system, as illustrated in Figure 11.5.

Sizing the photovoltaic generator.

To design the PV module it is important to take into consideration not only the RO unit power load but also other parameters such as inverter losses, battery losses and the PV thermal losses [118]

The peak power of the PV generator (P_{pv}) is obtained as: [119]

$$P_{pv} = \frac{E_l}{PSSH * \eta_b * \eta_{inv}} S_F.$$
(11-17)

where *PSSH* is the peak sunshine hours and it was found for the Palestinian territories to be 5.4 hours [119]. η_{inv} = Inverter losses, η_b = Battery losses = 15%, and S_F = Safety factor, for PV thermal losses for Palestinian environment =1.15%

Using above values in Equation 9.17, we obtain the peak power of PV array:

$$P_{pv} = \frac{518.4}{5.4 * 0.85} * 1.15 = 130W$$

The PV array should produce 130 W and to install this power, a high-power module using multi-crystalline silicon cells with 14.3% module conversion efficiency and a gross area of 129.3 cm x 33.8 cm rated at open circuit voltage 21.3 volts, and a short circuit current of 3.2 A is necessary. A peak power of P_{mpp} = 50 W_p was selected. Then the necessary number of PV modules (N_{pv}) is 3.

$$N_{pv} = \frac{P_{pv}}{P_{mmp}} = \frac{130}{50} = 3.$$
(11-18)

Sizing of the battery storage

Battery storage is required to stabilize the energy input to the RO unit and to compensate for solar insolation variations due to cloudy days and temperature

variations. Hence, battery storage should be selected to be able to operate the system for 24 hours. The battery block capacity can be determined based on the ampere hour capacity (C_{Ah}) and watt hour capacity (C_{wh}) of the battery block, which is necessary to cover the load demands, as follows [119]:

$$C_{Ah} = \frac{E_l}{V_b * DOD * \eta_b * \eta_{inv}} ;$$

(11-19)

$$C_{wh} = C_{Ah} * V_b .$$

(11-20)

By assuming the maximum battery discharge to be 50% and considering 24 V output is required from battery block

$$C_{Ah} = \frac{518.4}{24*0.5*0.9} = 48 Ah ;$$

and

$$C_{wh} = 48 * 24 = 1152 \, Wh .$$

In order to satisfy the power load of the battery block capacity, two batteries (each one rated at 12 V/50 A h) were selected and connected in series to build a battery block with an output at 24 VDC/ 50 A h.

The charge regulator

An appropriate battery charge regulator should be able to cope with the short circuit current of the PV array 3.2 Amp and it is necessary to protect the battery block against deep discharge [119] and overcharge and prevent reverse current flow at night. Hence a charge regulator was selected for 24 V and 10 A.

11.3.3 Economic analysis of RO system

The economic analysis was conducted in the way identical to that for a multi stage still plant.

To study the economics of RO water desalination system coupled with photovoltaic solar modules to produce potable drinking water from underground brackish water with total dissolved solids up to 2500 mg/L, it was necessary to estimate the

capital cost according to present prices. Table 11.4 represents breakdown of the capital cost of the desalination system components.

Item	Dimensions	Unit	Price per unit (US$)	Total cost (US$)
RO desalination residential unit	50 GPD	1	250	250
PV array	(150W)	150	9	1350
Battery bank	50 AH/12V	2	330	660
Battery charge controller 0.60US$/Wp	1.2mx0.34m	150	0.60	90
Installation	LS	1	100	100
RO unit replacement	3 times	3	250	750
Membrane filter set replacement	36 times	36	35	1260
Battery replacement	One time	1	660	660
Sub Total				**5120**
Profit, auxiliaries and any additional fittings	10% of capital cost	0.1	5120	512
Total cost				**5632**

Table 11-4: RO -Desalination system components and cost breakdown

Based on the manufacturer recommendation for the photovoltaic modules, it was assumed that the working life of the system is 20 years, while the RO unit is expected to last for 5 years and the batteries will need to be replaced every ten years. This means that the RO unit will be replaced after 5, 10 and 15 years and the batteries will be replaced after 10 years. Meanwhile the RO cartridge filter set should be replaced every 6 months so this will result in 36 replacements during the system is life equal to 20 years. All replacement parts were included in the capital cost, as shown in table 11.4.

The estimated cost of a cubic meter of desalinated water was determined according to the economic analysis model for cost prediction as shown in above It was assumed that the annual maintenance cost would be 2% of the initial capital cost, and bank interest rate would be 5%. The annual operation days of the desalination system was assumed to be 350.

The salvage value was taken to be 20% of the initial system cost. More information on the economic implications of various rates of interest and various annual maintenance percentages is shown in Appendix F. The performed calculations

demonstrated that such variations had a very small affect on the output costs and could be ignored.

The annual expected output of desalinated water was 66.15 m^3 and the annual cost was 463 US$. Hence the cost of 1 m^3 of desalinated water was 7.0 US$ (463/66.15).

However, this cost varies greatly with the quality of the influent saline water. It was found that the total dissolved solids concentration should be less than 2,500 mg/L because TDS concentrations greater than that result in dramatic increases in the cost of desalination. For example, the desalination cost of 1 m^3 of sea water using RO units is five times the cost of 1 m^3 of brackish water.

From the above results it can be concluded that reverse osmosis desalination units coupled with photovoltaic modules could help to solve the scarcity and shortage in water in remote and rural areas and especially in poor regions such as the Gaza Strip.

Maximizing the size of a RO unit decreases the output cost because larger RO units show dramatic increases in water production with smaller increases in the power required. Increasing the time of operation of RO units would improve the water productivity with most economical cost where the relation between the cost price and RO unit size is not proportional linearly.

11.4 Summary

In summary, it can be concluded that the study of reverse osmosis units connected to photovoltaic cells proved this to be a viable and feasible option with lower costs compared with multi stage distillation but its high initial capital cost could restrict its widespread use.

.The highly reliable multi stage solar desalination operation makes its installations possible to help to solve water scarcity in remote and rural areas where there is a lack of experienced technicians and especially in the poor areas like the Gaza Strip. Because any serious fault during the operation of a RO unit can ruin its membranes, these plants should be operated and maintained by skilled technicians. Also it is still expensive to collect solar energy by photovoltaic cells and store it in batteries.

Eventually in polluted areas, distillation processes especially in a multi stage solar still are preferred for desalination because water is boiled and this ensures that the distilled water does not contain any biological contaminants.

12 Conclusion and Future Work

12.1 Conclusion

A new promising technology of solar water desalination has been thoroughly studied through experimental investigation and theoretical analysis. A multi-stage solar still coupled with an evacuated tube solar collector panel was tested and simulated under conditions of a typical mid-summer day in the Middle East region.

It was found that the fresh water production capacity of the system was 4.94 litre/m²/day with a distillation efficiency of 89.7%. This is higher than that of both conventional stills and stills coupled with flat plate collectors. An Engineering Equation Solver program code was developed to calculate the experimental results and these showed a good correlation with the results of the theoretical analysis.

It was also found that the depth of water body had a direct effect on the system's performance; when the depth of water in the still was increased, the water production decreased and the system needed more time to reach a steady state condition.

A mathematical model based on differential equations of mass and energy conservations was developed for transient numerical simulation and calibrated by the experimental results. Experimental validation of the model demonstrated that it provides an acceptable level of accuracy in the prediction of the performance of the system. Therefore it can be used for the determination of rational design parameters of the multi-stage basin for a given aperture area of the solar collector.

A rational design simulation analysis was carried out for design parameters, such as the number of stages and the evaporation area relative to the solar collector area for real dynamic variations in the solar insolation. This showed that the evaporation area of the system should be increased by a factor of 2.

The simulation and optimization results also demonstrated that the performance of the system could be considerably improved and that the production of fresh water could reach as high as 11 kg/m² day.

A computational fluid dynamic (CFD) model using FLUENT 6.2 with multiphase segregated solver and VOF model was developed to simulate the evaporation and condensation processes inside one of stages of the solar still. At this stage the obtained

CFD results can be used for qualitative analysis of certain details of the heat transfer processes taking place inside the distillation still.

A water quality analysis for total dissolved solids, electrical conductivity and pH was performed on the distilled water and the results showed that quality was well within the range defined by the World Health Organization guidelines for drinking water.

An economic model was developed to determine the cost of the system and It was found that the cost of the fresh water produced would be 0.016 US$/litre and that the payback period would be 6 months based on the price for bottled water in Palestine. The capital cost is relatively high, but the system could be viable if it is manufactured in other regions, such as China, where the cost of the components and labour is lower.

However the proposed multi-stage solar desalination still is a prospective technology which could prove to be viable in remote and rural areas and particularly in politically unstable regions with an intermittent electricity supply like the Gaza Strip. Though the operating costs are low, the capital costs of the system are likely to inhibit its development and widespread use in the near future unless these capital costs are paid or subsidised by international aid.

The other advantage of the desalination system is that it is powered by a completely environment-friendly and sustainable energy source. This advantage could, in itself, attract international aid from countries interested in reducing climate change, especially if they were given credit for such aid by some of the carbon trading schemes currently under international discussion.

12.2 Future Work

Potentially, a multi-stage solar still coupled with an evacuated tube solar collector could achieve higher thermal efficiency and greater fresh water production. Hence, further research should be conducted to investigate the effect of non-condensing gases and pressure evacuation to enhance water evaporation at lower temperatures.

In practical terms, the recommendation would be to increase the evaporation area of the still and to couple the fourth stage with a saline water storage tank in order to utilize the latent heat of condensation in the last stage as much as possible. The increase in salt concentrations during the distillation process also needs to be studied. Finally, greater attention must be paid to reducing heat losses from the system.

Bibliography

[1] United Nations Environment Programme, http://www.unep.org/themes/freshwater.html 10 April 2008).

[2] Al-Kharabsheh, S., (2003). Theoretical and experimental analysis of water desalination system using low grade solar heat . PhD dissertation – University of Florida, USA.

[3] Colombo, D., De Gerloni, M., and Reali, M. (1999). An energy-efficient submarine desalination plant. *Desalination,* 122(2-3): 171-176.

[4] WHO/EU drinking water standards comparative table, Water treatment & Air Purification and other Supporting Information, http://www.lenntech.com/WHO-EU-water-standards.html (26 October 2007). .

[5] Tiwari, G. N., Singh, H. N., and Tripathi, R. (2003). Present status of solar distillation. *Solar Energy,* 75(5):367-373

[6] Buros, O.K., (1999), The ABCs of Desalting, International Desalination Association, Massachusetts, USA, 31 pages.

[7] Gleick, P.H.(Editor), (1998). The World's Water: the Biennial Report of Fresh Water Resources 1998-1999, Island Press, Washington, D.C., USA.

[8] WDI Water Desalination International: Introduction□ published by WDI. http://www.aterdesalination.com/introduction.htm., (21 April 2008).

[9] Al-Kharabsheh, S., and Yogi?Goswami, D. (2003). Analysis of an innovative water desalination system using low-grade solar heat. *Desalination,* 156(1-3): 323-332.

[10] Winter, T. Pannell J. and McCann Mc, (2005). The Economics of Desalination and its Potential Application in Australia, University of Western Australia, Perth, WA 6009, Australia

[11] Raluy, R. G., Serra, L., Uche, J., and Valero, A. (2004). Life-cycle assessment of desalination technologies integrated with energy production systems. *Desalination,* 167(2004): 445-458.

[12] Multi Stage Flash, Halcrow Water Services. http://www.hwsdesalination.com/multi%20stage%20flash%20desalination.html, (2 October 2007)

[13] Water Desalination Technologies in the ESCWA Member Countries, (2001). UN-ESSWA, ASIN: E/ESCWA/TECH/2001/3, United Nations, New York, USA, 172 pages

[14] Buros, O.K., (2000). The ABCs of Desalting (The 2nd edition.) ASIN: B0006S2DHY, International Desalination Association, Massachusetts, USA, 30 pages.

[15] Introduction to Desalination Technologies http://www.texaswater.tamu.edu/readings/desal/IntrotoDesal.pdf. (2 October 2007)

[16] Khawaji, A. D., and Wie, J.-M. (1994). Potabilization of desalinated water at Madinat

Yanbu Al-Sinaiyah. *Desalination*, **98**(1-3), 135-146.

[17] Wangnick, K., (2000). IDA worldwide desalting plants inventory: report No. 16 Produced by Wangnick Consulting for the International Desalination Association. Gnarrenburg, Germany.

[18] Al-Shammiri, M., and Safar, M. (1999). Multi-effect distillation plants: state of the art. *Desalination*, **126**(1-3): 45-59.

[19] El-Dessouky H. and Ettouny H., (2001). Study on water desalination technologies, prepared for ESCWA., United Nations.

[20] Khawaji, A. D., Kutubkhanah, I. K., and Wie, J.-M. (2008). Advances in seawater desalination technologies. *Desalination*, **221**(1-3):47-69.

[21] Darwish, M. A., and El-Dessouky, H. (1996). The heat recovery thermal vapour-compression desalting system: A comparison with other thermal desalination processes. *Applied Thermal Engineering*, **16**(6):523-5 37.

[22] El-Nashar, A. M. (2001). Cogeneration for power and desalination - state of the art review. *Desalination*, **134**(1-3): 7-28.

[23] Voivontas, D., Misirlis, K., Manoli, E., Arampatzis, G., & Assimacopoulos, D. (2001). A tool for the design of desalination plants powered by renewable energies. *Desalination*, **133**(2): 175-198.

[24] Zejli, D., Benchrifa, R., Bennouna, A., and Zazi, K. (2004). Economic analysis of wind-powered desalination in the south of Morocco. *Desalination*, **165**(2004): 219-230.

[25] The Desalting and Water Treatment Membrane Manual: A Guide to Membranes for Municipal Water Treatment, Water Treatment Technology Program, Report No. 1, September 1993, published by the United States Department of the Interior, Bureau of Reclamation, Denver Office, Research and Laboratory Services Division, Applied Sciences Branch (R-93-15), http://www.usbr.gov/pmts/water/publications/reportpdfs/report001.pdf (15 March 2008)

[26] Ayyash, Y., Imai, H., Yamada, T., Fukuda, T., Yanaga, Y., and Taniyama, T. (1994). Performance of reverse osmosis membrane in Jeddah Phase I plant. *Desalination*, **96**(1-3): 215-224.

[27] Khawaji, A. D., Kutubkhanah, I. K., and Wie, J.-M. (2007). A 13.3 MGD seawater RO desalination plant for Yanbu Industrial City. *Desalination*, **203**(1-3): 176-188.

[28] AL Mobayed, AA., and Balaji, S., Successful Operation of Pretreatment in Al – Jubail SWRO Plant, paper presented at *IDA World Congress on desalination & Water reuse conference*, September 11-16, 2005. Singapore, pp12.

[29] Helal, A. M., Al-Malek, S. A., and Al-Katheeri, E. S. (2008). Economic feasibility of alternative designs of a PV-RO desalination unit for remote areas in the United Arab Emirates. *Desalination*, **221**(1-3): 1-16.

[30] Al-Sheikh, A. H. H. (1997). Seawater reverse osmosis pretreatment with an emphasis on the Jeddah Plant operation experience. *Desalination*, **110**(1-2): 183-192.

[31] Kayyal M., (2000) Study on wastewater treatment and water desalination technologies for ESCWA countries, United Nations.

[32] Bou-Hamad, S., Abdel-Jawad, M., Al-Tabtabaei, M., and Al-Shammari, S. (1998). Comparative performance analysis of two seawater reverse osmosis plants: Twin hollow fine fiber and spiral wound membranes. *Desalination,* **120**(1-2): 95-106.

[33] Strathmann H. Winston W.S. and Sirkar, K.K. (Author.), (1992), Membrane Handbook, ISBN- 0-442-23747-2, Van Nostrand Reinhold, New York, pp. 246–254.

[34] Kalogirou, S. A. (2005). Seawater desalination using renewable energy sources. *Progress in Energy and Combustion Science,* **31**(3): 242-281.

[35] Fritzmann, C., Löwenberg, J., Wintgens, T., and Melin, T. (2007). State-of-the-art of reverse osmosis desalination. *Desalination,* **216**(1-3): 1-76.

[36] Stover R L. (2006)., Energy Recovery Devices for Seawater Reverse Osmosis Retrieved May 04, 2008 from the World Wide Web. Source: http://www.energyrecovery.com/news/documents/ERDsforSWRO.pdf.

[37] Delyianni E. and Belessiotis B., (1995). Methods and Desalination Systems - Principles of the Desalination Process, NCSR *"Demokritos"*, Athens, Greece.

[38] Avlonitis, S. A. (2002). Operational water cost and productivity improvements for small-size RO desalination plants. *Desalination,* **142**(3): 295-304.

[39] Al-Wazzan, Y., Safar, M., Ebrahim, S., Burney, N., and Mesri, A. (2002). Desalting of subsurface water using spiral-wound reverse osmosis (RO) system: technical and economic assessment. *Desalination,* **143**(1): 21-28.

[40] Jaber, I. S., and Ahmed, M. R. (2004). Technical and economic evaluation of brackish groundwater desalination by reverse osmosis (RO) process. *Desalination,* **165**(2004): 209-213.

[41] Sambrailo, D., Ivic, J., and Krstulovic, A. (2005). Economic evaluation of the first desalination plant in Croatia. *Desalination,* **179**(1-3): 339-344.

[42] IDA Desalination Yearbook 2006–2007, Water Desalination Report, Global Water Intelligence and International Desalination Association, Topsfield, MA, USA.

[43] Ashkelon Desalination Plant, Seawater Reverse Osmosis (SWRO) Plant, Water technology net . http://www.water- technology.net/projects/Israel, (21 April 2008)

[44] Wilf, M., and Bartels, C. (2005). Optimization of seawater RO systems design. *Desalination,* **173**(1): 1-12.

[45] Karagiannis, I. C., and Soldatos, P. G. (2008). Water desalination cost literature: review and assessment. *Desalination,* **223**(1-3): 448-456.

[46] Mahmoudi, H., Abdellah, O., and Ghaffour, N. (2008) Capacity building strategies and policy for desalination using renewable energies in Algeria. *Renewable and Sustainable Energy Reviews, In Press,* March 2008.

[47] Mathioulakis, E., Belessiotis, V., and Delyannis, E. (2007). Desalination by using alternative energy: Review and state-of-the-art. *Desalination,* **203**(1-3): 346-365.

[48] Tzen, E., (2006), Renewable energy sources for desalination, Paper presented at Workshop on Desalination Units Powered by RES, Athens.

[49] Kalogirou, S. A. (2005). Seawater desalination using renewable energy sources. *Progress in Energy and Combustion Science,* **31**(3): 242-281.

[50] Delyannis, E. (2003). Historic background of desalination and renewable energies. *Solar Energy,* **75**(5): 357-366.

[51] Kreith F, Kreider JF., (Author), (1978) Principles of solar engineering., McGraw-Hill, New York., USA.

[52] Kalogirou, S. A. (2004). Solar thermal collectors and applications. *Progress in Energy and Combustion Science,* **30**(3): 231-295.

[53] Intermediate Technology Development Group. Solar distillation: Technical brief. Rugby, UK: The Schumacher Centre for Technology & Development, http://www.itdg.org/docs/technical_information_service, (8 October 2007)

[54] Fath, H. E. S., and Ghazy, A. (2002). Solar desalination using humidification--dehumidification technology. *Desalination,* **142**(2): 119-133.

[55] Ali Samee, M., Mirza, U. K., Majeed, T., and Ahmad, N. (2007). Design and performance of a simple single basin solar still. *Renewable and Sustainable Energy Reviews,* **11**(3): 543-549.

[56] Abdel-Rehim, Z. S., and Lasheen, A. (2005). Improving the performance of solar desalination systems. *Renewable Energy,* **30**(13): 1955-1971.

[57] Hamed, O. A., Eisa, E. I., and Abdalla, W. E. (1993). Overview of solar desalination. *Desalination,* **93**(1-3): 563-579.

[58] The Encyclopedia of Desalination and Water Resources (DESWARE) http:://www.desware.net, (8 October 2007)

[59] Parekh, S., Farid, M. M., Selman, J. R., and Al-hallaj, S. (2004). Solar desalination with a humidification-dehumidification technique - a comprehensive technical review. *Desalination,* **160**(2): 167-186.

[60] Orfi, J., Galanis, N., and Laplante, M. (2007). Air humidification-dehumidification for a water desalination system using solar energy. *Desalination,* **203**(1-3): 471-481.

[61] Müller-Holst, H., Engelhardt, M., and Schölkopf, W. (1999). Small-scale thermal seawater desalination simulation and optimization of system design. *Desalination,* **122**(2-3): 255-262.

[62] Rice, W., and Chau, D. S. C. (1997). Freeze desalination using hydraulic refrigerant compressors. *Desalination,* **109**(2): 157-164.

[63] Xu, T. (2005). Ion exchange membranes: State of their development and perspective. *Journal of Membrane Science,* **263**(1-2): 1-29.

[64] Miller J. (2003) Review of Water Resources and Desalination Technologies, Materials chemistry department, Sandia National Laboratories, Albuquerque, New Mexico, USA. http://www.prod.sandia.gov/cgi-bin/techlib/access-control.pl/2003/030800.pdf . (3 March 2008).

[65] Introduction to Desalination Technologies in Australia, (2002). http://www.environment.gov.au/water/publications/urban/desalination-summary.html. (13 April, 2008).

[66] The World Factbook, http://www.cia.gov/cia/publications/factbook/geos/gz.html (2 October, 2007).

[67] Hamdan, L. K., Zarei, M., Chianelli, R. R., and Gardner, E. (2008). Sustainable water and energy in Gaza Strip. *Renewable Energy*, 33(6): 1137-1146.

[68] Water Desalination Plan", Draft Report, (2000). Palestinian Water Authority / Palestinian Energy Authority, Gaza, Palestine

[69] Escalating Water Scarcity and Prospects for Demand Management Solutions, (1999). Palestinian Environment Quality Authority, Gaza, Palestine.

[70] Coastal Aquifer Management Program (CAMP), (2000). Integrated Management Plan, Palestinian Water Authority / USAID, Gaza, Palestine.

[71] Statistical Monitoring of the Socio-economic Conditions of the Palestinian Society, (2004)., Palestinian Central Bureau of Statistics, Palestinian Authority, Palestine.

[72] Water Quality in Gaza strip report, (1999)., Palestinian Environment Quality Authority, Gaza, Palestine.

[73] Akash, B. A., Al-Jayyousi, O. R., and Mohsen, M. S. (1997). Multi-criteria analysis of non-conventional energy technologies for water desalination in Jordan. *Desalination*, 114(1):1-12.

[74] Goto, T., and Hakuta, T. (1966). Pollution problems in a distillation process. *Desalination*, 23(1-3): 245-253.

[75] Bartram, J., and Ballance, R. S. (Editor). (1996). Water Quality Monitoring : A Practical Guide to the Design and Implementation of Freshwater Quality Studies and Monitoring Programmes. ISBN: 0419217304 London, E & FN Spon, 1996, 383 pages.

[76] Davis, M. L., and Cornwell, D. A. (Author). (1991). Introduction to environmental engineering (2nd edition.). ISBN: 0071008284. McGraw-Hill, New York, USA 822 pages.

[77] pH and Water Quality, Internet information server. http://www.kywater.org/ww/ramp/rmph.htm, (10 October 2007).

[78] The Distilled, deionised and demineralised water and measuring of the purity. http://www.lenntech.com/deionised-demineralised-water.htm. (1 April 2008).

[79] Water. (2nd Edition), Geological Survey Water Supply Paper 1473. United States Department of the Interior, United States Government Printing Office. Washington, D.C. http://water.usgs.gov/pubs/wsp/wsp2254. (5 April 2008).

[80] Surface water Water quality report, Department of health, North Dakota. http//www..health.state.nd.us/WQ/SW/Z6_WQ_Standards/WQ_TSS.htm. (13 October 2007).

[81] Wilkes University Center for Environmental Quality, Environmental Engineering and Engineering Department. Total Dissolved Solids. http//www.water-

research.net/totaldissolvedsolids.htm. (12 October 2007).

[82] Total Dissolved Solids. http//www.en.wikipedia.org/wiki/Total_dissolved_solids. (12 October 2007).

[83] Water treatment handbook. (1991). (6th Edition) ISBN: 2950398413 Lavoisier, Paris, France, 592 pages.

[84] Gray, N. F. (Author). (1994). Drinking water quality : problems and solutions. ISBN: 0471948187. John Wiley and Sons Ltd. Chichester, UK, 315 pages.

[85] Nicolson, N. J. (Author). (1993). An introduction to drinking water quality., Institution of Water & Environmental Management ISBN:187075218X. London, UK, 62 pages.

[86] Saline water, The United States Geological Survey (USGS). http://www.ga.water.usgs.gov/edu/saline.html. (October 13, 2007)

[87] Open University. Oceanography Course Team. (1997). (2nd Edition) Seawater : its composition, properties and behaviour, ISBN: 0750637153. Butterworth-Heinemann in association with the Open University, Oxford, UK, 168 pages.

[88] El-Dessouky, H.T., Ettouney, H.M. (Author). (2002) Fundamentals of salt water desalination, ISBN- 13: 9780444508102. Elsevier Science, University of Kuwait, Safat, Kuwait, 690 pages.

[89] Hanson, A., Zachritz, W., Stevens, K., Mimbela, L., Polka, R., and Cisneros, L. (2004). Distillate water quality of a single-basin solar still: laboratory and field studies. *Solar Energy*, **76**(5): 635-645.

[90] Abou Rayan, M., and Khaled, I. (2003). Seawater desalination by reverse osmosis (case study). *Desalination*, **153**(1-3): 245-251.

[91] Yuan, G., and Zhang, H. (2007). Mathematical modeling of a closed circulation solar desalination unit with humidification-dehumidification. *Desalination*, **205**(1-3): 156-162.

[92] Eames, I. W., Maidment, G. G., and Lalzad, A. K. (2007). A theoretical and experimental investigation of a small-scale solar-powered barometric desalination system. *Applied Thermal Engineering*, **27**(11-12): 1951-1959.

[93] Voropoulos, K., Mathioulakis, E., and Belessiotis, V. (2001). Experimental investigation of a solar still coupled with solar collectors. *Desalination*, **138**(1-3): 103-110.

[94] Schwarzer, K., Vieira, M. E., Faber, C., and Müller, C. (2001). Solar thermal desalination system with heat recovery. *Desalination*, **137**(1-3): 23-29.

[95] Bouchekima, B. (2003). A solar desalination plant for domestic water needs in arid areas of South Algeria. *Desalination*, **153**(1-3): 65-69.

[96] Chaibi, M. T. (2000). Analysis by simulation of a solar still integrated in a greenhouse roof. *Desalination*, **128**(2): 123-138.

[97] Badran, A. A., Al-Hallaq, I. A., Eyal Salman, I. A., and Odat, M. Z. (2005). A solar still augmented with a flat-plate collector. *Desalination*, **172**(3): 227-234.

---

[98] Abu-Jabal, M. d. S., Kamiya, I., and Narasaki, Y. (2001). Proving test for a solar-powered desalination system in Gaza-Palestine. *Desalination,* **137**(1-3): 1-6.

[99] Eames, I. W., Maidment, G. G., and Lalzad, A. K. (2007). A theoretical and experimental investigation of a small-scale solar-powered barometric desalination system. *Applied Thermal Engineering,* **27**(11-12): 1951-1959.

[100] Abkr, A. and Ismail, F. (2005). Theoretical and experimental investigation of a novel multi-stage evacuated solar still. *ASME Journal of Solar Energy Engineering,* **127**(3):381-385.

[101] Jubran, B. A., Ahmed, M. I., Ismail, A. F., and Abakar, Y. A. (2000). Numerical modelling of a multi-stage solar still. *Energy Conversion and Management,* **41**(11):1107-1121.

[102] Abdel Dayem, A. M. (2006). Experimental and numerical performance of a multi-effect condensation-evaporation solar water distillation system. *Energy,* **31**(14): 2710-2727.

[103] Hou, S., and Zhang, H. (2008). A hybrid solar desalination process of the multi-effect humidification dehumidification and basin-type unit. *Desalination,* **220**(1-3): 552-557.

[104] Garg, H. P., Adhikari, R. S., and Kumar, R. (2003). Experimental design and computer simulation of multi-effect humidification (MEH)-dehumidification solar distillation. *Desalination,* **153**(1-3): 81-86.

[105] Adhikari, R. S., Kumar, A., and Sootha, G. D. (1995). Simulation studies on a multi-stage stacked tray solar still. *Solar Energy,* **54**(5): 317-325.

[106] Toyama, S., Aragaki, T., Salah, H.M., Murase, K. and Sando, M. (1987). Simulation of a multi-effect solar still and the static characteristics, *Journal of Chemical Engineering of Japan,* **20**(5):473-478..

[107] Fernandez, J. and Chargoy, N. (1990). Multi-stage, indirectly heated solar still. *Solar Energy,* **44**(4):215-223.

[108] Mahkamov, K., Makhkamova, I., Orda E. and Korobkov, A. Water Supply Using a Solar Fluid Piston Stirling Engine. *Proceedings of the 13th International Stirling Engine Conference,* September 23-26, 2007. Waseda University, Tokyo, Japan, pp. 275-279.

[109] Cooper, P. I. (1969). The absorption of radiation in solar stills. *Solar Energy,* **12**(3):333-346.

[110] Incropera, F. P. and DeWitt, D. P. (1996). Fundamentals of heat and mass transfer. ISBN-13: 978-0471163541, John Wiley & Sons, New York, 912 pages.

[111] Tiwari G.N. (Editor). (2002) Solar Energy: Fundamentals, Design, Modelling and Applications. ISBN-13: 978-0849324093. Narosa Publishing House, New Delhi, 2002, 525 pages.

[112] FLUENT Inc, FLUENT 6.2 Documentation; 2005.

[113] Troshko A. (2002). Multiphase with Heat and Mass Transfer and Phase Change presentation. Fluent Users' Group Meeting.

[114] Rehovot weather station, Department of Soil and Water Sciences, The Hebrew University of Jerusalem, Israel, http://www.agri3.huji.ac.il/~margolin (18 October 2007)..

[115] Introduction to Engineering Equation solver Software. http://www.fchart.com/ees/ees.shtml., (27 January 2008).

[116] Miller, J. N. (Author). (2005). Statistics and chemometrics for analytical chemistry. ISBN-13: 9780131291928. Prentice Hall. England, UK. 268 pages.

[117] Goosen, M. F. A., Sablani, S. S., Shayya, W. H., Paton, C., and Al-Hinai, H. (2000). Thermodynamic and economic considerations in solar desalination. *Desalination*, **129**(1): 63-89.

[118] Ahmad, G. E., and Schmid, J. (2002). Feasibility study of brackish water desalination in the Egyptian deserts and rural regions using PV systems. *Energy Conversion and Management*, **43**(18): 2641-2649.

[119] Mahmoud, M. M., and Ibrik, I. H. (2006). Techno-economic feasibility of energy supply of remote villages in Palestine by PV-systems, diesel generators and electric grid. *Renewable and Sustainable Energy Reviews*, **10**(2): 128-138.

Appendices Contents

Appendix A: Engineering Equation Solver program code

Description of Engineering Equation Solver software - EES

EES is a powerful tool for solving engineering problems and it is particularly useful in solving thermodynamic and heat transfer problems since it offers several built-in libraries comprising of thermodynamic and thermo physical properties,

EES provides capabilities not found in any other equation solving program. EES will solve large sets of non-linear algebraic and differential equations. EES also provides publication-quality plots, linear and non-linear regression, optimization, unit conversion and consistency checking, Built-in functions are provided for thermodynamic and transport properties of many substances, including steam, air, refrigerants, cryogenic fluids. Additional property data can be added. EES also allows user-written functions, procedures, modules, and tabular data. EES can also interface with REFPROP and other NIST fluid property programs.

"MODULE FOR CALCULATION OF FIRST STAGE PARAMETERS"

MODULE Evaporation1 (Ts,Tc,Tci,Tco,As,mc,Ms,G:me,DT,mfresh,Qc,mehfgo,Collector_Effeciency)

```
cpc=(4.2101-0.0022*Tco+0.00005*((Tco)^2)-0.0000003*((Tco)^3))*1000      "Specific Heat [J/kg.°C]"
cp=(4.2101-0.0022*Ts+0.00005*((Ts)^2)-0.0000003*((Ts)^3))*1000         "Specific Heat [J/kg.°C]"
hfg=((3165.5-2.40741*(Ts+273))*1000)              "Latent Heat of Vaporization [J/kg]"
Hfg_o=hfg+cp*(0.68*(Ts-Tc))                       " Refined Latent Heat of Vaporization [J/kg]"
Qc=mc*cpc*(Tco-Tci)                               "Solar collector heat input [W]"
ps=exp(25.317-5144/(Ts+273))                      "Partial Pressure [N/m² ] at Surface Water"
pc=exp(25.317-5144/(Tc+273))                      "Partial Pressure [N/m² ] at Bottom Surface of Next
Stage"
hsc=0.884*((Ts-Tc)+(Ts+273)*(ps-pc)/(268.9*1000-ps))^(1/3)  "Heat Transfer coeficient [W/m².C]"
hew=16.273*0.001*hsc*(ps-pc)/(Ts-Tc)             "Mass Evaporation Transfer coeficient [W/m².C]"
me=(Ts-Tc)*hew*As/hfg                            "Mass Evaporation Flow Rate [kg/sec]"
mfresh=me*60
mehfgo=me*Hfg_o
Qc-me*hfg=Ms*cp*dTdt
Ts=Ti+Integral(dTdt, time,0,60)
DT=Ts-Ti
Collector_Effeciency=(Qc*100)/(G)                 "Collector Efficiency [%]"

END
```

"MODULE FOR CALCULATION OF THE SECOND STAGE PARAMETERS"

MODULE Evaporation2(Ts,Tc,heat1,As,Ms:me,DT,mfresh,mehfgo)

```
cp=(4.2101-0.0022*Ts+0.00005*((Ts)^2)-0.0000003*((Ts)^3))*1000        "Specific Heat  [J/kg.C]"
hfg=((3165.5-2.40741*(Ts+273))*1000)                "Latent Heat of Vaporization [J/kg]"
Hfg_o=hfg+cp*(0.68*(Ts-Tc))                " Refined Latent Heat of Vaporization [J/kg]"
ps=exp(25.317-5144/(Ts+273))                "Partial Pressure [N/m^2] at Surface Water"
pc=exp(25.317-5144/(Tc+273))            "Partial Pressure [N/m^2] at Bottom Surface of Next Stage"
hsc=0.884*((Ts-Tc)+(Ts+273)*(ps-pc)/(268.9*1000-ps))^(1/3)        "Heat Transfer coefficient [W/m^2.C]"
hew=16.273*0.001*hsc*(ps-pc)/(Ts-Tc)            "Mass Evaporation Transfer coefficient [W/m^2.C]"
me=(Ts-Tc)*hew*As/(1000*(3165.5-2.40741*(Ts+273)))        "Mass Evaporation Flow Rate [kg/sec]"
mfresh=me*60
mehfgo=me*Hfg_o
heat1-(Ts-Tc)*hew*As=Ms*cp*dTdt
Ts=Ti+Integral(dTdt, time,0,60)
DT=Ts-Ti
```

END

"MODULE FOR CALCULATION OF THE THIRD STAGE PARAMETERS"

MODULE Evaporation3(Ts,Tc,heat2,As,Ms:me,DT,mfresh,mehfgo)

```
cp=(4.2101-0.0022*Ts+0.00005*((Ts)^2)-0.0000003*((Ts)^3))*1000        "Specific Heat  [J/kg.C]"
hfg=((3165.5-2.40741*(Ts+273))*1000)                "Latent Heat of Vaporization [J/kg]"
Hfg_o=hfg+cp*(0.68*(Ts-Tc))                " Refined Latent Heat of Vaporization [J/kg]"
ps=exp(25.317-5144/(Ts+273))                "Partial Pressure [N/m^2] at Surface Water"
pc=exp(25.317-5144/(Tc+273))            "Partial Pressure [N/m^2] at Bottom Surface of Next Stage"
hsc=0.884*((Ts-Tc)+(Ts+273)*(ps-pc)/(268.9*1000-ps))^(1/3)        "Heat Transfer coefficient [W/m^2. °C]"
hew=16.273*0.001*hsc*(ps-pc)/(Ts-Tc)            "Mass Evaporation Transfer coefficient [W/m^2. °C]"
me=(Ts-Tc)*hew*As/(1000*(3165.5-2.40741*(Ts+273)))        "Mass Evaporation Flow Rate [kg/sec]"
mfresh=me*60
mehfgo=me*Hfg_o
heat2-(Ts-Tc)*hew*As=Ms*cp*dTdt
Ts=Ti+Integral(dTdt, time,0,60)
DT=Ts-Ti
```

END

"MODULE FOR CALCULATION OF THE FOURTH STAGE PARAMETERS"

MODULE Evaporation4(Ts,Tc,heat3,As,Ms:me,DT,mfresh,mehfgo)

```
cp=(4.2101-0.0022*Ts+0.00005*((Ts)^2)-0.0000003*((Ts)^3))*1000        "Specific Heat  [J/kg. °C]"
hfg=((3165.5-2.40741*(Ts+273))*1000)                "Latent Heat of Vaporization [J/kg]"
Hfg_o=hfg+cp*(0.68*(Ts-Tc))                " Refined Latent Heat of Vaporization [J/kg]"
ps=exp(25.317-5144/(Ts+273))                "Partial Pressure [N/m^2] at Surface Water"
pc=exp(25.317-5144/(Tc+273))            "Partial Pressure [N/m^2] at Bottom Surface of Next Stage"
hsc=0.884*((Ts-Tc)+(Ts+273)*(ps-pc)/(268.9*1000-ps))^(1/3)        "Heat Transfer coeficient [W/m2. °C]"
hew=16.273*0.001*hsc*(ps-pc)/(Ts-Tc)            "Mass Evaporation Transfer coeficient [W/m2. °C]"
me=(Ts-Tc)*hew*As/(1000*(3165.5-2.40741*(Ts+273)))        "Mass Evaporation Flow Rate [kg/sec]"
mfresh=me*60
mehfgo=me*Hfg_o
```

heat3-(Ts-Tc)*hew*As=Ms*cp*dTdt
Ts=Ti+Integral(dTdt, time,0,60)
DT=Ts-Ti

END

"PROCEDURE TO SOLVE THE NET HEAT INPUT TO THE DESALINATION SYSTEM AND HEAT EXCHANGER EFFECTIVENESS"

PROCEDURE heattransfer(Thxci,Ts,Thxco,mc,Pa:uh,Qhe,efhx)

```
mu=Viscosity(Water,T=Thxci,P=Pa)              "Viscosity [kg/m.s]"
re=4*mc/(3.14*0.015*mu)                       "Renold Number"


If re<=2300 then
nu=3.66
     else

pr=Prandtl(Water,T=Thxci,P=Pa)                "Prandil Number"
nu=0.023*re^0.8*pr^0.4                         "Nussel Number"


     endIf

k=Conductivity(Water,T=Thxci,P=Pa)            "Conductivity[W/m.K]"
hf=nu*k/0.015
uh=1/(1/hf+0.0006)
cp=(4.2101-0.0022*Ts+0.00005*((Ts)^2)-0.0000003*((Ts)^3))*1000     "Specific Heat [J/kg.°C]"
m=-3.14*0.015*7*uh/(mc*cp)
n=exp(m)
Qhe=mc*cp*(Thxci-Ts)*(1-n)
efhx=1-n                                       "Heat exchanger effectiveness"


END
```

```
$ifnot ParametricTable
T1                                            "Temprature at Surface water of stage 1 [°C]"
T2                                            "Temprature at Surface water of stage 2 [°C]"
T3                                            "Temprature at Surface water of stage 3 [°C]"
T4                                            "Temprature at Surface water of stage 4 [°C]"
Tc1                                           "Temprature of condensing Surface at stage 1 [°C]"
Tc2                                           "Temprature of condensing Surface at stage 2 [°C]"
Tc3                                           "Temprature of condensing Surface at stage 3 [°C]"
Tc4                                           "Temprature of condensing Surface at stage 4 [°C]"
As1                                           "Surface Area of Water Body at Stage 1 [m²]"
As2                                           "Surface Area of Water Body at Stage 2 [m²]"
As3                                           "Surface Area of Water Body at Stage 3 [m²]"
As4                                           "Surface Area of Water Body at Stage 4 [m²]"
Ms1                                           "Mass of Water at Stage 1 [kg]"
Ms2                                           "Mass of Water at Stage 2 [kg]"
Ms3                                           "Mass of Water at Stage 3 [kg]"
Ms4                                           "Mass of Water at Stage 4 [kg]"
Tci                                           "Temprature of Influent Solar Collector [°C]"
Tco                                           "Temprature of Effluent Solar Collector [°C]"
Thxci                                         "Temprature of Influentof Heat Exchanger [°C]"
Thxco                                         "Temprature of Effluent Heat Exchanger [°C]"
G1                                            "Solar Radiation Insolation [W/m²]"
```

mc1   "Mass Flow Rate of Fluid through the Collector"
P1   "Atmospheric pressure [Pa]"
$endif

CALL Evaporation1(T1,Tc1,Tci,Tco,As1,mc1,Ms1,G1:me1,DT1,mfresh1,Qc1,mehfgo1,Collector_Effeciency)

heat1=mehfgo1

CALL Evaporation2(T2,Tc2,heat1,As2,Ms2:me2,DT2,mfresh2,mehfgo2)

heat2=mehfgo2

CALL Evaporation3(T3,Tc3,heat2,As3,Ms3:me3,DT3,mfresh3,mehfgo3)

heat3=mehfgo3
CALL Evaporation4(T4,Tc4,heat3,As4,Ms4:me4,DT4,mfresh4,mehfgo4)

CALL heattransfer(Thxci,T1,Thxco,mc1,P1:uh,Qhe,efhx)

Appendix B: MATLAB Simulation Model Program Code

```
%%%%%Matlab Water Desalination Modelling Code for Water Prediction %%%%%%%%%
%%%%%%%%%%% Optimization of Different Evaporation Area %%%%%%%%%%%%%%%%%%%%%%%%%

L=[0.4,0.6,0.8,1,1.2,1.5,1.75,2,2.25,2.5,2.75,3,3.5,4]   %%Multi stage still
length
for n=1:max(size(L))
for L1=L(n)
     L2=L(n)
          L3=L(n)
               L4=L(n)


               h1i=0.04; h2i=0.025; h3i=0.025; h4i=0.025; %%% initial height
of water stages - dimention in m
               Ms1=0.4*L1*h1i*1000-1.24;  %%/mass at first stage= volume*rho
               Ms2=(0.2*L2*(h2i))*1000;   %%/mass at second stage= volume*rho
               Ms3=(0.2*L3*(h3i))*1000;   %%/mass at third stage= volume*rho
               Ms4=(0.2*L4*(h4i))*1000;   %%/mass at fourth stage= volume*rho


               As1n=0.4*L1;  %%/ area of water surface at the beginning
               As2n=0.4*L2;  %%/ area of water surface at the beginning
               As3n=0.4*L3;  %%/ area of water surface at the beginning
               As4n=0.4*L4;  %%/ area of water surface at the beginning

Ta=18.44;Ts1=12.5;Ts2=12.4;Ts3=12.3;Ts4=12.2; %// Initial Temperatures of each
stage

Qc=[483,740,923,1048,1116,1106,1017,857,658,422,0,0,0,0,0,0,0,0,0,0,0,0,0,0];
%//Variation of Solar radiation(W/m2)during the day

Mw1=Ms1; Mw2=Ms2;Mw3=Ms3;Mw4=Ms4; %//Initial Mass of water at each stage
time=1; %Time in second

%%%%%%%%%%%%%%%%%%%%%%%%%Loop iteration for period division %%%%%%%%%%%%%%%%%%%%%%%

%%%%%%%%%%%%%%%%%%%%%%%%%%%%%% loop for segmentation and interpolation of the solar
insolation for each second %%%%%%%%%%%%%%%%%%%%%%%

s=1;
for i=1:(max(size(Qc))-1);
     dk=(Qc(i+1)-Qc(i))/3600;
     Q(s)=Qc(i); %#ok<AGROW>
     for j=2:3600;
          s=s+1;
          Q(s)=Qc(i)+(j-1)*dk; %#ok<AGROW>
     end
end

Q(s+1)=Qc(i+1);
for i=1:max(size(Q));
Qci=Q(i);
```

```
%%%%%%%%%%%%%%%%%% Call function for Stage (1)Calculations %%%%%%%%%%%%%%%%%%%

[cp1,hfg1,Tc1,hsc1,me1,mfresh1,DT1,Tsn1,mehfg1,Mn1,As1,h1]=Evaporation1(Ts1,Ts
2,Ta,Qci,Ms1,L1,time);%// First Stage Function
Ts1o(n,i)=Tsn1; %#ok<AGROW>
me1o(n,i)=me1; %#ok<AGROW>
mec1o(n,i)=Mw1-Mn1; %#ok<AGROW>
Tc1o(n,i)=Tc1; %#ok<AGROW>
As1o(n,i)=As1;
Ts1=Tsn1;
Ms1=Mn1;
Mt1o(n)=Mw1-Mn1; %%% Total production of water
Mnet1o(n,i)=Mn1; %% net stage water mass for each iteration decreasing
h1o(n)=h1*100; %%//height in cm
h1of(n)=h1i;    %%%%1stage water depth(Mw1+1.24)*100/(As1*1000)
As1of(n)=As1n;  %%%% Area of 1st stage at the begining
L1o(n)=L1
DT1o(n,i)=DT1;  %%// Temperature difference at the 1st stage
heat2=mehfg1;


%%%%%%%%%%%%%%%%%%%%%%%%%%%Call function for Stage (2) Calculations %%%%%%%%%%%%%%%

[cp2,hfg2,Tc2,hsc2,me2,mfresh2,DT2,Tsn2,mehfg2,Mn2,As2,h2]=Evaporation2(Ts2,Ts
3,Ta,heat2,Ms2,L2,time); %// First Stage Function
Ts2o(n,i)=Tsn2; %#ok<AGROW>
me2o(n,i)=me2; %#ok<AGROW>
mec2o(n,i)=Mw2-Mn2; %#ok<AGROW>
Tc2o(n,i)=Tc2;
As2o(n,i)=As2;
Ts2=Tsn2;%#ok<AGROW>
Ms2=Mn2;
Mt2o(n)=Mw2-Mn2; %%% Total production of water
Mnet2o(n,i)=Mn2; %% net stage water mass for each iteration decreasing
h2o(n)=h2*100; %%//height in cm %%% the remaining depth
%%%%%%%%%%%%%%%%%%%%%%%%%%%%%%
As2of(n)=As2n;  %%%% Area of 4th stage at the beginning
L2o(n)=L2
DT2o(n,i)=DT2;  %%// Temperature difference at the 2nd stage
heat3=mehfg2;


%%%%%%%%%%%%%%%%%%%%%%%%%% Call function for Stage (3) Calculations %%%%%%%%%%%%%%

[cp3,hfg3,Tc3,hsc3,me3,mfresh3,DT3,Tsn3,mehfg3,Mn3,As3,h3]=Evaporation3(Ts3,Ts
4,Ta,heat3,Ms3,L3,time); %// First Stage Function
Ts3o(n,i)=Tsn3;
me3o(n,i)=me3;
mec3o(n,i)=Mw3-Mn3;
Tc3o(n,i)=Tc3;
As3o(n,i)=As3;
Ts3=Tsn3;
Ms3=Mn3;
Mt3o(n)=Mw3-Mn3; %%% Total production of water
Mnet3o(n,i)=Mn3; %% the remaining net water mass at each stage
h3o(n)=h3*100; %%//height in cm %%% the remaining depth
heat4=mehfg3;
As3of(n)=As3n;  %%%% Area of 3rd stage at the beginning
```

```
L3o(n)=L3
DT3o(n,i)=DT3;   %%// Temperature difference at the 3rd stage


%%%%%%%%%%%%%%%%%%%%%% Call function for Stage (4) Calculations %%%%%%%%%%%%%

[cp4,hfg4,Tc4,hsc4,me4,mfresh4,DT4,Tsn4,mehfg4,Mn4,As4,h4]=Evaporation4(Ts4,Ta
,heat4,Ms4,L4,time); %// First Stage Function
Ts4o(n,i)=Tsn4; %#ok<AGROW>
me4o(n,i)=me4; %#ok<AGROW>
mec4o(n,i)=Mw4-Mn4; %#ok<AGROW>
As4o(n,i)=As4;
Tc4o(n,i)=Tc4; %#ok<AGROW>
Ts4=Tsn4;
Mt4o(n)=Mw4-Mn4; %%% Total production of water
Mnet4o(n,i)=Mn4; %% net stage water mass for each iteration decreasing
h4o(n)=h4*100; %%//height in cm %%% the remaining depth
As4of(n)=As4n;   %%%% Area of stages at the begining
L4o(n)=L4
DT4o(n,i)=DT4;   %%// Temprature diffrence at the 4th stage
h4of(n)=2.5+(Mw4*100/(1000*As4))-0.0125*100; %%% the depth of water at the
begining
Ms4=Mn4;

end


    end


TotalDistillate1(n)=sum(me1o(n,:));
TotalDistillate2(n)=sum(me2o(n,:));
TotalDistillate3(n)=sum(me3o(n,:));
TotalDistillate4(n)=sum(me4o(n,:));
AllTotalDistillate4(n)=TotalDistillate1(n)+TotalDistillate2(n)+TotalDistillate
3(n)+TotalDistillate4(n);
        end



%%%%%%%%%%%%%%%%%%%%%%%%%%%% First Stage Function %%%%%%%%%%%%%%%%%%%%%%%%%%%%%%%%

function
[cp,hfg,Tc,hsc,me,mfresh,DT,Tsn,mehfg,Mn,As,h]=Evaporation1(Ts,Tsc,Ta,Qci,Ms,L
,time)
cp=(4.2101-0.0022*Ts+0.00005*((Ts)^2)-0.0000003*((Ts)^3))*1000; %//
"Specific Heat  [J/Kg.C]"
hfg=(3165.5-2.40741*(Ts+273))*1000; %//"Latent Heat of Vaporization [J/Kg]"

if Ts<=100
    Ts=Ts;
else
    Ts=100;
end

if Tsc+2.0<=Ts;
Tc=Tsc+2.0;
else
    Tc=Ts-0.0000001;
```

```matlab
end

As=0.4*L;
h=(Ms+1.24)/(0.4*L*1000); %%% Depth of water in m and 1.24kg=heat exchanger
weight volume
cpc=(4.2101-0.0022*(Tc)+0.00005*((Tc)^2)-0.0000003*((Tc)^3))*1000; %//
"Specific Heat  [J/Kg.C]"
ps=exp(25.317-5144/(Ts+273));   %// "Partial Pressure [N/m2] at Surface Water"
pc=exp(25.317-5144/(Tc+273));   %// "Partial Pressure [N/m2] at Bottom Surface
of Next Stage"
hsc=0.884*((Ts-Tc)+(Ts+273)*(ps-pc)/(268.9*1000-ps))^(1/3);    %//"Heat
Transfer coeficient [W/m2.C]"
hew=16.273*0.001*hsc*(ps-pc)/(Ts-Tc);   %// "Mass Evaporation Transfer
coeficient [W/m2.C]"
me=(Ts-Tc)*hew*As/(1000*(3165.5-2.40741*(Ts+273)));    %// "Mass Evaporation
Flow Rate [Kg/sec]"
mfresh=me*time;
Hfg_o=hfg+cp*(0.68*(Ts-Tc));          %//"Modified Latent Heat of Vaporization
[J/Kg]"
Ut=((1/hsc)+(0.15/0.044))^-1;         %//"Total heat loss transfer coefficient
[W/m2.K]"

if Ta>=Ts
    Ta=Ts;
      else
    Ta=Ta;
            end

if (Ms-me*time)>0

DT=((Qci*2.2*0.7517-me*hfg-me*cpc*(Tc+273)-
((Ut)*(0.16*(1.2*2+0.4*2)+0.4*1.2))*(Ts-Ta))*time)/((Ms-me*time)*cp);
      else
        DT=0
            end

Tsn=Ts+DT;

mehfg=me*Hfg_o; %%// The input heat of the next stage
Mn=Ms-me*time; %%The remaining water mass at each stage
As=As;

%%%%%%%%%%%%%%%%%Second, Third, and Fourth Stages Function %%%%%%%%%%%%%%%%

function
[cp,hfg,Tc,hsc,me,mfresh,DT,Tsn,mehfg,Mn,As,h]=Evaporation2(Ts,Tsc,Ta,heat,Ms,
L,time)
cp=(4.2101-0.0022*Ts+0.00005*((Ts)^2)-0.0000003*((Ts)^3))*1000; %//
"Specific Heat  [J/Kg.C]"
hfg=(3165.5-2.40741*(Ts+273))*1000; %//"Latent Heat of Vaporization [J/Kg]"


if Ts<=100
    Ts=Ts;
else
```

```
        Ts=100;
end


if Tsc+2.7<=Ts;
Tc=Tsc+2.7;
else
        Tc=Ts-0.0000001;
end



h=sqrt(Ms/(8000*L));  %% length in (m)
As=16*h*L;     %% Area in (m2)


cpc=(4.2101-0.0022*(Tc)+0.00005*((Tc)^2)-0.0000003*((Tc)^3))*1000; %//
"Specific Heat  [J/Kg.C]"
ps=exp(25.317-5144/(Ts+273));    %// "Partial Pressure [N/m2] at Surface Water"
pc=exp(25.317-5144/(Tc+273));    %// "Partial Pressure [N/m2] at Bottom Surface
of Next Stage"
hsc=0.884*((Ts-Tc)+(Ts+273)*(ps-pc)/(268.9*1000-ps))^(1/3);     %//"Heat
Transfer coeficient [W/m2.C]"
hew=16.273*0.001*hsc*(ps-pc)/(Ts-Tc);    %// "Mass Evaporation Transfer
coeficient [W/m2.C]"
me=(Ts-Tc)*hew*As/(1000*(3165.5-2.40741*(Ts+273)));     %// "Mass Evaporation
Flow Rate [Kg/sec]"
mfresh=me*time;
Hfg_o=hfg+cp*(0.68*(Ts-Tc));           %//"Modified Latent Heat of Vaporization
[J/Kg]"
%%//hfg_c=(3165.5-2.40741*(Tc+273))*1000 %//"Latent Heat of Vaporization
[J/Kg]"
Ut=((1/hsc)+(0.15/0.044))^-1;
if Ta>=Ts
        Ta=Ts;
else
        Ta=Ta;
end
if (Ms-me*time)>0
DT=(heat-(Ts-Tc)*hew*As-me*cpc*(Tc+273)-(Ut)*(0.125*(1.2*2+0.4*2)*(Ts-
Ta)))*time/((Ms-me*time)*cp);
else
        DT=0;
end


Tsn=Ts+DT;



mehfg=me*Hfg_o;
Mn=Ms-me*time;
```

Appendix C: FLUENT 6.2 CFD Simulation Model Input File

The CFD modeling is divided into two stages the first one is generating the multi stage system by using GAMBIT software to generate and mesh the solar still as shown in Figure 1 in addition to specify the boundary conditions and the second one is simulation of the system by using FLUENT 6.2 software.
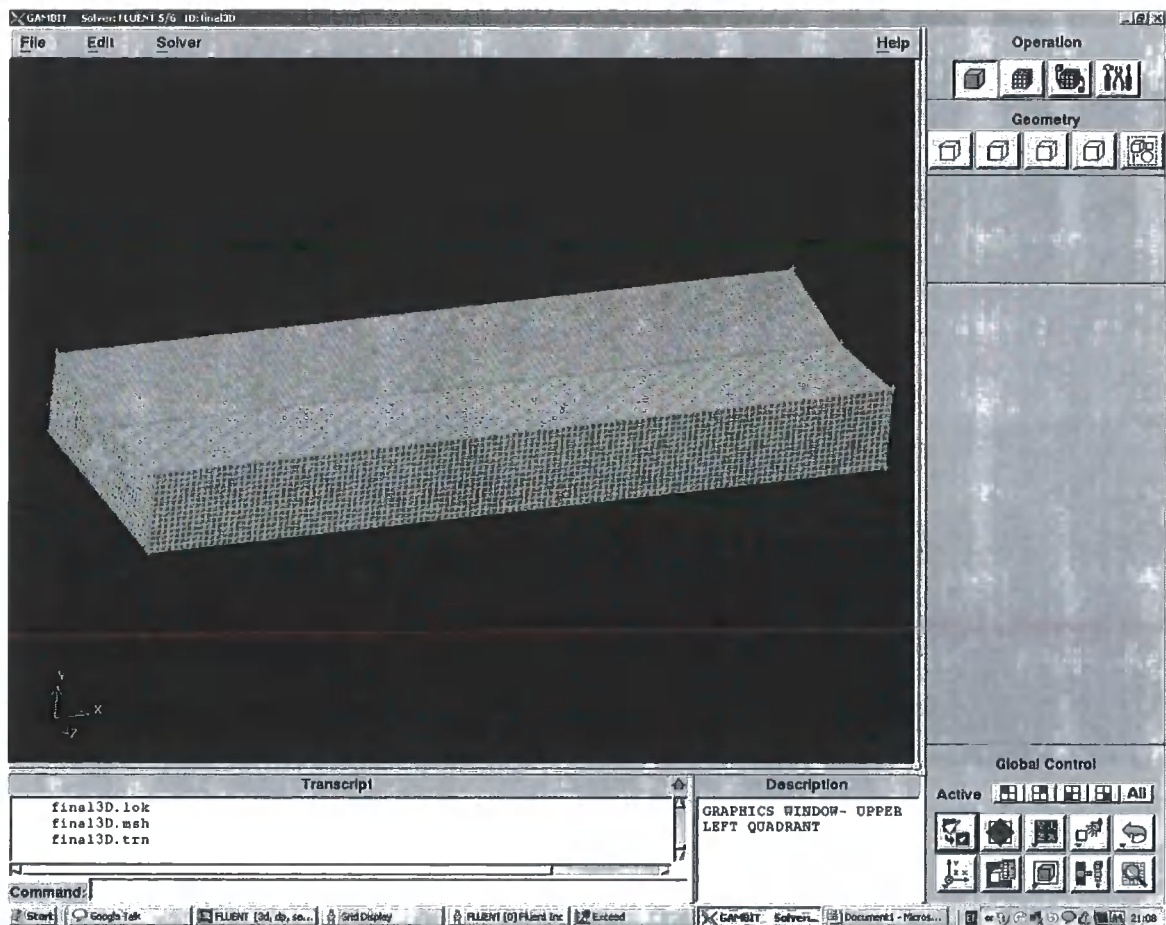
Figure 1: 3D solar water still meshing using GAMBIT software

Fluent input file

1. **Step 1: Set up and read case model**
   - Read the mesh file Multi-stage-still.msh
   - Check and display the grid

2. **Step 2: Model**
   - Select Solver Unsteady
   - Define Multi phase model

     (a) Select the Volume of Fluid multiphase model.

     (b) Enable the Implicit Body Force formulation.

3. **Step 3: Enable the Energy Equation.**

4. **Step 4: Materials**
   - Create two new fluid materials, liquid water and vapour water, and steel material solid from the fluent build in library

5. **Step 5: Phases**
   - Define the primary phase as water vapour phase.
   - Define the secondary phase as water liquid phase.
   - Specify the interphase interaction and specify the surface tension coefficient value 0.0608 N/m

6. **Step 6: Operating Conditions**
   - Define Operating Conditions...

     (a) Enable Gravity and set the Gravitational Acceleration in the Y direction to -9.81 m/s^2.

     (b) Enable specified Operating Density and set the Operating Density to 0.5542 kg/m^3.

7. **Step 7: User-defined Function - UDF**

   In this model a UDF is used to specify the mass transfer between the phases. The mass transfer terms for each phase (vapor and liquid), are equal and have Opposite signs. They are specified as source terms in volume fraction equations and have units of kg-sec/m^3. In addition, there is an energy source temperature to take into account the latent heat absorbed/released, which has units of W/m3 and is prescribed for mixture energy equation as shown in the UDF code.

UDF – Heat and Mass Transfer

```
#include "udf.h"
#include "sg_mphase.h"
#define T_SAT 373
#define LAT_HT 1.e3

DEFINE_SOURCE(liq_src, cell, pri_th, dS, eqn)
{

  Thread *mix_th, *sec_th;
  real m_dot_l;

  mix_th = THREAD_SUPER_THREAD(pri_th);
  sec_th = THREAD_SUB_THREAD(mix_th, 1);
  if(C_T(cell, mix_th)>=T_SAT){
    m_dot_l = -0.1*C_VOF(cell, pri_th)*C_R(cell, pri_th)*
          fabs(C_T(cell, pri_th) - T_SAT)/T_SAT;
    dS[eqn] = -0.1*C_R(cell, pri_th)*
      fabs(C_T(cell, pri_th) - T_SAT)/T_SAT;
                    }
  else {
    m_dot_l = 0.1*C_VOF(cell, sec_th)*C_R(cell, sec_th)*
          fabs(T_SAT-C_T(cell,mix_th))/T_SAT;

  dS[eqn] = 0.;

    }

  return m_dot_l;

}

DEFINE_SOURCE(vap_src, cell, sec_th, dS, eqn)

{
  Thread * mix_th, *pri_th;
  real m_dot_v;

  mix_th = THREAD_SUPER_THREAD(sec_th);
  pri_th = THREAD_SUB_THREAD(mix_th, 0);
  if(C_T(cell, mix_th)>=T_SAT){
    m_dot_v = 0.1*C_VOF(cell, pri_th)*C_R(cell, pri_th)*
          fabs(C_T(cell, mix_th) - T_SAT)/T_SAT;
    dS[eqn] = 0.;
```

```
                    }
   else {
     m_dot_v = -0.1*C_VOF(cell, sec_th)*C_R(cell, sec_th)*
             fabs(T_SAT-C_T(cell,mix_th))/T_SAT;

     dS[eqn] = -0.1*C_R(cell, sec_th)*
       fabs(C_T(cell, sec_th) - T_SAT)/T_SAT;

       }

   return m_dot_v;

}

DEFINE_SOURCE(enrg_src, cell, mix_th, dS, eqn)
{
   Thread *pri_th, *sec_th;
   real m_dot;
   pri_th = THREAD_SUB_THREAD(mix_th, 0);
   sec_th = THREAD_SUB_THREAD(mix_th, 1);

   if(C_T(cell, mix_th)>=T_SAT){
     m_dot = -0.1*C_VOF(cell, pri_th)*C_R(cell, pri_th)*
             fabs(C_T(cell, pri_th) - T_SAT)/T_SAT;

     dS[eqn] = -0.1*C_VOF(cell, pri_th)*C_R(cell, pri_th)/T_SAT;
                     }

   else {
     m_dot = 0.1*C_VOF(cell, sec_th)*C_R(cell, sec_th)*
             fabs(T_SAT-C_T(cell,mix_th))/T_SAT;

     dS[eqn] = -0.1*C_VOF(cell, sec_th)*C_R(cell, sec_th)/T_SAT;}

   return LAT_HT*m_dot;
}
```

8. **Step 8: Boundary Conditions**

- Set the boundary conditions for fluid based on the interpreted function for vapour, water liquid and energy mixture.

- Set the boundary conditions for heat source at the bottom surface temperature to be 368 K (95°C)

- all other still walls were defined as a diabetic flux = 0

- Distillate water and upper outlets were assigned to be at temperature 363 K and pressure 101325 Pa

- Set the surface tension calculation options using the following TUI commands:

9. **Step 9: Set the solution parameters.**

- Set the Under-Relaxation Factors for Pressure 0.3 and Momentum to 0.7.

- Select PRESTO! for Pressure, and QUICK for Momentum and Energy under Discretization

- Select PISO from the Pressure-Velocity Coupling drop-down list.

10. **Step 10: Define a custom field function**

- For initializing the temperature profile as shown in the following.

368 - y * 5 / 0.135.
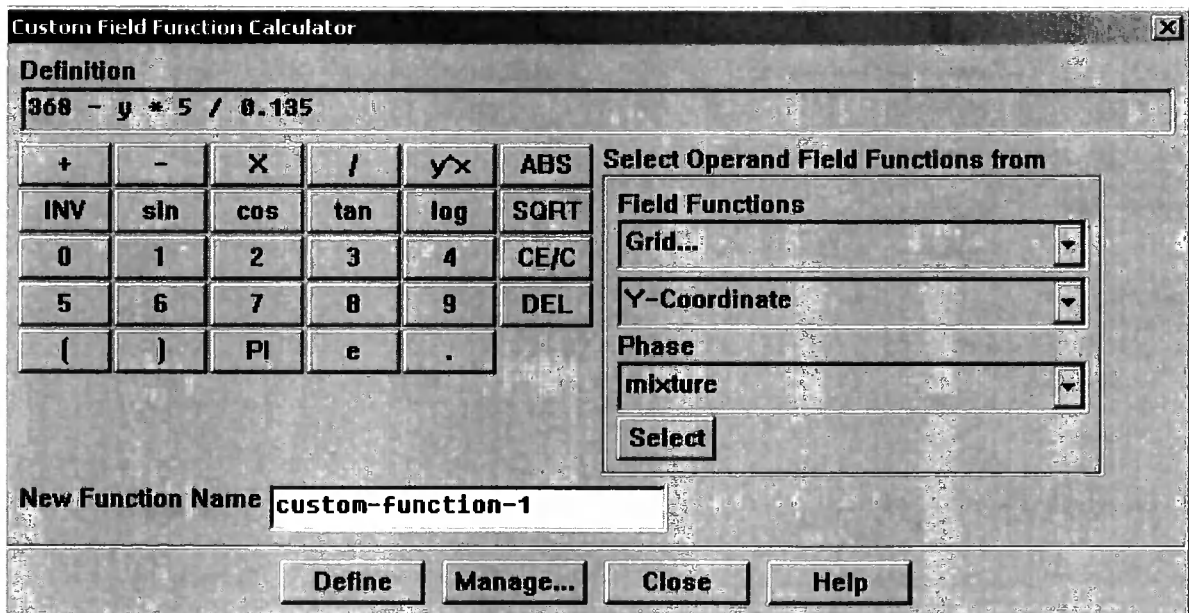
Figure 2: Custom field function for patching temperatures variation inside still

11. **Step 11: Initialize and patch the solution.**

- Initialize with pressure and velocity components at zero.

- Set the fluid Volume Fraction to 0.296.

- Set the value for Temperature to 363 k.

- Click Init and close the Solution Initialization panel.

- 5. Patch a temperature using custom-function-0 for the fluid zone.

- 6- Patch the water liquid by using defined adapt region as shown in figure 3

12. **Step 12: Start the calculation.**

- Set Time Step Size to 0.01.

- Set the Number of Time Steps to 1000.

- Click Iterate as shown in Figure 3.
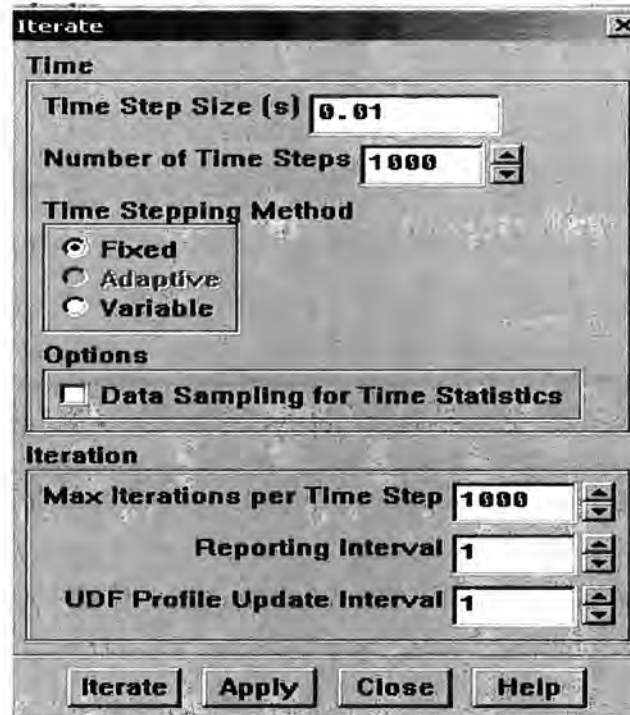
Figure 3: Iteration menu and its input time step

Appendix D: Experimental results and theoretical calculations

Measurements and calculations of calibration of Insolation variable simulator

Variable Voltage (%)	Area			Corner Voltage			Middle Voltage			Corner	Middle	Average
	Lamps (m²)	Columns (m²)	Rows (m²)	Lamp Volts	Column Volts	Row Volts	Lamp Volts	Column Volts	Row Volts	Insolation		
										(W/m²)	(W/m²)	(W/m²)
20	0.964	0.233	0.666	0.04	0.04	0.04	0.05	0.05	0.05	12	15	14
30	0.964	0.233	0.666	0.185	0.185	0.18	0.23	0.23	0.23	55	69	62
40	0.964	0.233	0.666	0.38	0.41	0.55	0.57	0.59	0.51	133	165	149
50	0.964	0.233	0.666	0.83	0.79	1.07	1.07	1.09	1.07	273	322	297
55	0.964	0.233	0.666	1.08	1.13	1.58	1.44	1.5	1.58	379	449	414
60	0.964	0.233	0.666	1.4	1.47	1.78	1.91	1.96	1.98	463	582	523
65	0.964	0.233	0.666	1.72	1.81	2.16	2.27	2.33	2.42	567	699	633
70	0.964	0.233	0.666	2.09	2.18	2.67	2.85	3	2.98	693	875	784
72	0.964	0.233	0.666	2.29	2.4	2.91	3.1	3.28	3.34	758	962	860
75	0.964	0.233	0.666	2.54	2.63	3.21	3.45	3.65	3.68	837	1067	952
78	0.964	0.233	0.666	2.84	2.99	3.61	3.99	3.84	4.05	940	1198	1069
80	0.964	0.233	0.666	2.91	3.07	3.82	4.08	4.29	4.23	977	1248	1112
82	0.964	0.233	0.666	3.23	3.38	4.05	4.2	4.37	4.41	1063	1289	1176

Measurement results and calculation of simulator Voltage versus Insolation

Experimental Results of Multi Stage still

Date: __12/03/2008__   **coupled with Evacuated Tube Solar Collector**   **Condition:**   *Partially Insulated*

Time	Insolation (W/m²)	Voltage (%)	1st Stage °C		2nd Stage °C		3rd Stage °C		4th Stage °C		Heat Exchanger		Solar Collector		Ambient	Distilled Water Product (Grams)			
			T1	T2	T3	T4	T5	T6	T7	T8	T-Inlet	T-Outlet	T-Outlet	T-Inlet	Ta	Stage1	Stage2	Stage 3	Stage4
08:00	483	60.04	12.9	12.7	12.4	12.9	12.4	12.7	12.8	12.4	12.9	13.3	13.5	13.1	13.1				
08:20	569	63.32	16.1	14.9	13.4	12.2	12.1	12.3	12.4	12.0	27.9	26.4	28.1	25.9	16.7				
08:40	654	66.28	18.5	16.0	12.9	12.4	12.4	12.5	12.2	37.4	35.9	37.7	35.3	17.9	17.9				
09:00	740	68.99	35.6	24.3	20.9	14.4	13.1	12.6	12.6	12.4	46.6	45.0	46.9	44.2	18.8				
09:20	801	70.79	44.8	32.0	28.1	17.2	14.9	13.0	12.9	12.6	55.1	53.5	55.6	52.7	19.5				
09:40	862	72.50	53.3	39.8	36.4	21.6	18.2	13.9	13.5	13.0	63.0	61.3	63.4	60.3	20.2				
10:00	923	74.14	60.7	47.3	45.2	27.5	23.2	15.5	14.7	13.5	70.0	68.3	70.5	67.3	20.4				
10:20	965	75.21	67.6	56.0	53.4	34.9	30.1	18.3	17.0	14.2	76.5	74.8	77.0	73.8	20.6				
10:40	1006	76.25	73.7	64.1	61.3	41.6	38.3	22.6	20.7	15.4	82.4	80.6	83.0	79.5	21.2				
11:00	1048	77.26	79.1	71.1	68.2	50.5	46.8	28.8	26.0	17.5	87.4	85.6	88.0	84.5	21.5				
11:20	1071	77.80	83.9	77.4	74.8	59.4	55.2	35.5	33.1	21.2	91.9	90.1	92.5	89.0	22.4	423	172		
11:40	1093	78.34	88.3	83.1	80.5	66.9	62.6	43.5	41.0	26.0	96.0	94.1	96.6	93.0	22.9				
12:00	1116	78.86	91.8	88.1	85.7	74.7	70.0	52.2	49.6	31.8	99.3	97.1	99.9	95.9	23.3				
12:20	1113	78.78	94.7	92.1	90.0	81.1	76.9	61.1	58.4	37.7	102.1	100.0	102.7	98.8	23.4	219	175	165	
12:40	1109	78.71	97.6	95.2	93.2	85.9	81.9	67.3	64.8	42.6	103.6	101.4	104.2	100.3	23.0				
13:00	1106	78.63	100.0	98.0	96.2	90.3	86.3	72.6	70.1	46.9	103.9	101.8	104.5	100.6	22.9	230	210	194	155
13:20	1076	77.94	100.4	99.11	97.85	94.18	90.52	77.28	74.73	52.7	104.04	101.84	104.62	100.67	22.52				
13:40	1047	77.23	100.4	99.45	98.63	96.13	93.06	80.47	77.68	56.6	103.96	101.745	104.54	100.59	22.16	176	271	310	245
14:00	1017	76.51	100.4	99.54	98.81	96.72	93.94	81.96	78.88	58.9	103.82	101.64	104.39	100.49	22.2				
14:20	964	75.18	100.4	99.65	99.06	97.19	94.51	83.56	80.49	61.63	103.73	101.61	104.3	100.46	22.08	96.3	282	295	288.5
14:40	910	73.80	100.4	99.52	98.83	96.21	93.35	81.8	78.73	33.6	103.65	101.54	104.2	100.43	22.13				
15:00	857	72.37	100.3	99.2	98.16	94.26	90.59	78.11	75.13	57.29	103.26	101.415	103.81	100.32	22.15	141	255	336	305
15:20	791	70.49	100.3	99.13	98	93.39	89.6	76.53	73.44	47.82	103.17	101.39	103.7	100.32	22.75				
15:40	724	68.51	100.1	98.99	97.78	92.77	89.17	77.17	74.4	54.14	102.99	101.285	103.5	100.26	22.82				
16:00	658	66.40	99.54	97.93	96.97	92.22	88.62	76.99	74.1	54.36	102.52	101.015	103.02	100.01	22.84	230	260	332	315

Experimental Results of Multi Stage still

Date: __12/03/2008__   coupled with Evacuated Tube Solar Collector   Condition: *Partially Insulated*

Time	Insolation (W/m²)	Voltage (%)	1st Stage °C		2nd Stage °C		3rd Stage °C		4th Stage °C		Heat Exchanger		Solar Collector		Ambient	Distilled Water Product (Grams)			
			T1	T2	T3	T4	T5	T6	T7	T8	T-Inlet	T-Outlet	T-Outlet	T-Inlet	Ta	Stage1	Stage2	Stage 3	Stage4
16:20	579	63.71	98.43	96.88	95.95	91.18	87.53	75.96	73.24	56.48	101.83	100.43	102.3	99.48	22.68				
16:40	501	60.75	97.34	95.71	94.4	88.3	84.87	72.51	69.87	49.3	100.85	99.64	101.32	98.69	22.65	172	243	304	288
17:00	422	57.46	95.9	93.92	92.88	87.57	84	72.23	69.68	54	99.173	98.125	99.63	97.21	22.57	102	143	195	186
After 24 hours																110	180	390	480
Total																1899.3	2191	2521	2262.5

Theoretical Calculations of Multi Stage solar still

Date: 12/03/2008   coupled with Evacuated Tube Solar Collector   Condition: Partially Insulated

| Time | Solar Insolation | Mass Flow rate | Q_h (J) Solar | Q_h (J) Heat | Cumulative Distilled Water | | | | Total |
(hr:min)	(W/m²)	(Kg/sec)	Collector	Exchanger	(Kg) 1st Stage	(Kg) 2nd Stage	(Kg) 3rd Stage	(Kg) 4th Stage	(Kg) Cumulative
08:00	483	0.1000	9551	0	0.00	0.00	0.00	0.00	0.00
08:20	569	0.1000	56194	35874	0.00	0.00	0.00	0.00	0.00
08:40	654	0.0967	58701	34868	0.00	0.00	0.00	0.00	0.00
09:00	740	0.0967	65552	38601	0.02	0.00	0.00	0.00	0.02
09:20	801	0.0967	70245	39435	0.04	0.01	0.00	0.00	0.05
09:40	862	0.0967	74699	41301	0.09	0.02	0.00	0.00	0.11
10:00	923	0.0967	77435	42186	0.16	0.04	0.00	0.00	0.20
10:20	965	0.0967	79417	41778	0.25	0.08	0.01	0.00	0.34
10:40	1006	0.0967	83807	45254	0.35	0.15	0.03	0.00	0.53
11:00	1048	0.0967	84271	44451	0.46	0.24	0.06	0.01	0.77
11:20	1071	0.0967	86172	44551	0.58	0.35	0.12	0.02	1.06
11:40	1093	0.0967	88295	46342	0.69	0.48	0.20	0.04	1.40
12:00	1116	0.0967	96241	54509	0.78	0.62	0.31	0.07	1.78
12:20	1113	0.0967	93729	51670	0.85	0.75	0.46	0.13	2.19
12:40	1109	0.0967	94408	52372	0.91	0.87	0.63	0.24	2.65
13:00	1106	0.0967	95366	52245	0.97	0.98	0.82	0.38	3.16
13:20	1076	0.0967	95848	53274	1.02	1.07	1.05	0.55	3.68
13:40	1047	0.0917	90893	51038	1.04	1.11	1.29	0.75	4.19
14:00	1017	0.0917	89748	50062	1.06	1.15	1.52	0.95	4.68
14:20	964	0.0917	88370	48683	1.08	1.18	1.74	1.15	5.14
14:40	910	0.0917	86762	48454	1.10	1.21	1.93	1.35	5.59
15:00	857	0.0917	80330	42532	1.12	1.27	2.13	1.54	6.06
15:20	791	0.0917	77801	40865	1.15	1.33	2.30	1.71	6.49
15:40	724	0.0917	74584	39198	1.17	1.41	2.45	1.85	6.88
16:00	658	0.0917	69301	34599	1.21	1.49	2.59	1.97	7.26
16:20	579	0.0917	64942	32131	1.25	1.56	2.71	2.09	7.60
16:40	501	0.0917	60586	27763	1.28	1.63	2.83	2.21	7.96
17:00	422	0.0917	55776	24146	1.33	1.70	2.93	2.30	8.26
After 24 hours					1.79	2.10	3.46	2.83	10.18
Total			43211845	23123188	1.79	2.10	3.46	2.83	10.18

Mout *
hfg   20737729   Joule

Distillation Efficiency   89.7   %

Overall Efficiency   32.42   %

Appendix E: Water quality analysis and experimental results

Water quality results

Condition 1 -Fully Insulated

	Before Distillation			After Distillation											
				1st Stage			2nd Stage			3rd Stage			4th Stage		
Time	EC	pH	TDS	EC-1	pH-1	TDS-1	EC-2	pH-2	TDS-2	EC-3	pH-3	TDS-3	EC-4	pH-4	TDS-4
	(µS/cm)		(mg/L)	(µS/cm)		(mg/L)	(µS/cm)		(mg/L)	(µS/cm)		(mg/L)	(µS/cm)		(mg/L)
08:00															
09:00															
10:00															
11:00															
12:00	3136	7.3	2407	35.9	6.47	23.11	36.95	6.86	24.2						
13:00				40.12	6.48	25.88	17.35	7.22	10.71	21.35	7.25	13.26			
14:00				14.32	6.15	8.85	19.57	7.28	12	23.99	7.57	14.8	36.48	7.22	22.83
15:00				32.47	5.77	20.34	27.6	6.98	17.04	36.98	7.57	23.04	44.52	7.38	28.02
16:00				24.5	5.2	16.1	49.39	6.64	31.1	75.31	7.47	47.73	73.22	7.09	46.51
17:00				29.46	6.01	18.86	61.40	7.00	39.07	39.41	7.47	24.71	51.41	7.23	32.45
Average	3136	7.3	2407	29.46	6.01	18.86	30.17	7.00	19.03	39.41	7.47	24.71	51.41	7.23	32.45

EC: Electrical conductivity (µS/cm)

TDS: Total dissolved solids (mg/L)

Water quality results
Condition 2 -Partially Insulated - 1

| | Before Distillation | | | After Distillation | | | | | | | | | | | | |
| | | | | 1st Stage | | | 2nd Stage | | | 3rd Stage | | | 4th Stage | | |
Time	EC	pH	TDS	EC-1	pH-1	TDS-1	EC-2	pH-2	TDS-2	EC-3	pH-3	TDS-3	EC-4	pH-4	TDS-4
	(µS/cm)		(mg/L)	(µS/cm)		(mg/L)	(µS/cm)		(mg/L)	(µS/cm)		(mg/L)	(µS/cm)		(mg/L)
08:00															
09:00															
10:00															
11:00															
12:00	3056	7.07	2323	40.31	6.74	25.78	46.4	7.62	26.24	37.3	7.73	23.51	49.01	7.5	31.25
13:00				22.88	6.6	14.12	30.34	7.83	18.72	27.11	8.01	16.96	45.65	8.1	28.91
14:00				63.48	7.61	39.86	29.41	7.93	17.91	25.69	8.04	15.6	38.83	7.7	24.08
15:00				35.75	7.8	22.26	29.13	8.01	17.9	28.18	8.16	17.41	35.75	7.8	22.26
16:00				26.5	7.91	16.59	27.2	7.74	16.78	29.91	8.01	18.43	30.68	8.1	18.91
17:00				44.18	6.14	28.88	26.94	6.65	17.34	28.07	7.45	18.08	29.98	7.4	19.34
Average	3056	7.07	2323	38.85	7.13	24.58	31.57	7.63	19.15	29.38	7.90	18.33	38.32	7.77	24.13

EC: Electrical conductivity (µS/cm)
TDS: Total dissolved solids (mg/L)

Water quality results
Partially Insulated – 2

Time	Before Distillation			After Distillation											
				1st Stage			2nd Stage			3rd Stage			4th Stage		
	EC	pH	TDS	EC-1	pH-1	TDS-1	EC-2	pH-2	TDS-2	EC-3	pH-3	TDS-3	EC-4	pH-4	TDS-4
	(µS/cm)		(mg/L)	(µS/cm)		(mg/L)	(µS/cm)		(mg/L)	(µS/cm)		(mg/L)	(µS/cm)		(mg/L)
08:00															
09:00															
10:00															
11:00															
12:00	2888	2196	7.11	15.23	6.22	9.49	49	6.6	31.64						
13:00				12.39	6.48	7.73	25.51	7.3	16	31.67	7.1	20.06			
14:00				13.92	6.41	8.6	28.48	7.55	17.8	26.48	7.26	16.62			
15:00				15.95	6.23	9.29	29.14	7.78	18.19	27.85	7.65	17.49			
16:00				16.33	6.09	10.27	28.95	7.85	18.22	29.23	7.72	18.32	46.11	7.04	29.55
17:00				18.62	6.05	11.92	29.76	7.03	19.1	28.18	7.23	18.06			
Average	2888	2196	7.11	15.41	6.25	9.55	31.81	7.35	20.16	28.68	7.39	18.11	46.11	7.04	29.55

EC: Electrical conductivity (µS/cm)
TDS: Total dissolved solids (mg/L)

Appendix F: Economic study

PV Module catalogues

MIL-PV-50W-M01
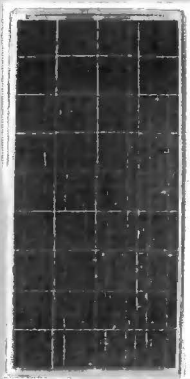
Features & Benefits

☒ High efficiency - maximizing power and reducing installation costs.

☒ High energy generating kWh/kWp performance.

☒ High power tolerance.

☒ High reliability through enhanced processing technology.

Millennium's photovoltaic modules offer industry-leading performance, durability, and reliability for a variety of electrical power requirements. Using breakthrough technology, these modules use a textured cell surface to reduce reflection of sunlight, and structure to improve conversion efficiency. An anti-reflective coating provides uniform blue color and increases the absorption of light in all weather conditions.

Common applications include grid connected houses, solar houses, solar power stations, telecom and cellular base stations, beacons and lighting equipment. Designed to withstand rigorous weather conditions, a junction box is also provided for easy electrical connections in the field, making Millennium's modules the perfect combination of advanced technology and reliability.

☑ **High Performance**

High-power module using 36 125mm square multi-crystalline silicon cells with 14.3 % module conversion efficiency. Photovoltaic modules with bypass diodes minimize the power drop cause by shade.

☑ **High Quality**

Advanced EVA encapsulation with highest quality strengthened glass embedded with years of manufacturing experience and quality assurance procedures.

☑ **Lifetime Guarantee**

Manufacturer lifetime guarantee for 25 year. Warranty for module 80% performance after 20 years
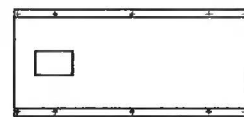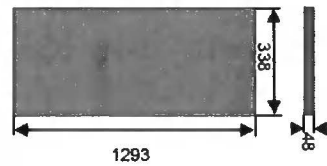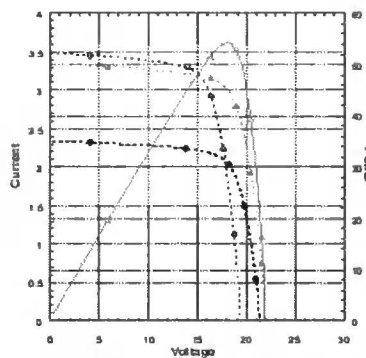
Weight: 5.3kg

Max power	50 watt peak +-5%
Max power voltage	17.3 Volts
Max power current	2.9 Amps
Open circuit voltage	21.7 Volts
Short circuit current	3.2 Amps

Cells	Multicrystalline Si, textured and anti-reflectivity layered
Contacts	Redundant contact on each cell for circuit reliability
Laminate	EVA
Front face	Tempered glass with improved light transmission

Note: Test conditions 1 Kw/m, 25°c, AM1.5

Back face	Tough multi layered back sheet tedlar
Frame	Anodized aluminum
Connection Box	1xIP65 with built-in bypass diodes
Grounding connection	Yes
Specification	IEC 61215, class II TUV certificate

Economical analysis calculations

Stainless Steel Multi stage still
Optimization of various stages with different R ratios for the capital cost (US$):

No of stages	Useful life year	Capital Cost (US$)	Rate of interest	Annual mainte nance	Capital recovery factor CRF	Sinking Salvage Factor SFF	First annual cost M (US$)	Annual maintenance cost AMC (US$)	Annual salvage value N	Annual cost AC (US$)	Annual output Y (kg)	Product water cost PC US$/kg	Annual useful energy (kWh)	Annual cost per (kWh)	Payback period (year)
1	15	848	5%	5%	0.096	0.046	82	4	16	70	933	0.075	607	0.115	2.2
2	15	972	5%	5%	0.096	0.046	94	5	18	80	1447	0.055	941	0.085	1.6
3	15	1095	5%	5%	0.096	0.046	106	5	20	91	1723	0.053	1120	0.081	1.6
4	15	1219	5%	5%	0.096	0.046	117	6	23	101	1866	0.054	1213	0.083	1.6
5	15	1343	5%	5%	0.096	0.046	129	6	25	111	1941	0.057	1261	0.088	1.7
6	15	1467	5%	5%	0.096	0.046	141	7	27	121	1989	0.061	1293	0.094	1.8
7	15	1590	5%	5%	0.096	0.046	153	8	29	131	2036	0.065	1324	0.099	1.9
1	15	1056	5%	5%	0.096	0.046	102	5	20	87	1505	0.058	978	0.089	1.7
2	15	1179	5%	5%	0.096	0.046	114	6	22	97	2359	0.041	1533	0.064	1.2
3	15	1303	5%	5%	0.096	0.046	126	6	24	108	2836	0.038	1843	0.058	1.1
4	15	1427	5%	5%	0.096	0.046	137	7	26	118	3094	0.038	2011	0.059	1.1
5	15	1551	5%	5%	0.096	0.046	149	7	29	128	3233	0.040	2101	0.061	1.2
6	15	1674	5%	5%	0.096	0.046	161	8	31	138	3313	0.042	2153	0.064	1.2
7	15	1798	5%	5%	0.096	0.046	173	9	33	149	3374	0.044	2193	0.068	1.3
1	15	1263	5%	5%	0.096	0.046	122	6	23	104	2087	0.050	1357	0.077	1.5
2	15	1387	5%	5%	0.096	0.046	134	7	26	115	3285	0.035	2135	0.054	1.0
3	15	1511	5%	5%	0.096	0.046	146	7	28	125	3967	0.031	2579	0.048	0.9
4	15	1634	5%	5%	0.096	0.046	157	8	30	135	4347	0.031	2826	0.048	0.9
5	15	1758	5%	5%	0.096	0.046	169	8	33	145	4555	0.032	2961	0.049	0.9
6	15	1882	5%	5%	0.096	0.046	181	9	35	155	4673	0.033	3038	0.051	1.0
7	15	2006	5%	5%	0.096	0.046	193	10	37	166	4754	0.035	3090	0.054	1.0
1	15	1504	5%	5%	0.096	0.046	145	7	28	124	2673	0.046	1737	0.072	1.4
2	15	1627	5%	5%	0.096	0.046	157	8	30	134	4215	0.032	2739	0.049	0.9

No of stages	Useful life year	Capital Cost (US$)	Rate of Interest	Annual mainte nance	Capital recovery factor CRF	Sinking Salvage Factor SFF	First annual cost M (US$)	Annual maintenance cost AMC (US$)	Annual salvage value N	Annual cost AC (US$)	Annual output Y (kg)	Product water cost PC US$/kg	Annual useful energy (kWh)	Annual cost per (kWh)	Payback period (year)
3	15	1751	5%	5%	0.096	0.046	169	8	32	145	5102	0.028	3316	0.044	0.8
4	15	1875	5%	5%	0.096	0.046	181	9	35	155	5604	0.028	3643	0.043	0.8
5	15	1999	5%	5%	0.096	0.046	193	10	37	165	5884	0.028	3825	0.043	0.8
6	15	2122	5%	5%	0.096	0.046	204	10	39	175	6043	0.029	3928	0.045	0.9
7	15	2246	5%	5%	0.096	0.046	216	11	42	186	6146	0.030	3995	0.046	0.9
1	15	1711	5%	5%	0.096	0.046	165	8	32	141	3260	0.043	2119	0.067	1.3
2	15	1835	5%	5%	0.096	0.046	177	9	34	152	5143	0.029	3343	0.045	0.9
3	15	1959	5%	5%	0.096	0.046	189	9	36	162	6233	0.026	4052	0.040	0.8
4	15	2082	5%	5%	0.096	0.046	201	10	39	172	6858	0.025	4458	0.039	0.7
5	15	2206	5%	5%	0.096	0.046	213	11	41	182	7211	0.025	4687	0.039	0.7
6	15	2330	5%	5%	0.096	0.046	224	11	43	192	7412	0.026	4818	0.040	0.8
7	15	2454	5%	5%	0.096	0.046	236	12	45	203	7539	0.027	4900	0.041	0.8
1	15	1919	5%	5%	0.096	0.046	185	9	36	159	3847	0.041	2501	0.063	1.2
2	15	2042	5%	5%	0.096	0.046	197	10	38	169	6070	0.028	3945	0.043	0.8
3	15	2166	5%	5%	0.096	0.046	209	10	40	179	7360	0.024	4784	0.037	0.7
4	15	2290	5%	5%	0.096	0.046	221	11	42	189	8104	0.023	5268	0.036	0.7
5	15	2414	5%	5%	0.096	0.046	233	12	45	199	8530	0.023	5544	0.036	0.7
6	15	2537	5%	5%	0.096	0.046	244	12	47	210	8774	0.024	5703	0.037	0.7
7	15	2661	5%	5%	0.096	0.046	256	13	49	220	8927	0.025	5803	0.038	0.7
1	15	2126	5%	5%	0.096	0.046	205	10	39	176	4434	0.040	2882	0.061	1.2
2	15	2250	5%	5%	0.096	0.046	217	11	42	186	6992	0.027	4545	0.041	0.8
3	15	2374	5%	5%	0.096	0.046	229	11	44	196	8479	0.023	5512	0.036	0.7
4	15	2497	5%	5%	0.096	0.046	241	12	46	206	9343	0.022	6073	0.034	0.7
5	15	2621	5%	5%	0.096	0.046	253	13	49	217	9840	0.022	6396	0.034	0.7
6	15	2745	5%	5%	0.096	0.046	264	13	51	227	10128	0.022	6583	0.034	0.7
7	15	2869	5%	5%	0.096	0.046	276	14	53	237	10307	0.023	6699	0.035	0.7

Aluminum Multi stage still
Optimization of various stages with different R ratios for the capital cost (US$):

No of stages	Useful life year	Capital Cost (US$)	Rate of interest	Annual mainte nance	Capital recovery factor CRF	Sinking Salvage Factor SFF	First annual cost M (US$)	Annual maintenance cost AMC (US$)	Annual salvage value N	Annual cost AC (US$)	Annual output Y (kg)	Product water cost PC US$/kg	Annual useful energy (kWh)	Annual cost per (kWh)	Payback period (year)
1	15	709	5%	5%	0.096	0.046	68.3	3.4	13.1	58.6	933	0.063	607	0.097	1.9
2	15	833	5%	5%	0.096	0.046	80.3	4.0	15.4	68.8	1447	0.048	941	0.073	1.4
3	15	957	5%	5%	0.096	0.046	92.2	4.6	17.7	79.0	1723	0.046	1120	0.071	1.4
4	15	1052	5%	5%	0.096	0.046	101.4	5.1	19.5	87.0	1866	0.047	1213	0.072	1.4
5	15	1204	5%	5%	0.096	0.046	116.0	5.8	22.3	99.5	1941	0.051	1261	0.079	1.5
6	15	1328	5%	5%	0.096	0.046	127.9	6.4	24.6	109.7	1989	0.055	1293	0.085	1.6
7	15	1452	5%	5%	0.096	0.046	139.9	7.0	26.9	119.9	2036	0.059	1324	0.091	1.7
1	15	825	5%	5%	0.096	0.046	79.5	4.0	15.3	68.1	1505	0.045	978	0.070	1.3
2	15	948	5%	5%	0.096	0.046	91.4	4.6	17.6	78.4	2359	0.033	1533	0.051	1.0
3	15	1072	5%	5%	0.096	0.046	103.3	5.2	19.9	88.6	2836	0.031	1843	0.048	0.9
4	15	1179	5%	5%	0.096	0.046	113.6	5.7	21.9	97.4	3094	0.031	2011	0.048	0.9
5	15	1320	5%	5%	0.096	0.046	127.1	6.4	24.5	109.0	3233	0.034	2101	0.052	1.0
6	15	1443	5%	5%	0.096	0.046	139.1	7.0	26.8	119.3	3313	0.036	2153	0.055	1.1
7	15	1567	5%	5%	0.096	0.046	151.0	7.5	29.1	129.5	3374	0.038	2193	0.059	1.1
1	15	940	5%	5%	0.096	0.046	90.6	4.5	17.4	77.7	2087	0.037	1357	0.057	1.1
2	15	1064	5%	5%	0.096	0.046	102.5	5.1	19.7	87.9	3285	0.027	2135	0.041	0.8
3	15	1188	5%	5%	0.096	0.046	114.4	5.7	22.0	98.1	3967	0.025	2579	0.038	0.7
4	15	1306	5%	5%	0.096	0.046	125.9	6.3	24.2	107.9	4347	0.025	2826	0.038	0.7
5	15	1435	5%	5%	0.096	0.046	138.3	6.9	26.6	118.6	4555	0.026	2961	0.040	0.8
6	15	1559	5%	5%	0.096	0.046	150.2	7.5	28.9	128.8	4673	0.028	3038	0.042	0.8
7	15	1683	5%	5%	0.096	0.046	162.1	8.1	31.2	139.0	4754	0.029	3090	0.045	0.9
1	15	1089	5%	5%	0.096	0.046	104.9	5.2	20.2	89.9	2673	0.034	1737	0.052	1.0
2	15	1212	5%	5%	0.096	0.046	116.8	5.8	22.5	100.2	4215	0.024	2739	0.037	0.7
3	15	1336	5%	5%	0.096	0.046	128.7	6.4	24.8	110.4	5102	0.022	3316	0.033	0.6

No of stages	Useful life year	Capital Cost (US$)	Rate of interest	Annual mainte nance	Capital recovery factor CRF	Sinking Salvage Factor SFF	First annual cost M (US$)	Annual maintenance cost AMC (US$)	Annual salvage value N	Annual cost AC (US$)	Annual output Y (kg)	Product water cost PC US$/kg	Annual useful energy (kWh)	Annual cost per (kWh)	Payback period (year)
4	15	1470	5%	5%	0.096	0.046	141.6	7.1	27.2	121.4	5604	0.022	3643	0.033	0.6
5	15	1584	5%	5%	0.096	0.046	152.6	7.6	29.4	130.8	5884	0.022	3825	0.034	0.7
6	15	1707	5%	5%	0.096	0.046	164.5	8.2	31.6	141.1	6043	0.023	3928	0.036	0.7
7	15	1831	5%	5%	0.096	0.046	176.4	8.8	33.9	151.3	6146	0.025	3995	0.038	0.7
1	15	1204	5%	5%	0.096	0.046	116.0	5.8	22.3	99.5	3260	0.031	2119	0.047	0.9
2	15	1328	5%	5%	0.096	0.046	127.9	6.4	24.6	109.7	5143	0.021	3343	0.033	0.6
3	15	1451	5%	5%	0.096	0.046	139.8	7.0	26.9	119.9	6233	0.019	4052	0.030	0.6
4	15	1597	5%	5%	0.096	0.046	153.8	7.7	29.6	131.9	6858	0.019	4458	0.030	0.6
5	15	1699	5%	5%	0.096	0.046	163.7	8.2	31.5	140.4	7211	0.019	4687	0.030	0.6
6	15	1823	5%	5%	0.096	0.046	175.6	8.8	33.8	150.6	7412	0.020	4818	0.031	0.6
7	15	1946	5%	5%	0.096	0.046	187.5	9.4	36.1	160.8	7539	0.021	4900	0.033	0.6
1	15	1319	5%	5%	0.096	0.046	127.1	6.4	24.5	109.0	3847	0.028	2501	0.044	0.8
2	15	1443	5%	5%	0.096	0.046	139.0	7.0	26.8	119.2	6070	0.020	3945	0.030	0.6
3	15	1567	5%	5%	0.096	0.046	151.0	7.5	29.0	129.5	7360	0.018	4784	0.027	0.5
4	15	1724	5%	5%	0.096	0.046	166.1	8.3	32.0	142.4	8104	0.018	5268	0.027	0.5
5	15	1814	5%	5%	0.096	0.046	174.8	8.7	33.6	149.9	8530	0.018	5544	0.027	0.5
6	15	1938	5%	5%	0.096	0.046	186.7	9.3	35.9	160.1	8774	0.018	5703	0.028	0.5
7	15	2062	5%	5%	0.096	0.046	198.6	9.9	38.2	170.4	8927	0.019	5803	0.029	0.6
1	15	1435	5%	5%	0.096	0.046	138.2	6.9	26.6	118.5	4434	0.027	2882	0.041	0.8
2	15	1559	5%	5%	0.096	0.046	150.2	7.5	28.9	128.8	6992	0.018	4545	0.028	0.5
3	15	1682	5%	5%	0.096	0.046	162.1	8.1	31.2	139.0	8479	0.016	5512	0.025	0.5
4	15	1851	5%	5%	0.096	0.046	178.3	8.9	34.3	152.9	9343	0.016	6073	0.025	0.5
5	15	1930	5%	5%	0.096	0.046	185.9	9.3	35.8	159.4	9840	0.016	6396	0.025	0.5
6	15	2054	5%	5%	0.096	0.046	197.8	9.9	38.1	169.7	10128	0.017	6583	0.026	0.5
7	15	2177	5%	5%	0.096	0.046	209.8	10.5	40.4	179.9	10307	0.017	6699	0.027	0.5

Multi stage still
Sensitivity analysis for various rates of interest and annual maintenance percentages on the economical calculations.

No.	Useful life year	Rate of interest	Annual maintenance	Capital recovery factor CRF	Sinking Salvage Factor SFF	First annual cost M (US$)	Annual maintenance cost AMC	annual salvage value N	Annual cost AC (US$)	Annual output Y (kg)	Product water cost PC US$/kg	Annual useful energy (kWh)	Annual cost per kWh	Payback period (year)
1	15	5%	2%	0.096	0.046	142	14	27	129	9343	0.014	6073	0.021	0.41
2	15	5%	5%	0.096	0.046	142	14	27	129	9343	0.014	6073	0.021	0.41
3	15	5%	10%	0.096	0.046	142	14	27	129	9343	0.014	6073	0.021	0.41
4	15	7%	2%	0.110	0.040	161	16	23	154	9343	0.016	6073	0.025	0.43
5	15	7%	5%	0.110	0.040	161	16	23	154	9343	0.016	6073	0.025	0.43
6	15	7%	10%	0.110	0.040	161	16	23	154	9343	0.016	6073	0.025	0.43

Based on Bottled water cost = 0.35 US$/kg

Reverse osmosis desalination system
Capital Cost: 5632 US$

No.	Useful life year	Rate of interest	Annual maintenance	Capital recovery factor CRF	Sinking Salvage Factor SFF	First annual cost M (US$)	Annual maintenance cost AMC	annual salvage value N	Annual cost AC (US$)	Annual output Y (kg)	Product water cost PC US$/kg	Annual useful energy (kWh)	Annual cost per kWh	Payback period (year)
1	20	5%	2%	0.080	0.030	452	45	34	463	66150	0.007	42998	0.011	7.9
2	20	5%	5%	0.080	0.030	452	45	34	463	66150	0.007	42998	0.011	7.9
3	20	5%	10%	0.080	0.030	452	45	34	463	66150	0.007	42998	0.011	7.9
4	20	7%	2%	0.094	0.024	532	53	27	557	66150	0.008	42998	0.013	8.1
5	20	7%	5%	0.094	0.024	532	53	27	557	66150	0.008	42998	0.013	8.1
6	20	7%	10%	0.094	0.024	532	53	27	557	66150	0.008	42998	0.013	8.1

Based on desalinated water cost by RO technology = 12 US$/m^3